

THESIS
C 173d
1975
c.3

THE DEPOSITIONAL ENVIRONMENT, PALEOCURRENTS, PROVENANCE
AND DISPERSAL PATTERNS OF THE ABO FORMATION IN
PART OF THE CERROS DE AMADO REGION, SOCORRO COUNTY,
NEW MEXICO

by
James A. Cappa

Geotechnical
Information Center

JUL 9 1980

N.M.I.M.T.
LIBRARY
SOCORRO, N.M.

Submitted in Partial Fulfillment
of the Requirements for the Degree of
Master of Science in Geology

NEW MEXICO INSTITUTE OF MINING AND TECHNOLOGY

Socorro, New Mexico

June, 1975

788 2 1984
6500058

TABLE OF CONTENTS

	Page
CHAPTER 1: INTRODUCTION	1
Purpose	1
Background	1
Scope and Methods	2
Previous Work	7
Economic Aspects	13
Significance of the Problem	14
CHAPTER 2: GENERAL GEOLOGY OF THE STUDY AREA	16
Introduction	16
Stratigraphy	18
Structural Geology	22
CHAPTER 3: PETROGRAPHY AND X-RAY ANALYSIS	27
Procedures	27
Arkoses and Arkosic Conglomerates	28
Siltstones	34
Granular Siltstone	38
Mudstones	39
Calcilithites	40
Diagenesis	46
Source Rocks	48
CHAPTER 4: THE DETAILED STRATIGRAPHY OF THE ABO FORMATION WITHIN THE STUDY AREA	53
Introduction	53
Lower Member	55
Upper Cyclic Member	55

CHAPTER 5: PALEOCURRENT ANALYSIS	76
Introduction	76
Procedure	76
Statistical Treatment	80
Test of Significance	82
Paleocurrent Data	83
Summary	89
CHAPTER 6: DEPOSITIONAL ENVIRONMENT	91
Introduction	91
Fluvial Models	91
Depositional Environment - Upper Member of the Abo ..	97
Depositional Environment - Lower Member of the Abo ..	106
Fluvial Paleochannels	106
CHAPTER 7: PROVENANCE AND DISPERSAL PATTERNS OF THE ABO FORMATION	110
Provenance	110
Dispersal Patterns	117
CHAPTER 8: SUMMARY AND CONCLUSIONS	122
Summary	122
Conclusions	125
Recommendations for Further Work	125
APPENDICES	
Appendix A: Classification Systems	127
Appendix B: Catalogue of Sedimentary Structures from the Abo Formation	131
REFERENCES	144

LIST OF FIGURES

Figure		Page
1	General Map of New Mexico showing modern uplifts in which the Abo Formation is exposed	3
2	Map of New Mexico showing distribution of late Paleozoic land masses	4
3	Generalized Pennsylvanian-Permian correlation chart of the Southwestern United States	10
4	Index and location map of study area	17
5	Photomicrograph of arkose	30
6	Photomicrograph of siltstone	36
7	Photomicrograph of calcilithite	41
8	Photomicrograph showing neomorphic regrowth between two micrite clasts	44
9	Stratigraphic section of the Abo Formation	54
10	A view down the axis of a channel fill composed of calcilithite	57
11	Channel fill composed mostly of siltstone	57
12	A view down the trough of small scale cross-lamination	60
13	Type A climbing ripples	60
14	Tabular-shaped medium scale cross-stratification	62
15	Trough-shaped medium scale cross-stratification	62
16	Large scale cross-stratification	63
17	Top view of catenary and linguoid ripple marks	65
18	A fossil plant stem	67
19	Stratigraphic section of Unit F	69
20	A partial cycle in Unit F	70

Figure		Page
21	Convolute laminations, Unit F	71
22	Interbedded calcilithite and siltstone, Unit F	71
23	Large scale cross-stratification, Unit F	73
24	Stratigraphic section of Unit K	74
25	Stratigraphic section of Unit G	74
26	Rayleigh Test of significance on summed sedimentary structures	84
27	Fluvial Models	93
28	A typical meandering stream deposit in the upper cyclic member	99

LIST OF TABLES

Table		Page
1	Point count data for arkoses in the Abo Formation	31
2	Point count data for clasts in the calcilithites in the Abo Formation	42
3	Summary of lithologic types in the Abo Formation	51
4	Types of primary sedimentary structures used for paleocurrent measurement	78
5A	Fluvial parameters and equations	107
5B	Fluvial parameters from two localities in the Abo Formation	107

LIST OF PLATES

Plate		
1	Geologic Map of Study Area	rear pocket
2	Structure Sections	"
3A	Rose Diagrams of Sedimentary Structures, Units A-F	"
3B	Rose Diagram of Sedimentary Structures, Units G-O	"

ACKNOWLEDGMENTS

I am deeply grateful to my thesis advisor, Dr. John MacMillan, for his guidance and assistance from the original suggestion of the problem to the preparation of the final manuscript.

Thanks to the New Mexico Geological Society for a grant which partially covered field expenses, photographic supplies and drafting expenses. I am also indebted to the New Mexico Institute of Mining and Technology for a teaching assistantship.

I would like to thank Michael Jaworski and Dr. Karl Vonder Linden both formerly of the New Mexico Bureau of Mines and Mineral Resources for the use of their topographic base map of the Chupadero Mines area.

Many thanks to my colleagues, teachers, and friends who have in many ways contributed to the final completion of this thesis. My deepest thanks are reserved for my wife, Sherry, who performed such diverse tasks as editor, critic, and surveyor and provided moral support during the production of this thesis.

ABSTRACT

Lower Permian red-beds of the Abo Formation were studied in a small area in the Cerros de Amado region about 7 miles east of Socorro, New Mexico, to quantitatively determine their source area, paleocurrents, dispersal patterns and depositional environment.

The Abo Formation has been divided into two informal members. The lower member consists primarily of arkose with minor mudstone and limestone. The arkose is thick bedded, very coarse to pebbly, internally homogenous to graded and is composed of composite grains of quartz and slightly rounded euhedra of pink perthitic microcline. The abundance, size, shape and petrographic characteristics of the microcline and composite quartz grains indicate a local source (a few tens of miles) such as the Precambrian granitic gneiss of the Joyita Hills, which was a positive area in Pennsylvanian and Early Permian times.

The upper member consists of several cycles of calcilithite, overlain by siltstone, overlain by mudstone. The clasts in the calcilithites are composed of micrite, biomicrite, calcareous and quartzose siltstone, and minor sparite. The siltstones of the upper member are composed primarily of quartz. The mudstones are similar but also contain kaolin, chlorite, and illite/smectite mixed layer clays.

The paleocurrent directions are bimodal with the

dominant mode southerly; the secondary mode westerly. The calcilithite clasts are petrographically similar to subjacent Pennsylvanian carbonate and clastic rock sequences.

The fine grained rocks suggest derivation from weathered "granitic" rocks, so that the source areas were mixed sedimentary and crystalline highlands to the north.

Vertical sequences of large scale cut-and-fill structures, planar alignment of pebbles, medium scale cross lamination and horizontal lamination, ripple and ripple-drift cross lamination; and finally mud cracks, vertebrate tracks and plant fragments in the upper cyclic member, suggest point bar and flood plain deposits. The environment of deposition is interpreted as a low gradient alluvial plain with meandering streams.

The depositional environment of the lower member was probably a braided stream.

CHAPTER 1: INTRODUCTION

Purpose

The purpose of this thesis is to determine, quantitatively where possible, the depositional environment, paleocurrent and dispersal patterns, and provenance of the Lower Permian red-beds of the Abo Formation near Socorro in central New Mexico. The primary tools in this investigation are statistical analysis of paleocurrent data, petrographic analysis, and detailed stratigraphic sections.

Paleoenvironments of the Abo Formation are inferred by the comparison of mineralogical composition, texture, primary sedimentary structures, and fossil organisms with modern deposits in specific environments. Fossil organisms, such as plant fossils, or the evidence of organisms, such as vertebrate tracks, occur in the Abo Formation but are not studied for their paleoenvironmental significance.

Background

The exact age of the red-beds of the Abo Formation has been the subject of some controversy (King, R. E., 1945; Kottowski and Stewart, 1970). In this thesis the Abo is taken to be of partly Wolfcampian and partly Leonardian age.

The Abo Formation occurs throughout New Mexico (see Figure 1) from the Nacimiento Mountains of northern New Mexico, southward to the Zuni and Sandia Mountains,

and in the southern part of the state in the Manzano, Lucero, Sacramento, San Andres, Caballo and Los Piños Mountains (Darton, 1928). There has been mention by oilmen of the "Abo reef" which occurs in subsurface of the Permian Basin in the southeastern part of the state. This unit is a light colored, porous, coarse grained dolomite of Leonardian age (Wright, 1962). It is distinct lithologically and stratigraphically from the terrigenous red-beds of the Abo Formation found in outcrop throughout New Mexico (Meyer, 1966).

Most previous workers agree that the Abo red-beds are dominantly continental in origin on the basis of mud cracks, lenticular bedding, land vertebrate tracks and impressions and carbonized remains of land plants. Moreover, most previous workers propose a fluvial-alluvial environment of deposition based largely on the association of interbedded conglomerates, sandstones, siltstones and mudstones.

Numerous source areas have been proposed by previous workers based largely on the stratigraphic relationships of the Abo Formation with other rock units, and to a lesser extent on petrography. Figure 2 shows the location, extent and names of areas which are thought to have been highlands which shed detritus into adjacent subaerial and/or submarine basins during Late Pennsylvanian and Early Permian time.

Scope and Methods

Most of the previous studies of the Abo Formation

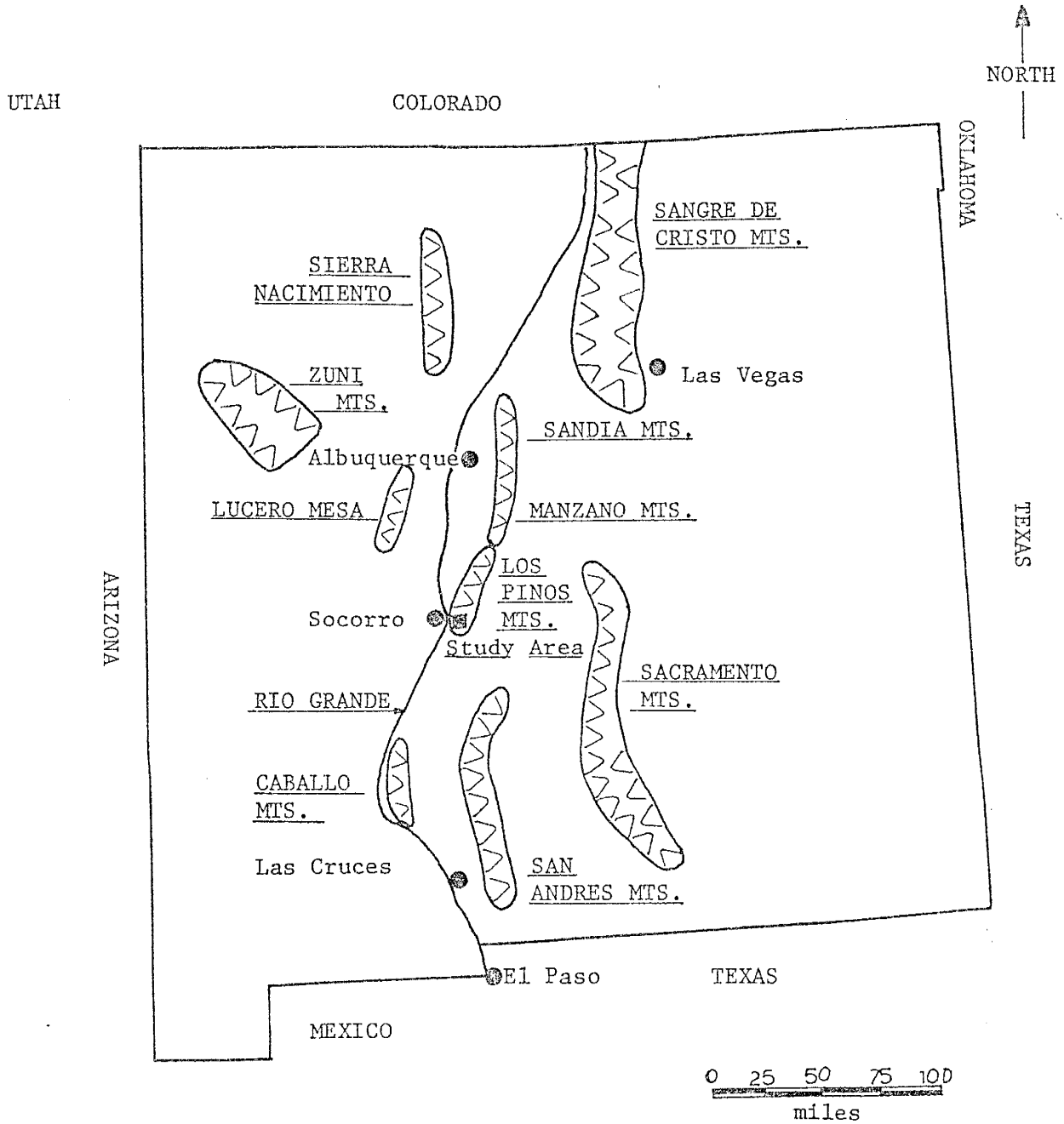


Figure 1. General map of New Mexico showing modern uplifts in which the Abo Formation is exposed.

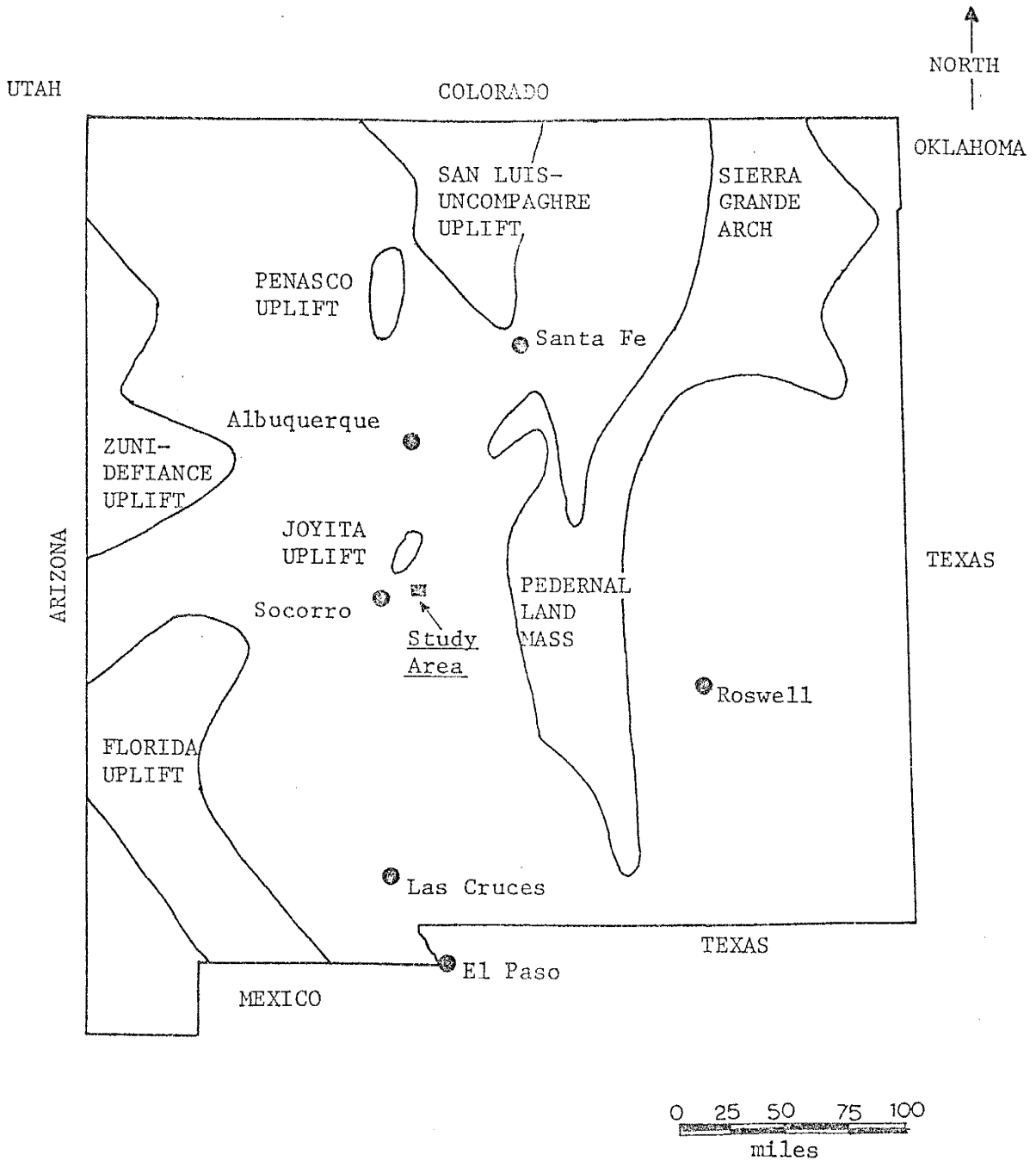


Figure 2. Map of New Mexico showing distribution of late Paleozoic land masses. Modern cities are shown for reference (after Kottlowski and Stewart, 1970; McKee, 1967).

are concerned with stratigraphic relationships, and do not employ detailed or quantitative methods in reaching conclusions about the depositional environment and provenance of the Abo Formation.

In this study a small area (≈ 1 sq. mile) of outcrop of the Abo Formation is mapped in detail in the Cerros de Amado region (Figure 1). Petrographic analysis of thin sections and X-ray diffraction of the rocks of the Abo Formation combined with study of published and unpublished descriptions of older rocks in the area is used to determine the type and variety of the source rocks. Statistical analysis of paleocurrent directions measured from primary sedimentary structures in the Abo Formation is used to determine the relative geographic position of source areas throughout the time of deposition of the Abo Formation. Changes in the location of source areas through time may be used to infer the nature and extent of tectonism during deposition of the Abo red-beds.

The mineralogic composition, texture, primary sedimentary structures and their relationships in the Abo Formation are compared with modern sediments of known environment of deposition in order to interpret the depositional environment of the Abo Formation. Quantitative data on the thickness (depth) and lateral extent (width) of major sedimentary structures, such as channels, are used to quantitatively estimate the parameters of a depositional environment, such as gradient, sinuosity and discharge.

This investigation deals with only a limited portion of the outcrop area of the Abo Formation in the Cerros de Amado region. Reconnaissance indicates similar lithologic types, textures and structures in the Sacramento, Manzano and Zuni Mountains. Published descriptions of the Abo red-beds from other areas such as the San Andres Mountains (Kottlowski, et al., 1956), the Caballo Mountains (Kelley and Silver, 1952), the Lucero Uplift (Tonking, 1957), and the Sandia Mountains (Kelley, 1963) are similar to the area studied in the Cerros de Amado.

Therefore, many of the broad conclusions and interpretations reached in this thesis are probably applicable to the Abo Formation over the broader region of central New Mexico.

The Abo Formation is similar to other red-bed deposits of Lower Permian (Wolfcampian to Leonardian) age found in northern New Mexico and southern Colorado and Utah, and to the west in the Colorado Plateau. The Abo has been correlated with the Supai Formation in Arizona and the lower part of the Cutler Formation in southern Colorado and Utah (Baars, 1962). The Lower Permian arkoses and red siltstones and shales of the Sangre de Cristo Formation (Miller, et al., 1963) in the Sangre de Cristo Mountains of northern New Mexico are also probable lateral equivalents of the Abo Formation.

In the central Sacramento Mountains of southern New Mexico, the Abo Formation interfingers with the limestones

and dolomites of the Pendejo Tongue of the Hueco Limestone (Pray, 1961).

Previous Work

Definition and contact relations: Willis Lee (1909) is the earliest worker to use the name "Abo" for a succession of dark red sandstones exposed in Abo Canyon at the southern end of the Manzano Mountains in New Mexico. N. H. Darton (1928) in his classic study of the "Red Beds" of New Mexico described the distribution of the "Abo red beds". Darton also recognized a facies change from the continental "Abo red beds" to marine, near-shore limestones in the Sacramento Mountains.

Needham and Bates (1943) formally defined the Abo Formation and described a total of 915 feet of sandstone, arkose and shale at the type section in Abo Pass at the southern end of the Manzano Mountains. They noted the non-marine character of the Abo Formation by its red color, clastic character, casts of halite, mud cracks, ripple marks, cross-bedding, bones and tracks of land vertebrates and plant remains.

An anonymous observer (New Mexico Geol. Soc. Guidebook, 1963) noted that a distinctive dolomite bed occurs 100 feet below the top of the type section of Needham and Bates. ^{5/}He proposed that this dolomite marks the base of a series of cross bedded sandstones found throughout central New Mexico which are assigned to the Meseta Blanca Member of the overlying Yeso Formation of Leonardian age. This

member is thought to represent a littoral to sub-littoral facies of a transgressing sea as indicated by increasing amounts of carbonate rocks and evaporites. Throughout New Mexico the contact between the Abo and Yeso Formations is gradational. In most of central New Mexico the lower contact of the Abo Formation with the underlying Bursum Formation is conformable (Wilpolt and Waneck, 1951). In other localities, such as the Zuni Mountains (Smith, 1957) and locally in the Sacramento Mountains (Pray, 1961; Otte, 1959), the Abo rests with angular unconformity on Precambrian crystalline rocks.

Age and correlation: The age of the Abo Formation has been the subject of much controversy. Some workers such as R. E. King (1945) and J. Hills (1961) suggest that the Abo Formation is totally of Leonardian age. Indeed, much of the upper Abo Formation throughout New Mexico contains fossils of the Supaia flora (Winters, 1963; Read and Mamay, 1964) which are characteristic of the Leonardian Stage. Other workers have felt that because the Abo Formation locally conformably overlies Wolfcampian marine strata that it too may be of Wolfcampian age (King, P. B., 1942; Baars, 1961; Kottowski and Stewart, 1970). In the southern Sacramento Mountains, the marine Hueco Limestone is interbedded with the middle portion of the Abo red-beds (Pray, 1961). The lower beds of the Hueco Limestone at Otero Mesa a few miles south of the Sacramento Mountains contain a Wolfcampian fusulinid fauna and the upper beds

contain a Leonardian fusulinid fauna (Kottlowski, 1965). These relationships indicate that the Abo Formation is both Wolfcampian and Leonardian in age.

Figure 3 is a correlation chart of the Abo Formation and other units in the surrounding area.

Depositional environments and source areas: Depositional environments and source areas for the Abo Formation are noted by several authors. L. C. Pray (1961) and Carel Otte (1959) in separate studies in the Sacramento Mountains both believe that the mudstones, siltstones, arkoses, quartzite pebble conglomerates and limestone pebble conglomerates of the Abo Formation were deposited on a broad flood plain or piedmont area near a major uplift. Otte (1959) mentions that the coarse detritus of the Abo Formation may have accumulated as channel deposits of shifting streams while the mudstones and siltstones represent flood plain deposits. Both authors believe that the Precambrian granitic rocks of the Pedernal land mass (Thompson, 1942) to the east were the most probable source for the "granitic" material in the coarse clastic rocks of the Abo Formation.

In the northern Sacramento Mountains, Bachman (1964) notes that the Abo Formation thins and overlaps Precambrian quartzite which is locally intruded by granitic rocks. The lower beds of the Abo Formation contain cobble conglomerates whose clasts are of the underlying quartzite and granite. Bachman concludes that this locality may have been the edge of the late Paleozoic Pedernal land mass.

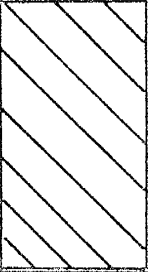
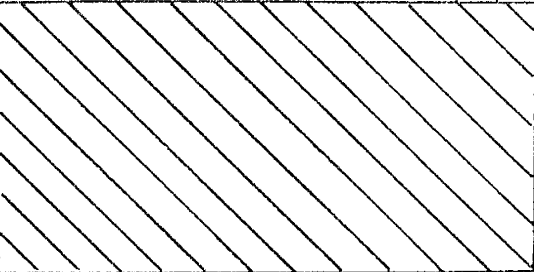
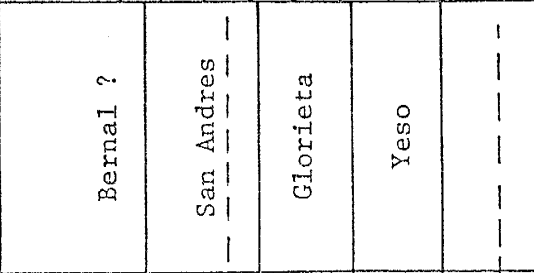

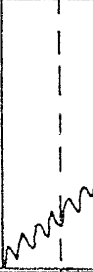

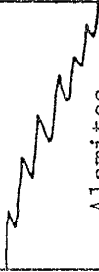
SYSTEM	SERIES	SOUTH CENTRAL NEW MEXICO	CENTRAL NEW MEXICO	NORTHERN NEW MEXICO	SOUTHERN COLORADO	GRAND CANYON, ARIZONA	
PERMIAN	Guadalupian		Bernal ?		Lykins	Kaibab	
		San Andres	San Andres				
	Leonardian		Glorieta	Glorieta		Lyons	Toroweap
		Yeso	Yeso				Coconino
	Wolfcampian						
		Hueco Abo	Abo	Sangre de Cristo	Maroon (west)	Supai	
PENNSYLVANIAN	Virgilian	Bursum	Bursum		Fountain (east)		
		Magdalena Group	Madera and Magdalena Groups			Naco	

Figure 3. Generalized Pennsylvanian-Permian correlation chart of the Southwestern United States: adapted from Dunbar, C. O. et al., (1960); Miller, J. P. et al., (1963); Winters, S. L., (1963); and McKee, E. D., (1967).

Kottowski and Stewart (1970) in their study of the Wolfcampian Joyita Hills uplift of central New Mexico believe, because of the presence of angular shards of quartz and large fresh clasts of feldspar in the lower Abo beds, that the Precambrian granitic gneiss of the Joyita Hills was a local source. By late Wolfcampian time the small Joyita "islands" and more distant land areas such as the Zuni land mass and Pedernal land mass were covered or partially covered by the clastic debris of the Abo Formation which flowed southward in stream channels and adjacent flood plains.

Meyer (1966), in his study of the Pennsylvanian and Wolfcampian rocks of southeastern New Mexico, concludes that the various structural elements, such as the Pedernal land mass, were buried by Wolfcampian marine and non-marine sediments.

Baars (1961) mentions that the Uncompaghre-San Luis uplift was a possible source area for the Abo Formation. He also suggests that deposition took place on a broad coastal plain, which was periodically flooded by marine waters in the southern part of the state.

Tonking (1957), in his study of the Puertocito area just south of the Lucero uplift, believes that the shales, shaley siltstones, arkoses and limestone pebble conglomerates of the Abo Formation represent non-marine deposition following withdrawal of the Pennsylvanian seas. The conditions of deposition were on a flood plain-deltaic system consisting

of meandering streams with fairly wide flood plains. The coarse material represents migrating channel deposits and the fine grained material represents flood plain deposits. Tonking also mentions the "Ancestral Rocky Mountains" and the Zuni uplift as possible source areas.

Kelley and Silver (1952) conclude that the Abo Formation in the Caballo Mountains is continental in origin and typical of wide flood plain deposits.

Smith (1957) believes that the Abo Formation in the Zuni Mountains are flood plain deposits which accumulated under fluvial and quiet water conditions.

McKee (1967), in a summary study of the paleotectonics of the Permian System in western New Mexico and Arizona, concludes that the Abo red-beds are of continental origin because of mud cracks, bones and tracks of land vertebrates, land plants and abundant channels and lenticular beds. The depositional environment is envisioned as one of flood plains and deltas across a wide lowland area. Possible source areas listed by McKee (1967) are the Florida positive element, Pedernal positive element, the Zuni-Defiance positive element and the San Luis-Uncompaghe positive element (see Figure 2).

LaPoint (1974) concludes that the copper-rich montmorillonite clays and/or copper-organic complexes in the lower clastic rocks of the Abo Formation in parts of northern New Mexico were derived from Precambrian metavolcanic rocks in the nearby late Paleozoic land masses.

Previous work in the study area: The earliest attempt at broad geological mapping in the study area is at a reconnaissance level (1" = 1 mile) by the now extinct Fuels Branch of the U. S. Geological Survey (Wilpolt and Waneck, 1951). Rejas (1965) describes the geology of the Cerros de Amado area which includes the study area of this thesis, but his primary concern was the stratigraphic relationships of the Pennsylvanian System in the area. Jaworski (1973) did detailed mapping in the area (1" = 200'). The topic of his study was copper mineralization in the Upper Moya Sandstone of Pennsylvanian age.

Economic Aspects

"Red-bed" type copper and lead deposits occur in the lower arkoses of the Abo Formation at several localities in New Mexico (U. S. Geological Survey, 1965). Chalcocite is the primary copper mineral and usually occurs as a replacement of original woody material in sand channels or as nodules in siltstones and shales. Malachite, azurite and chrysocolla are common oxidation products. Economic copper mineralization has been found in the Scholle district at the southern end of the Manzano Mountains, in the Zuni Mountain district, and in the High Rolls district of the Sacramento Mountains.

In the High Rolls district lead which occurs as galena, cerrusite and anglesite is found with copper in the Abo red-beds (Jerome, et al., 1965).

The ores which occur in the Abo of the High Rolls district are thought to be "syngenetic" with a later epigenetic stage involving redistribution by ground water (Jerome, et al., 1965).

LaPoint (1974) noted that it is possible that copper rich clays and/or copper-organic complexes from Precambrian sources may have been deposited in the Abo sediments, and then remobilization occurred due to dewatering during compaction of the sediment. It is obvious that the depositional environment has played an important part in the localization of copper and lead mineralization in the Abo Formation.

Significance of the Problem

Areas of provenance, paleoslopes, and depositional environments of the Lower Permian rocks of central New Mexico have been hypothesized by many authors primarily on the basis of lithofacies distribution and stratigraphic relationships. This thesis provides detailed quantitative information on the paleocurrent system and source rocks of the Lower Permian Abo Formation in central New Mexico.

As a result of this study the geographic distribution and varieties of source rocks during Lower Permian time in central New Mexico will be known with a greater degree of confidence. The study of the sedimentary structures allows a more precise determination of the depositional environment. Variances in the direction of sedimentary

structures reflect tectonism within the depositional basin or in the source areas.

The gross picture of the Lower Permian landscape envisioned by previous workers will not be changed significantly by this thesis, however much detail can be added to this picture so that the concepts of the Lower Permian paleogeography in central New Mexico become more realistic and approach the complexities observed in the modern world.

From an economic point of view, a quantitative awareness of the paleocurrent systems and depositional environments may lead to a better understanding of the origin and lateral and vertical distribution of copper and lead mineralization within the Abo Formation.

CHAPTER 2: GENERAL GEOLOGY OF THE STUDY AREA

Introduction

The study area is located in the Cerros de Amado region approximately 7 miles east of the town of Socorro, New Mexico. The exact location is the SW $\frac{1}{4}$ of section 23 and the NW $\frac{1}{4}$ of section 26, Township 2 South, Range 1 East, on the Loma de Las Cañas 7.5 minute quadrangle map. (See Figure 4 for a location map).

The area is easily reached by a Bureau of Land Management road (Quebrado road) which begins near the old village of Pueblito on the east side of the Rio Grande (see Figure 4).

The Cerros de Amado are characterized by low rolling hills to moderately steep cuesta scarps. Exposures of the Abo Formation, especially arkoses and siltstones, are good. Interbedded mudstones are largely covered by vegetated colluvium except in recent stream cuts.

Plates 1 and 2 (in pocket) show a detailed geologic map and cross sections of the study area. Field work and mapping was begun in July 1973 and continued intermittently through the fall to February 1974. The base map for the study area is a 1" = 100' topographic map which was commissioned by the New Mexico Bureau of Mines and Mineral Resources for a study of copper mineralization in the vicinity (Jaworski, 1973). A small area was added to the northeast corner of the existing map using a plane

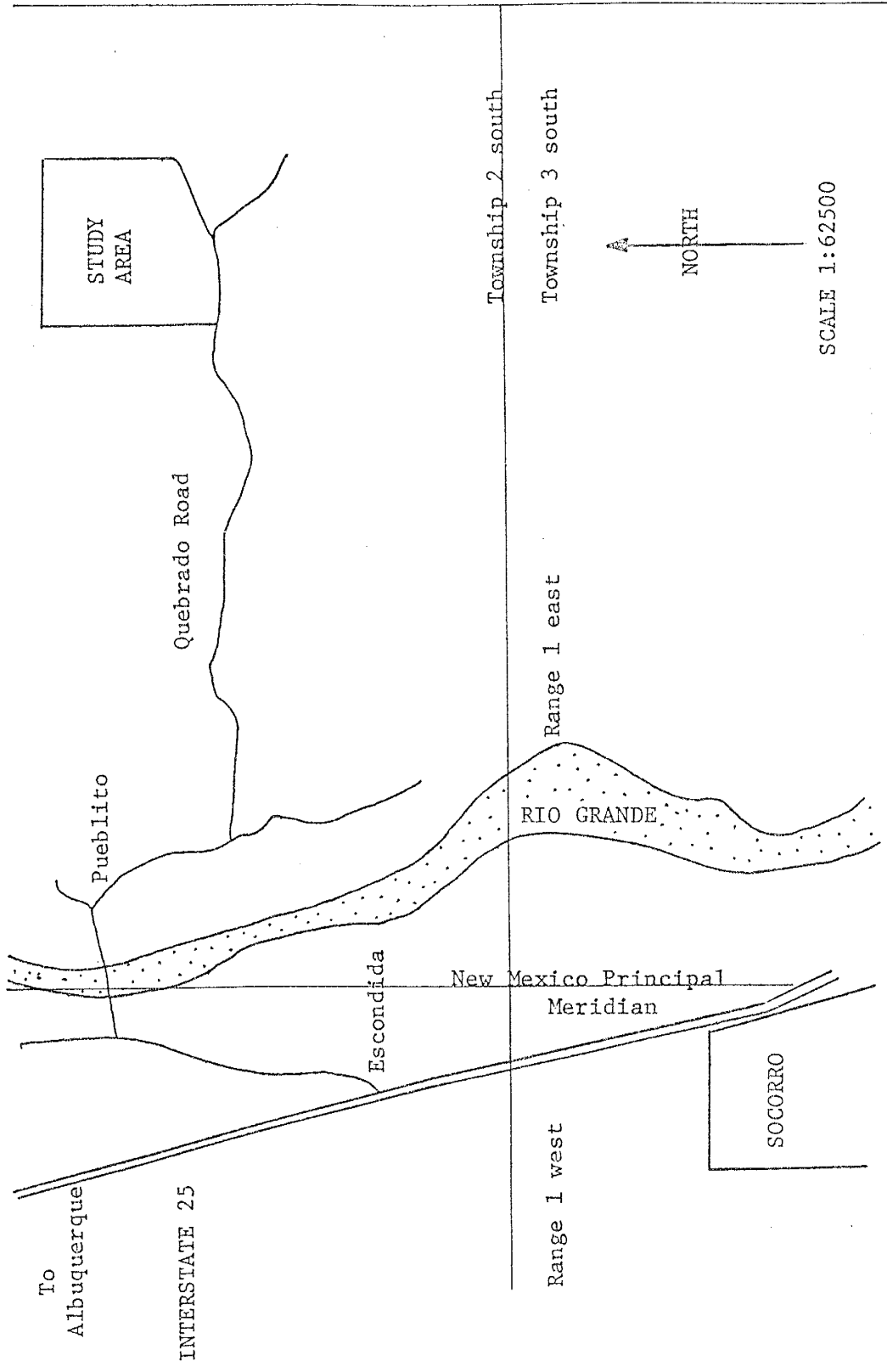


Figure 4. Index and location map of study area (after Socorro, New Mexico 15 minute Quadrangle, 1959).

table and alidade.

The units plotted on the geologic map (Plate 1) and cross sections (Plate 2) are lithofacies of the Abo Formation. Other formations in the study area were mapped but not divided into lithofacies. Areal photographs were used as an aid in mapping faults and the distribution of stratigraphic units.

Stratigraphy

The oldest rocks in the study area (Plate 1) are the Early Permian carbonate and clastic rocks of the Bursum Formation. The dominantly clastic rocks of the Abo and Yeso Formations, also of Early Permian age, conformably overlie the Bursum Formation. The Santa Fe Formation is of Middle to Late Tertiary age (Dane and Bachman, 1965) and overlies the older rocks with angular unconformity.

Bursum Formation: The Bursum Formation was named by Wilpolt et al. (1946) for exposures located on the Bursum Ranch a few miles south of the study area. Within the vicinity of the study area the Bursum Formation consists of thick beds of dark purplish-red and green shales separated by thinner beds of arkose, arkosic conglomerate, and gray micrite and biomicrite (Jaworski, 1973). Fusulinids found in the Bursum Formation of the Los Piños Mountains indicate a Wolfcampian age (Wilpolt and Waneck, 1951). The alternating marine and non-marine sediments of the Bursum Formation are thought to represent the gradual

withdrawal of the widespread Pennsylvanian seas from central New Mexico (Willpolt and Wanack, 1951). The upper contact of the Bursum Formation with the Abo Formation is a matter of some controversy as discussed below.

Abo Formation: Jaworski (1973) in his study of the Chupadero Mining district, which includes the study area, defined the Bursum Formation as a predominantly reddish-gray mudstone and siltstone with interbeds of gray shale. A quartz pebble conglomerate with several thin interbeds of gray (micrite and biomicrite) limestone and gray shale occurs in the lower two-thirds of the formation. The upper one-third consists of a coarse grained arkose with conspicuous grains of pink orthoclase feldspar. This upper member of Jaworski's is considered to be the lower coarse arkosic member of the Abo Formation by this author for the following reasons: 1) the arkose and the overlying siltstones and mudstones of the Abo Formation both have the same dark reddish-brown color, 2) there is a thin bed of coarse arkose with clasts of pink orthoclase feldspar 100 feet stratigraphically above the lowest siltstone unit of the Abo Formation in the study area, and 3) the clastic nature of the arkoses suggest a closer affinity to the Abo Formation than the Bursum Formation.

Within the study area the contact between the gray micrites and biomicrites of the Bursum Formation and the overlying lower coarse arkosic member of the Abo Formation

is conformable.

Overlying the basal pebbly arkoses is a 515 foot thick section consisting of several cycles of calcilithites (pebbly limestone conglomerate) which have erosional lower contacts and often a lenticular shape, overlain by dark reddish-brown laminated to cross laminated, quartzitic siltstone, which are in turn overlain by poorly exposed reddish brown mudstone. Two thin beds of gray nodular mottled micrite occur near the base. The entire formation consists of 25% siltstone, 70% mudstone and 5% arkose.

Graded bedding is common in the coarse pebbly arkoses. The siltstones contain abundant primary sedimentary structures such as ripple marks, tool marks, cross-lamination, rain-drop impacts, mud crack and channel forms.

The Abo Formation is easily recognizable because of its conspicuous reddish-brown color which stands in marked contrast to the gray, orange and tan colors of the subjacent Pennsylvanian and superjacent Permian rocks.

The upper contact of the Abo Formation with the Meseta Blanca Member of the Yeso Formation in the study area is gradational and is marked by a color change to reddish-orange and by the first appearance of halite casts and thin beds of dolomite.

For purposes of this investigation the Abo Formation has been subdivided into two informal members: the lower coarse arkosic member, and a upper cyclic member consisting of fourteen cycles of calcilithite, siltstone and mudstone.

On the geologic map (Plate 1) the siltstones and mudstones of the upper member are mapped as lithofacies of the upper member. Many of the calcilithites are too thin to be distinguished on the geologic map (Plate 1). The lower member is also divided into three lithofacies: arkose, limestone, and mudstone.

Meseta Blanca Member-Yeso Formation: The Yeso Formation of Leonardian age was formally described by Needham and Bates (1943) for exposures at Mesa del Yeso just a few miles north of the study area. The Yeso Formation has been divided into four members of which only the lower-most member, the Meseta Blanca, is exposed in the study area.

The Meseta Blanca Member (Wilpolt and Waneck, 1951) consists of uniformly bedded light red-brown to orange and variegated sandstone and sandy shale with occasional thin beds of dolomite and halite.

The Meseta Blanca Member was deposited during a transgression of the sea from the south (Wilpolt and Waneck, 1951).

Santa Fe Formation: The Santa Fe Formation is an alluvial deposit composed of coarse sand to cobble and boulder sized detritus derived from the erosion of older rocks. It is considered to be of Miocene (?) to Pleistocene age (Dane and Bachman, 1965).

Within the study area the Santa Fe Formation is found only on the hilltops where it overlies the Paleozoic

rocks with angular unconformity.

Recent alluvium and colluvium: Recent alluvial deposits are found in intermittent stream channels and are generally sandy gravels derived from the erosion of the surrounding rocks.

Colluvium is a general term used to designate "slope wash." In the study area this material is gravel to boulder sized, angular to subangular blocks derived from the erosion of the Santa Fe Formation and older rocks.

Structural Geology

Within the study area the structure is fairly simple. Dips of the Abo Formation and adjacent Paleozoic formations generally range between 10° and 20° to the north (see Plate 1).

Normal faulting is mostly confined to the southern part of the study area, and seems to have occurred in two distinct periods. The earlier period of faulting is shown by two faults which trend east-northeast to east. Faults of the early period are displaced by faults of the later period which trend almost exactly northeast. The easterly trending fault of the early period in the very southeast corner of the study area is a normal fault which has an uplifted southern block. The uplift upon this fault has been at least 100 feet but probably less than 150 feet. To the west this fault is covered with alluvium, and is inferred to reappear as a northeasterly trending

fault. The east-northeast trending fault of the early period separates the lower arkose member from the upper cyclic member. The displacement on this fault is not known. Judging from the average change in thickness of the Abo Formation from north of the study area to south of the study area (Wilpolt and Waneck, 1951) it is estimated that no greater than 50 feet of stratigraphic throw has occurred.

The second period of faulting was also normal faulting, but these faults strike northeast and generally involve displacements of less than twenty feet (see cross sections A-A' and E-E' on Plate 2). There are several of these later faults throughout the study area, however they are definitely concentrated in the southern part of the study area near the contact between the upper cyclic member and the lower coarse arkosic member. The dips of the normal faults of the second period are generally to the southeast at about 60°.

One fault, whose surface trace is confined to the Bursum Formation, has a north trend. This fault occurs in the southeastern corner of the study area. The amount of displacement on this fault is not known.

There seems to be a correlation between the location of the normal fault sets and stratigraphic position. The majority of the normal faults are located near the base of the Abo Formation and may, in part, be due to different rheological responses to stress between the arkose and

the overlying siltstones and mudstones. There are several factors which influence the uniaxial strength of rocks. Price (1966) notes that sandstones are, in general, stronger than mudstones and that sandstones with a clay mineral matrix are, in general, weaker than cemented sandstones. There is a possibility that the stresses which caused the normal faulting in the lower part of the section were absorbed as plastic deformation in the mudstones of the upper member. Any such features in the mudstone could easily be unnoticed because of the poor exposure of the mudstones or because of the fine grain size and homogeneity of the mudstones.

The faults, where exposed, are generally steep and have a breccia zone composed of pebble and cobble sized fragments of Abo reddish-brown siltstone, and knobby crystals of calcite ranging up to eight cm on a side set in a finer calcite matrix.

There is no folding in the study area except for three small areas. Some small folds occur in and around Unit E at Locality 9 (see cross section C-C', Plate 2). The folds have a wavelength of ten feet to twenty feet and occur in about a 500 square foot area. Attitudes measured on the limbs of the folds were plotted on an equal area stereonet to determine the direction and amount of plunge of the fold axis. The fold axes in this small system have a plunge of 2° in a direction of N66W. The cause of this fold is conjectural; it does not seem to be related to any normal faulting. The fold may be due to gravity sliding during

tilting of the Abo Formation by block faulting.

There is another small fold (25 square feet) in the lower arkosic member just south of Locality 26 (Plate 1). Stereographic analysis of bedding attitudes on the limbs of the fold indicates a horizontal fold axis trending N41W. This fold is spatially related to the intersection of two normal faults.

Another small fold occurs in a stream bottom 200 feet northeast of Locality 25. The axis of this fold has a plunge of 13° in a direction of N50W. This fold can also be related to movement on nearby normal faults.

There is a closely spaced (six inches) rectangular joint system in the lower coarse arkosic member. The joint system is well developed and ubiquitous, and gives the exposures of arkose an appearance of having columnar jointing. The "columns" of arkose tend to fall away from the main outcrop during erosion, which gives the lower arkose a "shattered" appearance.

Joint sets are also abundant in the Abo siltstones of the upper member. In fact, many of the exposures of the siltstones are joint faces coated by drusy calcite which obscures many of the primary sedimentary structures. The bisectrix of the acute angle of a joint set gives the direction of the greatest principal stress (Price, 1966). One joint set from the Abo siltstone was measured and gave a greatest principal stress direction of N15W, and a corresponding least principal stress direction of N75E.

It is expected that an east-west least principal stress component would be produced during the formation of the north-south trending Rio Grande Graben and associated normal faults.

Structural History: A. Rejas (1965) studied the geology of the Cerros de Amado region which includes the study area under consideration in this thesis. He observed two high angle normal fault systems. The first fault system has an average trend of N40E, and was probably formed during the Late Cretaceous or Paleocene. This tectonic event is widely known in the western United States and is referred to as the Laramide Orogeny. All the faults in the study area, except one, were probably formed during this tectonic episode. Rejas (1965) felt that many of the small folds in the Cerros de Amado region were formed shortly after or during the Laramide deformation. This is probably true also of the small folds spatially related to the faults in the study area.

The second period of normal faulting according to Rejas (1965) has a north trend and occurred from the Middle to Late Tertiary. These normal faults were caused by the same tensional forces that were forming the Rio Grande Graben. One fault in the Bursum Formation at the southern end of the study area (Plate 1) was probably formed during this episode. At least part of the joint sets were, also, probably formed during this episode.

CHAPTER 3: PETROGRAPHY AND X-RAY ANALYSIS

Procedures:

A total of 40 thin sections (fifteen of siltstone, seventeen of calcilithite, five of arkose and three of mudstone) were analyzed according to standard petrographic procedures (Folk, 1974). Point counts (Tables 1 and 2) were made on a small number of typical samples of arkose and calcilithite to give some statistical confidence to the visual percentage estimates made for the bulk of the thin sections. Grain diameters were measured directly from the thin sections by ribbon counts of 30 to 40 grains, or in the case of the larger grains, by averaging direct thin section measurements. Two of the thin sections of calcilithite were stained with Alizarin Red solution to distinguish between dolomite and calcite.

The petrographic data was supplemented with X-ray diffraction analysis on nine samples of mudstone, two samples of arkose, six samples of siltstone and one of calcilithite. The samples selected for X-ray analysis were crushed in a jaw crusher, then pulverized in a disk pulverizer. Samples still too coarse after this procedure were ground in a ball mill using porcelain balls. The whole rock samples were then pressed into Bakelite tablets by the application of two tons of pressure for 5 minutes. Samples of the Abo mudstone were further analyzed for their clay mineralogy by the following sedimentation technique.

Approximately 25-30 grams of pulverized samples were placed in a beaker with 100 ml of distilled water and stirred until completely in suspension. After a settling period of ten to fifteen minutes only clay size particles ($\leq 2\mu$) remain within the upper five mm due to differential settling velocities. The upper five mm of clay and water is drawn off by an eye dropper or pipette and placed on a glass slide and allowed to dry overnight. This sedimentation technique results in a parallel orientation of basal planes in layered clay minerals. The samples were run on a Norelco vertical diffractometer using a copper K_{α} source and a nickel filter.

Table 3 (at the end of this chapter) is a general summary of the results of the petrographic and X-ray analyses. Appendix A contains the classification systems used in this study.

Arkoses and Arkosic Conglomerates

The arkoses and arkosic conglomerates of the Abo Formation are found primarily in the lower member. A small bed of arkose occurs 100 feet above the base of the upper member interbedded with the siltstones of the upper member.

In hand specimen the arkoses of the Abo Formation are glassy, coarse grained to pebbly, and reddish-brown (10R 3/4) to orange pink (10R 7/4) in color. Large (up to 25 mm in diameter), pink, euhedral, poikilitic, perthitic microclines are abundant - making up to 30% to 40% of any

hand specimen. Clear quartz, with a maximum diameter of 5 cm, makes up most of remaining composition of the arkoses.

The grain sizes of the quartz and perthitic microcline range from .25 mm to 5 cm. The average grain size in the thin sections is .75 mm, which is coarse sand. The grains are moderately sorted, sub-angular, and generally equant to sub-equant. Sub-angular equant grains of sodic plagioclase are generally smaller and less abundant than the quartz and feldspar.

Typically the long axes of the grains are randomly oriented, though in a few hand specimens the long axes of quartz or microcline pebbles are slightly imbricated. The grains primarily have line contacts with free margins ranging up to 50% in specimens with abundant (>20%) matrix and/or cement.

Composite grains of quartz are the most abundant constituent of the arkoses (see Figure 5). They range from 50% to 60% (Table 1) of the point counted samples. The grains are almost invariably composite with individual, blocky crystals within the grains having sutured and welded contacts. Individual crystals within the grains show slight to strong undulatory extinction, range in size from .03 mm to nearly 1 mm, and generally, have no preferred orientation of optical axes as judged from their random positions of extinction within a grain. Generally there is a bimodal crystal size distribution within the grains. Graphic intergrowths of microcline and quartz are common.



Figure 5. Photomicrograph of arkose (sample number 1) showing a composite grain of quartz with an inclusion of plagioclase. Note the dark matrix with silt-size quartz to the right of the composite grain. Mottled grain in lower left is microcline. Magnification: 35X, crossed nicols.

Sample Number Constituents	1		3		34		Mean %
	n	%	n	%	n	%	
Quartz (CG)	236	51	353	60	200	50	53
Plagioclase	5	1	30	5	8	2	2
Microcline	93	20	182	31	92	23	25
Mica	3	<1	6	1	0	0	1
Calcite cement	23	5	6	1	72	18	9
Matrix	102	22	9	2	28	7	10
Totals	462	100	586	100	400	100	100

Table 1: Point count data for arkoses in the Abo Formation: n = number of counts, CG = composite grains.

Pink, perthitic microclines are a common clast in the arkoses, ranging in abundance from 20% to 31%. The clasts of microcline are commonly euhedral, usually sub-angular, and range in size from .8 mm to 25 cm with an average close to one mm. The crystals show fair to excellent perthitic intergrowths and occasionally twinning on the albite law. Poikilitic textures are common with microcline enclosing crystals of plagioclase and quartz. Calcite is common as a late authigenic replacement of microcline. Fine-grained white mica (sericite) is also found as an alteration product of microcline.

Sodic plagioclase occurs as smaller, sub-rounded, sub-equant grains ranging in size from .1 to 1.5 mm with an average size of .5 mm. Plagioclase makes up from 1% to 5% of the total composition of the arkose. The composition of the plagioclase as measured by the extinction angles of the (010) twins range from An₇ to An₁₅ with a mean composition of An₁₂, oligoclase. Twinning on the albite law is common, and Carlsbad twins are less common. Most of the plagioclase is somewhat replaced or altered either by authigenic calcite or by sericite.

Muscovite is the most common accessory mineral. It occurs as .5 to one mm laths which are often tattered and bent. Muscovite occasionally occurs as inclusions in microcline or, in one sample, as a constituent of the composite quartz grains.

Small, rare (<1%) crystals (.2 mm) of zircon occur

as inclusions in microcline and quartz.

Small opaque grains (.05 mm to .1 mm) are common in the matrix. These opaque grains are mostly magnetite which has been oxidized to a fine clay-size hematite. In some cases the crystal form of the magnetite is still visible. Other less common opaque minerals which do not have the characteristic reddish-brown color in reflected light might be copper or iron sulfides. One sample (#4) contained traces of chalcocite visible only under a hand lense.

The amount of matrix in the arkoses is variable. Point count estimates (Table 1) range from 2% to 22%. For example, sample number one of arkose contains 22% of matrix. The matrix is predominantly a dark reddish brown mass of nearly opaque hematite with approximately 20% of medium silt-sized, sub-angular quartz. Clay minerals and magnetite also occur. Approximately 5% of sample number one is a blocky sparite cement which surrounds grains of quartz.

The matrix in other samples of arkose is similar in composition and texture to sample number one. In other samples the calcite cement ranges from 1% of the total composition up to 18% of the total composition. In a few samples calcite cement replaces microcline along cleavage planes.

Anomalous results were obtained when pulverized whole rock samples of the arkose were analyzed by X-ray diffraction.

No peaks were obtained for the potassium feldspars, whereas fairly good peaks were obtained for albite. To further check on these anomalous results, a single crystal of the apparent microcline was chiseled out of the rock, pulverized and mounted in a Bakelite capsule. Diffraction analysis of this mount indicated a plagioclase with a composition of albite and no potassium feldspar whatever.

The limited X-ray diffraction data suggests that at least some of the microcline has been albitized by a diagenetic event. The introduction of sodium rich ground waters into the Abo Formation may have been the cause of the suggested alteration to albite. These waters are thought to have been derived from the dissolution of overlying evaporite beds in the Yeso Formation (R. E. Beane, 1974, oral communication). The majority of the knobby calcite which occurs along joints, fractures and faults may also have been introduced at this time. This event has been hypothesized (Beane, 1974) to have occurred during the Late Tertiary and may have been coincident with the normal block faulting that caused the formation of the Rio Grande Graben.

Siltstones

Above the basal arkoses, the Abo Formation consists primarily of dark reddish brown (10R 5/4) to pale reddish brown (10R 3/4) beds of quartzose siltstone and mudstone.

The siltstones show no preferred orientation of

grains in thin section. They are almost monomineralic in composition and have a mean grain size of 0.038 mm (coarse silt) with a range of 0.01 mm to 0.10 mm. The siltstones are generally well sorted. In a few thin sections a density/size sorting defines lamination; the laminations containing abundant hematite and hematized magnetite have quartz grains which were usually finer grained (0.03 mm - 0.06 mm) than the adjacent laminae which have negligible iron oxides and coarser quartz grains (0.08 mm - 0.1 mm). The quartz grains are generally sub-angular, occasionally sub rounded, and generally blocky and equant in shape.

Quartz comprises 80%-95% of the mineral composition of the siltstone. No composite grains were found in the siltstones as opposed to the arkoses which have predominantly composite grains. This may be due to the fine grained character of the siltstones. The individual crystals of quartz in the composite grains in the arkose are approximately the same size as the quartz particles in the siltstones. Most quartz grains show a slight to moderately undulatory extinction.

Hematite and magnetite occur in intimate association. The hematite commonly occurs as opaque to translucent circular "blobs" surrounding euhedral crystals of magnetite. This pair of minerals comprises anywhere from 3% to 40% of the siltstones (see Figure 6).

Sodic plagioclase occurs as a rare accessory mineral

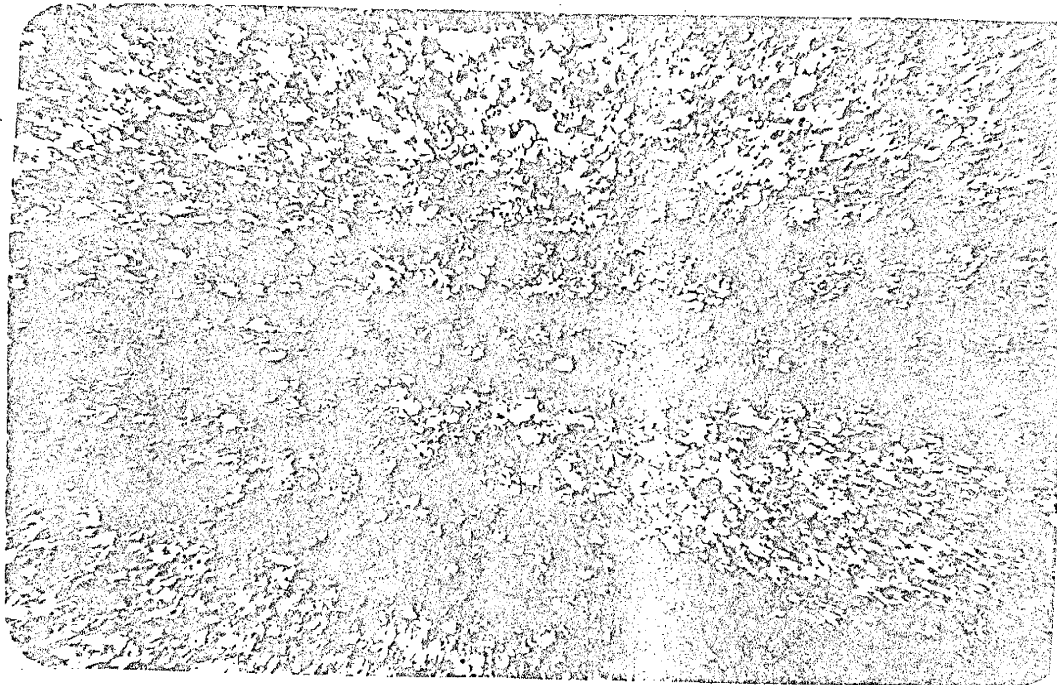


Figure 6. Photomicrograph of siltstone showing concentrations of hematite and opaque magnetite along laminations. Magnification: 35X, ordinary light. Sample number 31.

generally in concentrations of less than 1%. The equant-blocky, subangular to subrounded grains are usually altered to sericite and calcite. The grains range in size from 0.020 mm to 0.060 mm. Only one grain was sufficiently large and unaltered to estimate the composition of the plagioclase by the measurement of the extinction angle of the (010) twins. The grain in question has a composition of An₁₆, oligoclase.

Laths of muscovite ranging from 0.1 mm to 0.2 mm are also a rare accessory mineral. These laths are commonly bent and distorted around surrounding quartz grains.

Small (0.01 mm) crystals of zircon and hornblende occur in trace quantities in one thin section (sample number eleven).

Calcite occurs either as a sparry cement or as a later replacement of detrital minerals which may comprise up to 80% of a thin section, but a composition of less than 10% is most common. Sparry calcite is also found as a filling in burrow tubes.

In some siltstones the cement is composed entirely of hematite with rare local patches of micritic calcite. Cements of sparry calcite and hematite are the most common for the siltstones. Occasionally hematite occurs as elongate laths 0.1 mm to 0.3 mm in length which may represent replacement of an unstable mica, possibly biotite. Hematite is also found as a thin stain on most quartz grains in the siltstones.

Reduction spots ranging in size from one cm to 25 cm in diameter are common throughout the siltstones and mudstones. These spots are circular in cross section, have a pale green color (10G 6/2) and often contain manganese dendrites. A small grain of chalcocite was found in a reduction spot in sample number 20.

The reduction is presumably caused by a small amount of organic material which has a definite "sphere of influence", for actually the reduction spots are reduction spheres. These small zones of reduction create a favorable environment for the precipitation of Cu_2S , chalcocite, from solutions containing Cu^{++} and $\text{SO}_4^{=}$ ions (LaPoint, 1974).

X-ray diffraction of 6 samples of siltstone indicates the following mineralogy: quartz, sodic plagioclase, dolomite, calcite, and hematite. Dolomite may occur in the matrix as fine grained material too small to be noted by petrographic examination.

Granular Siltstone

Granular siltstone occurs only in Unit G within the Abo Formation. The granules which make up 50% of the rock are 2-3 mm in size, sub-rounded to sub-angular, equant to tabular in shape and are composed of quartzose siltstones with hematite-clay cement and authigenic calcite. About one-fourth of these clasts have a hematite cement. The siltstone clasts are very similar to the previously described siltstones and calcareous siltstones.

The matrix is composed of 40% to 70% silt-sized sub-angular quartz grains with 30% to 60% of euhedral sparry calcite.

Mudstones

The dark reddish brown (10R 5/4) mudstones are poorly exposed.

Thin sections of mudstone appear to be mostly a mixture of opaque to translucent hematite, rare magnetite, calcite and terrigenous clay minerals with 10% to 20% of silt-sized quartz grains.

X-ray diffraction of nine samples of mudstone indicates the following mineralogy: quartz, sodic plagioclase, hematite and minor dolomite and calcite. Two oriented slides were prepared (using the sedimentation technique outlined in the beginning of this chapter) in order to analyze the clay mineralogy. The peak heights on the diffractograms were measured so that relative percentages of clay minerals could be computed using the methods outlined by Johns et al. (1954). Kaolinite is the most abundant clay mineral, composing one-third to one-half of the clay minerals. The amount of chlorite is variable from none to one-half of the clay minerals. Illite/smectite mixed layer clays compose approximately one-tenth of the clay minerals. Illite also may occur without mixed layers in concentrations up to two-fifths of the clay minerals.

Calcilithites:

The average size of the clasts within the calcilithites is 3 mm ranging upward to 3 cm. In any given specimen the clasts are well to moderately sorted. The grain size distribution of the clasts is typically unimodal, though one sample (#52c) has a bimodal size distribution. Locally the clasts within the calcilithites are poorly imbricated (see Figure 7).

Moderate packing of the clasts is the most common texture, though tightly packed clasts occur less commonly. Most of the rocks studied had clasts with floating margins. Line and point contacts between clasts are found in samples with tight packing and correspondingly lesser amounts of matrix. Occasionally there are concavo-convex contacts between clasts which show neomorphic growths of sparry calcite (Folk, 1965).

The matrix between clasts is generally variable, commonly the matrix is composed of silt sized quartz, sparry calcite, hematite and clay minerals. The amount of matrix ranges from 28% to 37% with an average of 31% (see Table 2). Quartz generally makes up 30% to 60% of the matrix, but ranges from 80% to a trace. Medium silt sized particles of plagioclase occur in trace amounts in some samples. Calcite, which can make up to 90% of the matrix, occurs either as a sparry blocky mosaic or as micritic patches of unknown origin mixed with hematite and clay minerals. The blocky sparry calcite commonly



Figure 7. Photomicrograph of calcilithite (sample 52c). Dark clasts are micrite, except for mottled clast in the right hand corner which is microsparite. Note silt-size quartz in matrix. Magnification: 35X, ordinary light.

Sample Number Constituents	28		49		52c		54		Mean %	Clast type
	n	%	n	%	n	%	n	%		
Micrite	307	51	266	59	283	50	118	14	43	1
Hematized Micrite	84	14	26	5	74	13	134	16	12	1
Siltstone	42	7	12	3	-	-	25	3	3	2
Calcareous Siltstone	-	-	-	-	-	-	118	14	4	2
Sparite	-	-	-	-	tr.	tr.	202	24	6	3
Matrix	168	28	148	33	209	37	243	29	32	-
Total	601	100	452	100	566	100	840	100	100	-

Table 2. Point count data for clasts in the calcilithites of the Abo Formation: n = number of counts, tr. = trace amounts; Clast type refers to classification in the text. No clasts of microsparite (type 4) were found in the point counted samples.

appears as a neomorphic growth on the boundaries of the associated clasts of micrite (Figure 8).

There are 4 major types of clast lithology within the calcilithites: 1) micrite, 2) siltstone, 3) sparite, and 4) microsparite.

The most abundant type is micrite, which averages 55% of the clasts. In Table 2 this type has been divided into micrites with a pinkish to gray color and hematized micrites with a dark reddish brown color. Some biomicrites may also be present in this type. The clasts are sub-rounded to rounded. The grain shape is commonly irregular, but equant to sub-equant. The irregular shape is caused by breakage of the clast during transportation. The texture is mottled, and internal laminations within the micrite clasts have been disturbed.

Within the micrites there is from less than 1% to 10% of silt-sized, sub-rounded quartz and plagioclase.

Lunate-shaped fillings and veins of sparry calcite are common in the micrite. The lunate-shaped fillings of calcite might be recrystallized shell fragments.

Neomorphic growths to sparite and microsparite are common along clast edges (see Figure 8). The degree and form of hematization in the micrite clasts is variable.

Staining two of the calcilithites with Alizarin Red indicates that the micrite clasts are composed of calcite rather than dolomite.

The second major type of clast lithology are the

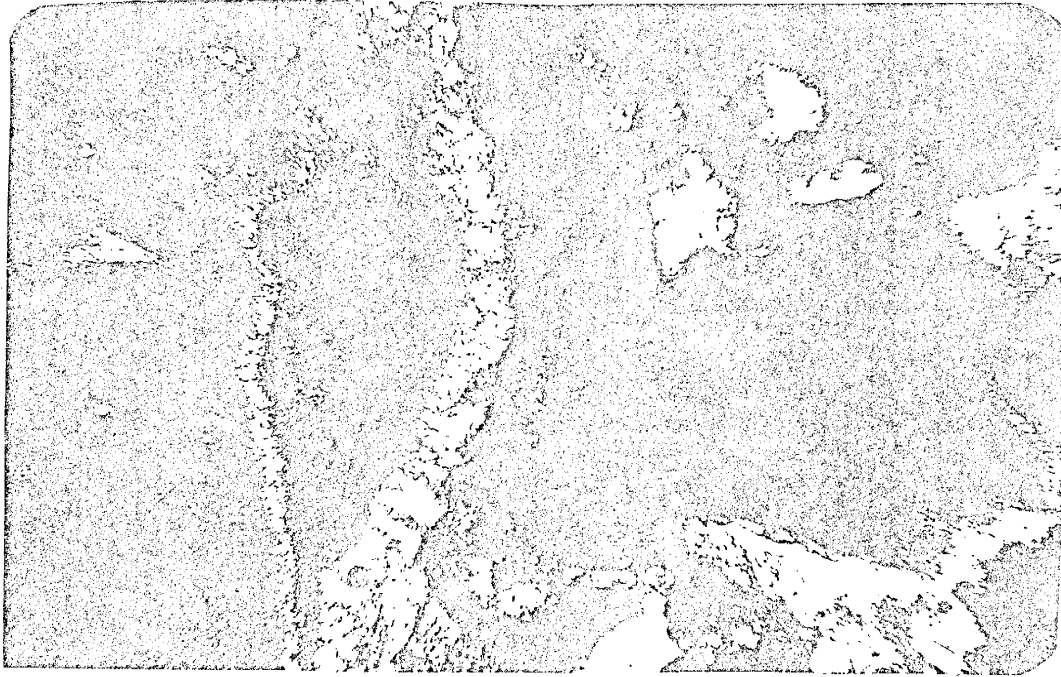


Figure 8. Photomicrograph showing neomorphic growth between two micrite clasts in a calcilithite (sample 36A). Note silt size quartz grains in clast to the left. Magnification: 35X, crossed nicols.

siltstones which comprise 7% of the calcilithite clasts (Table 2). One variety of siltstone is composed of 50% to 80% of medium to coarse silt-sized, sub-angular quartz with moderate to strong undulatory extinction. Plagioclase of the same size and shape is found in trace amounts. The clastic grains are set in a dark reddish-brown hematite and clay matrix. The clasts of siltstone average 1 mm to 2 mm in diameter, but range upward to 4 mm. They are subrounded to rounded, equant to tabular with irregular boundaries. Sparry calcite occasionally occurs as a replacement product.

The second variety of siltstone is similar in all respects to the quartzose siltstones described above, but contain up to 80% of microsparite calcite replacement. These clasts should be termed calcareous siltstone. One sample shows a progressive replacement of quartz by calcite.

The third type of clasts within the calcilithites is composed of sparite. These clasts occur as well rounded to rounded, equant to occasionally tabular shaped granules with an average diameter of 3 mm and constitute from trace amounts to 24% of the composition of the calcilithites (see Table 2). Approximately one-third of the sparite clasts are composed of 90% rhombohedral crystals of dolomite and 10% of a reddish-brown hematite and clay cement. The other two-thirds of the clasts are composed of a blocky mosaic of sparry calcite with very little cement.

The fourth and last type of clast is composed of

pinkish-gray microsparites. Clasts of microsparite are either absent or comprise about 5% of the calcilithite. Quantitative point count data for the microsparite clasts is not available because the thin sections selected for point counts (Table 2) do not contain any clasts of microsparite. Only about one-fourth of the calcilithites contain clasts of microsparite. The clasts are subrounded, have an equant to sub-equant shape and an average grain size of 2 mm.

Diagenesis

The earliest and most widespread diagenetic event in the Abo Formation was the hematization of iron-bearing minerals. The effects of this event are seen in the distinct dark reddish-brown color of the Abo Formation.

The petrographic evidence for this early diagenetic event is: 1) "blobby" haloes of translucent to opaque reddish-brown hematite replacing detrital grains of opaque, rhombic minerals, probably magnetite, 2) reddish-brown hematite replacing lath-like detrital particles of biotite. The detrital origin of both the biotite and magnetite is shown by their occurrence along laminations and cross-laminations within a given sample, 3) hematite coatings are commonly absent at contacts between grains in the arkoses and in the siltstones implying formation after deposition, and 4) one thin section (53A) contains penecontemporaneously ripped-up clasts of siltstone.

The laminations in the clasts of siltstone, which are discordant with laminations in the surrounding rock, have reddish-brown haloes of hematite surrounding detrital grains of magnetite. This suggests (but does not prove) an early age of hematization.

There have been several theories concerning the origin of red-beds, such as the Abo Formation, and how the existence of red-beds can be used as a paleoclimatic indicator. These theories can be divided into two main classes (Walker, 1967, 1974): 1) the detrital origin - this theory states that the hematite is formed in lateritic soils in moist tropical or sub-tropical climates and then either remains in situ and preserved as an ancient soil profile or the material is transported out of the laterite soil-forming area to a distant basin of deposition, 2) the authigenic origin - this theory states that the hematite forms after deposition owing to in situ alteration of iron-bearing detrital grains in an arid climate. T. R. Walker (1967, 1974) in two papers on the origin of red-beds gave convincing evidence that red-beds can form diagenetically by the intrastratal alteration of iron-bearing detrital grains, such as hornblende, biotite and magnetite. The alteration proceeds by the formation of ferric oxide in a favorable Eh-pH environment. Walker found diagenetic red-beds forming in a modern arid to semi-arid environment in Baja California (Walker, 1967) and also in a modern moist tropical environment in Puerto Rico and the

Orinoco Basin in South America (Walker, 1974). Walker concludes by stating that there is no way to distinguish tropical and arid red-beds in the ancient record and that red-beds should not be used as paleoclimate indicators.

Possibly during or shortly after the hematization sparry calcite cement was formed only in the lower arkose and may have replaced some of the matrix. Calcite also occurs as an alteration product of microcline and plagioclase in the lower arkoses, though this event may have occurred later than the formation of the cement. Most of the micritic material in the matrix of the siltstones, arkoses and calcilithites is of unknown origin.

Authigenic sparry calcite was introduced in a later diagenetic stage by neomorphic growth (Folk, 1965) of borders and edges of clasts of micrite in the calcilithites.

The last diagenetic event was the suggested albitization of the microcline in the arkoses by alkaline ground waters. This event has been postulated to have occurred in the Late Tertiary (Beane, 1974, oral communication).

Source Rocks

The lower arkoses of the Abo Formation contain composite grains of quartz with moderate to strong undulatory extinction, bimodal crystal size distribution, and sutured boundaries between the individual crystals. A genetic classification of quartz types by P. D. Krynine (in Folk, 1974) and a partly empirical, partly genetic classification

by Folk (1974) were both used to classify the quartz fragments as to possible source rocks. The presence of composite grains, the amount of undulatory extinction, and the size distribution of crystals in a composite grain (Blatt et al., 1972) can be used to discriminate between plutonic, low rank metamorphic, and high rank metamorphic rocks. Blatt and Christie (1963) studied the relationship between undulatory extinction in quartz from igneous and metamorphic rocks and provenance, and concluded that undulatory extinction is meaningless in provenance studies. However, Basu et al. (1974) concluded that the measurement of apparent extinction angles in quartz on a flat stage proved to be useful in discriminating between plutonic and metamorphic quartz.

The occurrence of quartz as composite grains with a bimodal crystal size distribution and moderate undulatory extinction are strong evidence for a recrystallized metamorphic rock as a source. Because there is not a strong alignment of individual crystals with the grains, it can be surmised that strong foliation is not a primary characteristic of the source rocks.

The large, pink, often euhedral microclines are characteristic of coarse grained igneous and metamorphic rocks with a "granitic" composition. The small amount of sodic plagioclase and muscovite indicates a source rock of "granitic" composition. Due to the size of the quartz, and the size and euhedral outlines of the microcline

a nearby source is indicated. The most likely composition of the source rock is "granitic". Metamorphism without a strong foliation is indicated by the moderate undulatory extinction and the lack of orientation of optical axes in the quartz composite grains.

The siltstones contain mostly quartz which is too fine grained to have many distinguishing characteristics. The quartz grains are similar in size and shape to the individual crystals within the composite grains in the arkoses. There is a possibility that the quartz grains come from the same type of source rock as the arkoses. Another equally possible source is sedimentary rocks of Pre-Permian age which contained silt or sand sized quartz grains.

Not enough information is available on the clay mineralogy throughout the Abo Formation to make a meaningful statement about the provenance of the clay minerals.

The calcilithites contain clasts of micrite, biomicrite, sparite, dolosparite and siltstone. The micrites and biomicrites often contain 5% to 10% silt sized quartz. The source rock of the calcilithites was probably a sequence of predominately carbonate rocks with interbedded clastic rocks, probably siltstone. There is a possibility that some of the siltstone clasts in the calcilithites are intraformational. A more specific discussion of source areas (provenance), as opposed to source rocks, is presented in Chapter 7 of this thesis.

Lithologic Types	Composition	Texture	Sedimentary Structures
Lower Arkose	<p><u>50%-60%</u>: Composite grains of quartz. Moderate undulatory extinction, graphic intergrowths.</p> <p><u>20%-30%</u>: Pink, commonly idiomorphic perthitic microcline. Poikilitic texture is common. Altered to albite.</p> <p><u>1%-5%</u>: Sodic plagioclase and muscovite.</p> <p><u>≈10%</u>: Matrix of silt size quartz, reddish-brown hematite, clay minerals. Some calcite cement.</p>	<p>Quartz and microcline are coarse sand to pebble size. Subangular. Sorting is moderate.</p> <p>Plagioclase occurs as medium sand-size grains.</p> <p>Grains have primarily line contacts.</p>	<p>Normal graded bedding</p> <p>Poorly defined cross-stratification.</p> <p>Poorly defined pebble imbrication.</p>
Siltstone	<p><u>80%-95%</u>: Quartz</p> <p><u><1%</u>: Sodic plagioclase and mica.</p> <p><u>15%-20%</u>: Matrix of hematite, calcite, magnetite and clay minerals.</p>	<p>Coarse silt size, sub-angular grains, well sorted.</p> <p>Distinct reddish-brown color</p>	<p>Planar lamination, cross-lamination deformed bedding, convolute lamination, ripple marks, tool marks, plant casts, vertebrate tracks, mud cracks, rain drop impressions, and burrows.</p>

Table 3. Summary of Lithologic Types in the Abo Formation

Lithologic Types	Composition	Texture	Sedimentary Structures
Mudstone	<p>Quartz, plagioclase, microcline, hematite, some calcite and dolomite.</p> <p>Kaolinite, chlorite and illite/smectite mixed layer clays.</p>	Silty mudstone.	Burrow tubes, plant root networks, and calcareous concretions.
Calcilithites	<p><u>Clasts</u></p> <p>1) 30%-60%: Pink-gray micrite and hematized micrite. Possibly some biomicrite. Micrites contain 5%-10% silt-size quartz.</p> <p>2) 3%-17%: Reddish brown quartzose siltstone with hematite and calcareous siltstone.</p> <p>3) ~8%: Sparite or dolosparite.</p> <p>4) ~5%: Microsparite.</p> <p><u>Matrix:</u> (20%-50%) Composed of silt-size quartz, hematite, calcite and clay minerals.</p>	<p>Conglomeratic texture.</p> <p>Clasts range from 1 mm to 8 mm, mean at 3 mm, generally rounded to subrounded, equant to tabular, well sorted.</p> <p>Grain contacts are mostly line contacts.</p> <p>Neomorphic growths common around clasts of micrite.</p>	<p>Lenticular beds to channel cut and fills.</p> <p>Rare pebble imbrication.</p>

Table 3. Summary of Lithologic Types in the Abo Formation (continued).

CHAPTER 4: THE DETAILED STRATIGRAPHY OF THE ABO FORMATION WITHIN THE STUDY AREA

Introduction:

The stratigraphy of the Abo Formation in the study area is similar to other stratigraphic sections of the Abo Formation in New Mexico described in the literature and/or studied on a reconnaissance level. The greatest differences between stratigraphic sections generally can be attributed to the variable lithology of the lower coarse units in the Abo Formation.

The Abo Formation within the study area can be divided into two informal members. The lower coarse arkosic member which consists of more than 60 feet of coarse and very coarse to conglomeratic arkose, reddish-brown mudstone, and a minor thin bed of mottled, nodular micrite.

The upper cyclic member consists of 515 feet of fourteen cyclic repetitions of gray pebbly calcilithite overlain by reddish-brown coarse siltstone overlain by reddish-brown mudstone (see Figure 9).

In the study area the Abo Formation is 575 feet thick, but there is a normal fault of unknown displacement which separates the lower member from the upper member (see Plate I and Figure 9). In Chapter 2 of this thesis it was estimated that the displacement is no more than 50 feet.

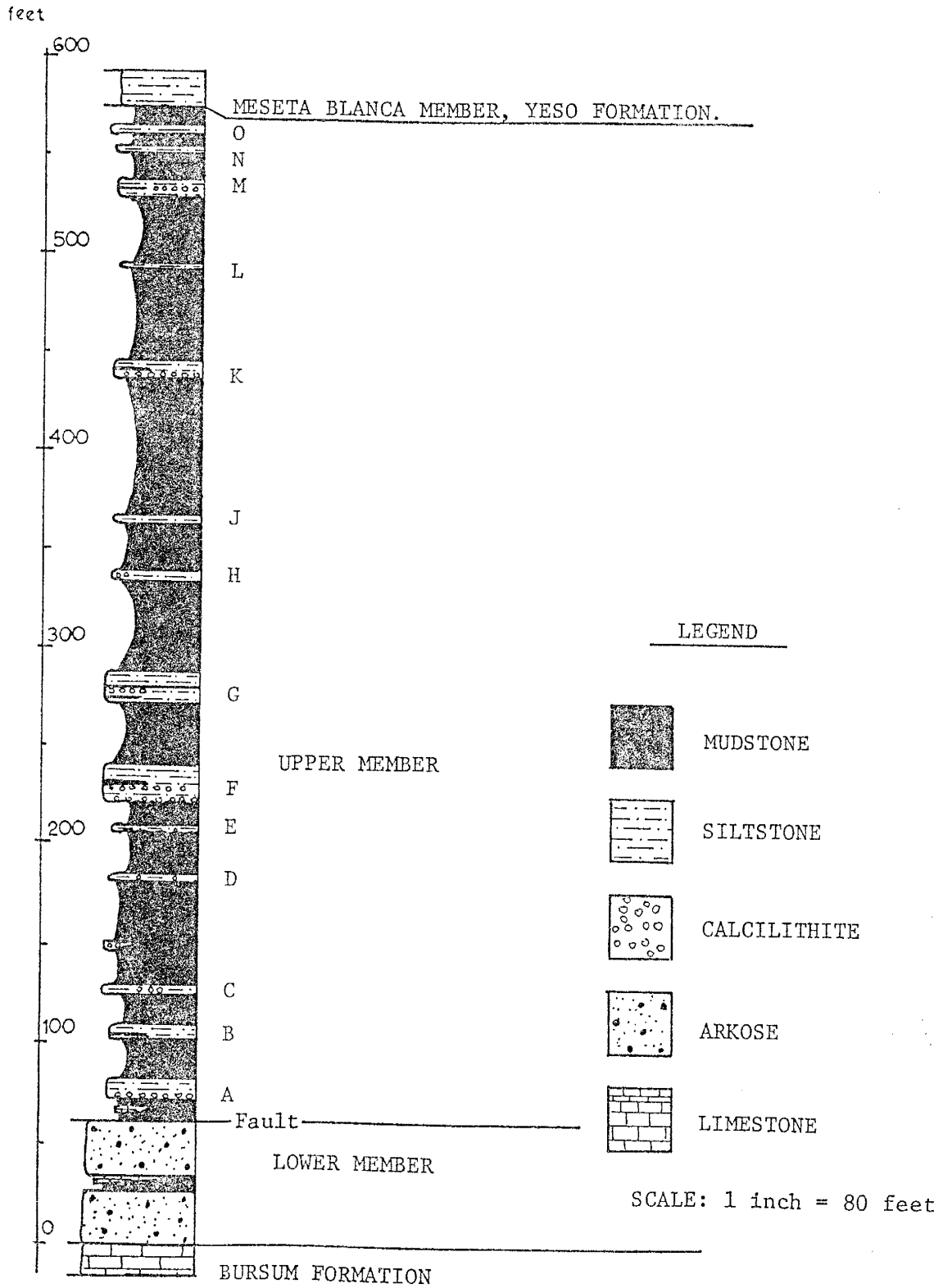


Figure 9. Stratigraphic section of the Abo Formation within the study area.

Lower Member

The lower member of the Abo is a reddish-brown to pinkish, very coarse to pebbly arkose with a medial six foot bed of reddish-brown mudstone overlain by a one foot thick nodular, argillaceous, mottled red and gray, micritic limestone. The lower member rests conformably upon gray micrites of the Bursum Formation. Sets of normal graded bedding approximately ten cm to fifteen cm in thickness are common in the lower member. Poorly developed pebble imbrication also occurs. Some poorly developed medium scale trough cross-stratification occurs, but these structures are difficult to describe because of the well developed, closely spaced rectangular fracture pattern in the lower arkoses and general homogeneity of the arkoses.

The mudstone in the lower member is similar to the reddish-brown mudstones of the upper member. Locally there are small "knobby" concretions of argillaceous micritic limestone. The concretions are generally five to ten cm in diameter. The limestone unit is truncated by the overlying arkose, indicating a minor unconformity between these units (see Plate 1).

Upper Cyclic Member

The upper member contains cycles of calcilithite overlain by siltstone overlain by mudstone.

Calcilithites: The lowest unit of a cycle is commonly a calcilithite with an irregular erosional basal contact.

Many of the calcilithite units are channel cut and fills. There is a variety of sizes, shapes and lithic types in the channel fills of the Abo Formation. Small channels such as the one exposed at Locality 2 near Unit C, are .7 m in width and .3 m in depth (Figure 10). In this particular example the channel has been cut into typical reddish-brown mudstone and is composed of a pebble calcilithite with poorly developed pebble imbrication. There are numerous other channel fills composed of calcilithite gravels within the mudstones of the Abo Formation but none so well exposed as the above described locality. Other channel deposits are commonly broadly lenticular in shape with an average length of 10 m and maximum thickness at the mid-point of .3 m to .7 m. Other channels are composed primarily of siltstone and commonly have a basal zone of calcilithite gravel. These channels range in depth from .7 m to approximately 8 m in thickness and have widths of up to 15 m (see Figure 11). The channels are typically cut into reddish-brown mudstone which at Locality 15 in Unit F shows evidence of bioturbation by burrowing organisms.

Calcilithites are also common in the siltstone and mudstone units of the upper cyclic member. They occur as thin to "knobby" lenticular beds.

Siltstones: The siltstones of the upper member are dark to pale reddish-brown in color except for a few local greenish-gray reduction spots. The siltstones form distinct

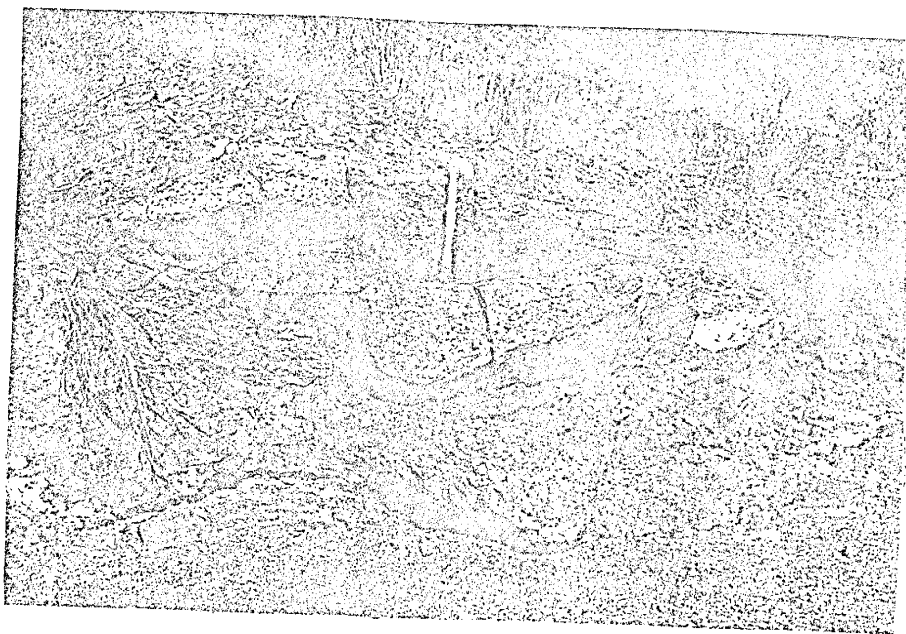


Figure 10. A view down the axis of a channel fill composed of calcilithite. Note steep side cut into mudstone on the left side. Current flowed into the photograph. Near Unit C, Locality 2.

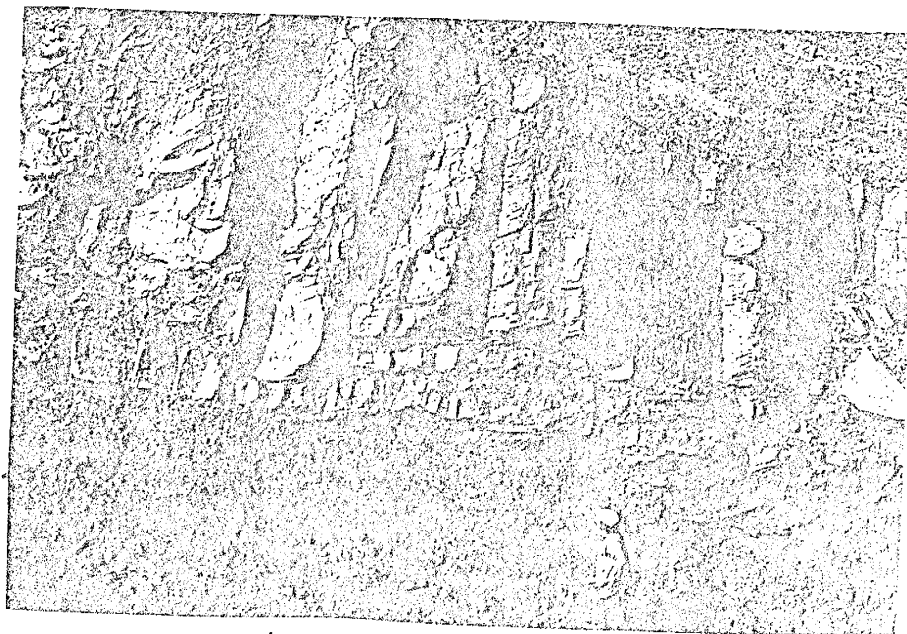


Figure 11. Channel fill composed mostly of siltstone, note lenticular calcilithite channel deposit to the right of the man, and pinching out of underlying mudstone beds. Unit F, Locality 23.

ledges ranging in thickness from 3 to 23 feet with an average thickness of 6 feet. The siltstones of the Abo Formation contain abundant and ubiquitous primary sedimentary structures such as small to large scale cross-stratification, ripple marks, ripple drift, planar lamination, tool marks, groove marks, plant casts, burrow tubes, casts of root networks, rain-drop impressions, mud cracks, channel fills, deformed bedding (planes of stratification have been broken and disrupted), convolute lamination (laminations are deformed and folded but remain intact), and tracks of small land vertebrates. The section immediately following is a more complete description of the primary sedimentary structures which were used for the paleocurrent analysis.

Small scale cross-lamination: Small scale cross-laminations are found in the siltstone units of the Abo Formation. Their stratigraphic positions within these units are variable, but they generally occur within the upper or middle portions of the units. The sets of cross-strata are usually trough shaped (Figure 12) with erosional bases, though tabular sets of cross strata with non-erosional bases are almost as common. The mean angle of inclination of fifty foresets of small scale cross-lamination is 20° with a range from 5° to 46° . The higher angles which are above the angle of repose ($\approx 30^{\circ}$) may indicate penecontemporaneous deformation of previously deposited cross-laminations. The angle of repose is variable itself within a sedimentary sequence,

and is a function of grain size and shape, and degree of saturation with water. The foreset strata are commonly concave upward. Sets of cross-strata range from two to four cm in thickness and cosets, though generally variable, range up to 40 cm in thickness. The laminations are marked by the accumulation of detrital grains of magnetite now altered to hematite.

Small scale cross-lamination commonly is formed by the down-current migration of ripples. This has been shown by laboratory investigations using flumes (McKee, 1965) and in modern fluvial deposits (Harms and Fahnestock, 1965). Small scale cross-lamination commonly occurs in the Abo Formation in the form known as climbing ripples or ripple drift. Climbing ripples in the Abo siltstones are generally composed entirely of climbing sets of lee side laminations with no preservation of stoss side laminations. This type of climbing ripple has been described and classified as Type A ripple drift (Jopling and Walker, 1968; Allen, 1973) (see Figure 13). Some of the climbing ripples in the Abo Formation are composed mostly of climbing sets of lee side laminae with thin, poorly developed stoss side laminae. This type of ripple drift is transitional between the above described Type A ripple drift and Type B ripple drift described by Jopling and Walker (1968). Type A and the transitional Type B climbing ripple lamination often occur vertically adjacent to each other in the Abo siltstones.

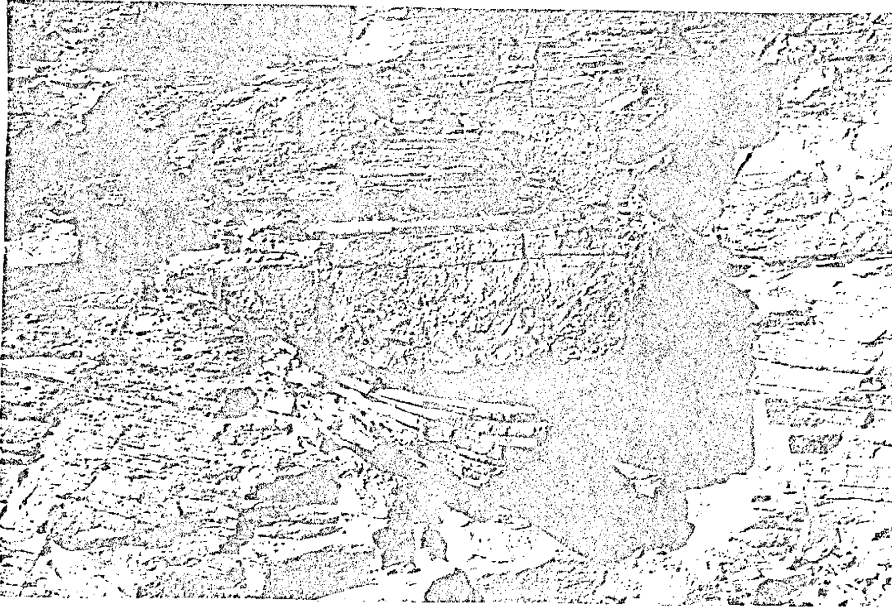


Figure 12. A view down the trough of small scale cross-lamination. Unit A, Locality 1. Pencil is six inches long.



Figure 13. Type A climbing ripples. Current from left to right. Unit F, Locality 20. Knife lies in the plane of true bedding.

Medium scale cross-stratification: Medium scale cross-bedding and cross-lamination commonly occur in the middle or lower portions of siltstone units in the Abo Formation. In Unit E medium scale cross-bedding comprises almost the entire unit in some places (Figure 14). The medium scale cross-stratifications occur in single sets ranging from .3 m to .8 m in thickness. The cross-strata are usually thinly bedded (1-4 cm) but are also thinly laminated. The strata are composed of alternating mudstone and siltstone beds. The mean angle of inclination of fifty foresets is 21° with a range from 4° to 36° . The sets of cross-strata are predominately tabular-shaped with planar cross-stratum, however, trough-shaped sets are also common (Figure 15). The lower contacts of the medium scale cross-stratification are not commonly exposed because of colluvial cover; however, one trough shaped set (Figure 15) shows an erosional lower contact.

Large scale cross-stratification: Large scale cross-stratification occurs within the Abo siltstones (Figure 16) and usually overlying channel fill deposits of calcilithite within the mudstone units. The height of the sets is variable but averages two m. The sets, which are generally trough-shaped, are composed of laminated or thinly bedded siltstone with occasional mudstone interbeds. The length of the exposed set shown in Figure 16 is approximately eight m. The mean angle of inclination of the foresets is 26° with a range from 2° to 43° .



Figure 14. Tabular-shaped medium scale cross-stratification. Hammer lies on foreset beds. Unit E, Locality 10. Current flowed from right to left.



Figure 15. Trough-shaped medium scale cross-stratification. Unit M, Locality 65.

calcilithite



Figure 16. Large scale cross-stratification. Unit E, Locality 10. Regional dip is 10° - 15° to the north (direction in which hammer is pointing). Foresets of large scale cross-stratification are dipping south. Note calcilithite at base of cross-strata.

Catenary and Linguoid Ripples: Catenary and linguoid ripple marks (Figure 17) occur only in the upper siltstone units of the Abo Formation (at Locality 21 in Unit G and Locality 60 in Unit H). The mean amplitude of the catenary and linguoid ripples is 2 cm. The wavelength varies from 9 cm to 15 cm. The mean angle of inclination on the lee side of the ripples is 20°. The ripple patterns are out of phase with each other - that is, the crest points of a line of ripples are not directly down current from the crest points of the ripples just upstream from it. Trough-shaped small scale cross-lamination is probably formed by the downcurrent migration of catenary and linguoid ripple marks.

Groove Marks: Groove marks occur on the tops of siltstone beds or laminations (as opposed to groove casts which are sole marks occurring on the bottom of beds) in Units A, D, and F. They often occur in groups and bear a remarkable similarity to each other in form and direction. Groove marks from Locality 45 in Unit D are .5 cm to 1.5 cm in length and are closely spaced with almost identical azimuths. These structures were cut into the underlying silt by some unknown tool which was carried by a current. Potter and Pettijohn (1963) list several possible engraving tools: algal anchor stones, sand grains, water logged wood, the bodies of soft bodied animals, shale fragments, skeletal debris or plant stems. Fossil plant stems are



Figure 17. Top view of catenary and linguoid ripple marks. Current flowed from right to left. Crest line has been accentuated by a black ink marker. Unit G, Locality 21.

abundant throughout the siltstone beds of the Abo Formation and are the most likely candidates for the engraving tool.

Tool Marks? Tool marks (?) of questionable origin were collected from two small (< 100 sq. ft.) localities, Locality 24 and 47, in Unit F. They are short linear structures with lengths ranging from 3 mm to 7 mm, closely spaced and thin (< 1 mm). They are similar in appearance to the groove, bounce, brush or skip casts figured by Potter and Pettijohn (1963).

Plant stems: Numerous fossil plants occur within the Abo Formation in all the siltstone beds. They seem to be more concentrated in the upper portions of the siltstone beds. Plant stems are variable in size but none greater than 40 cm occur in the study area (see Figure 18).

Symmetrical Ripple marks: Symmetrical ripple marks occur throughout the Abo Formation. These ripple marks have an average amplitude of 1.2 cm but range up to 2.5 cm. The mean wavelength is 12 cm but ranges up to 30 cm.

Within the study area the siltstone units are persistent along strike, that is, they do not thicken, thin, or pinch out appreciably except for Unit E, which pinches out in the central part of map area (Plate 1). Units F and G both pick up a medial reddish-brown mudstone unit in the western part of the map area (see Plate 1).

The vertical succession within a given siltstone unit is variable from one locality to the next, and from

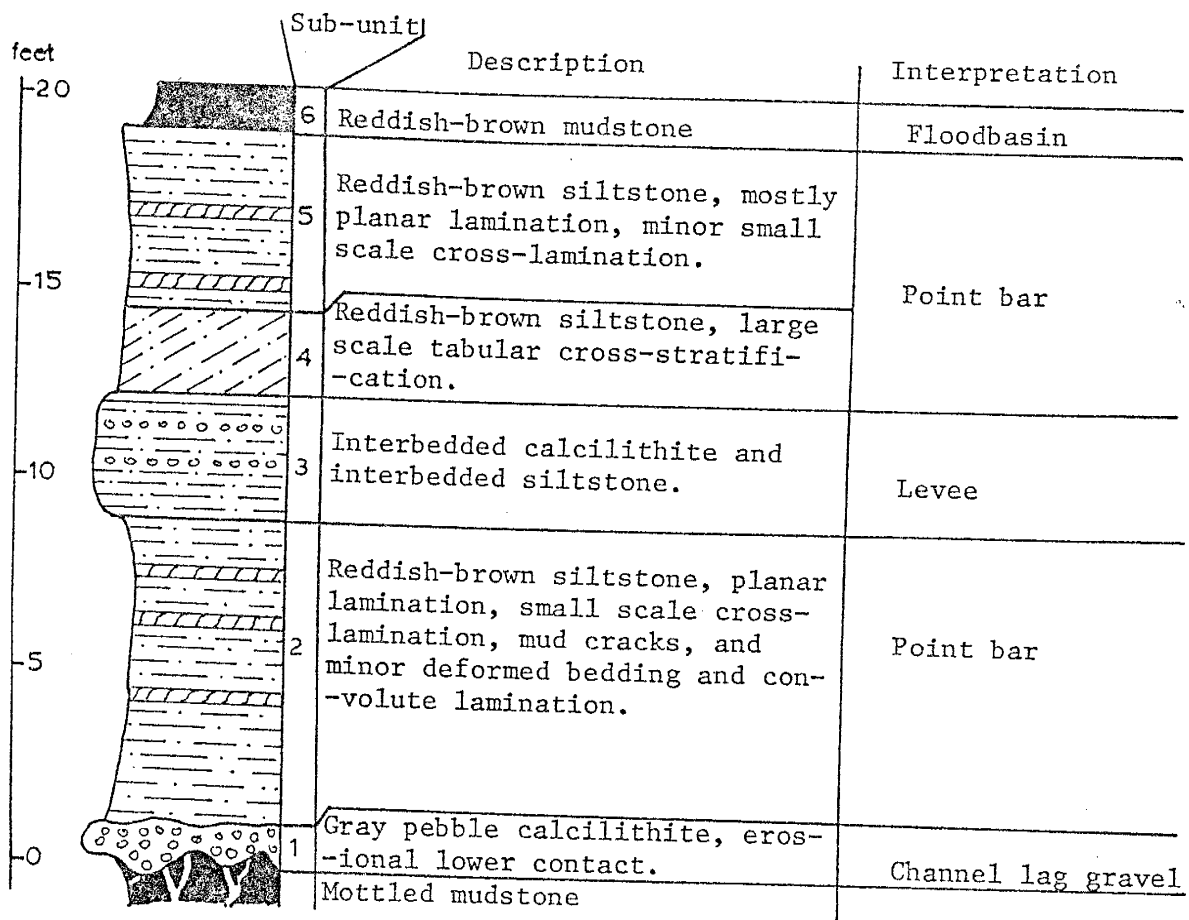


Figure 18. A fossil plant stem of the genus Walchia which is unusually complete. The current probably flowed from the top of the photograph to the bottom as indicated by the bending of the stem near the top (right side of photograph). Unit B, Locality 7.

one unit to another, as shown in Figures 19, 24, and 25. Figure 19 shows a detailed stratigraphic section of a single complete siltstone unit (Unit F). The lowest member of this unit, sub-unit one, is a gray to off-white pebbly calcilithite (see sample 52c - Table 2). The calcilithite overlies the mottled dark reddish-brown mudstone of the underlying cycle with an irregular erosional contact. The mudstones below the calcilithites contains anastomosing, branching and bifurcating greenish-gray reduction zones. These branching reduction zones may mark burrows of organisms, or they may represent a root network of land plants which grow upon the fine-grained muds (see Figure 20).

Sub-unit two is a sequence of reddish-brown, planar laminated to small-scale cross-laminated and ripple drifted coarse siltstone. Mud cracked bedding surfaces and zones of convolute lamination are also common in sub-unit two. The convolute laminations are mushroom-shaped antiforms with a height of ten to fifteen cm and a wavelength of 25 to 35 cm (see Figure 21). Sub-unit three is a three foot thick interval containing tabular to slightly lenticular interbeds of pebbly calcilithite, with irregular, erosional lower contacts and abrupt non-erosional upper contact, with interbeds of dark reddish-brown siltstone which has small scale cross-lamination and ripple drift cross-lamination (see Figure 22).

Sub-unit four is a 2.5 foot thick interval of large scale cross-laminated reddish-brown siltstone (see Figure



Legend for Figures 19, 24, and 25.

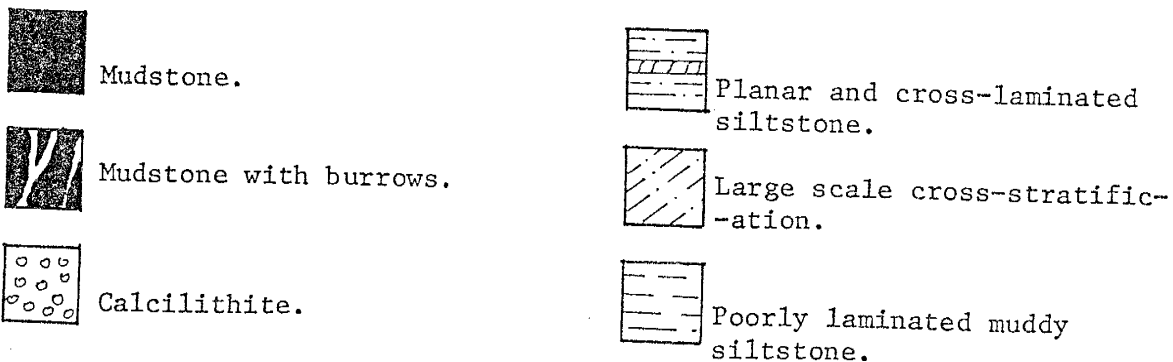


Figure 19. Stratigraphic section of Unit F, Locality 15.

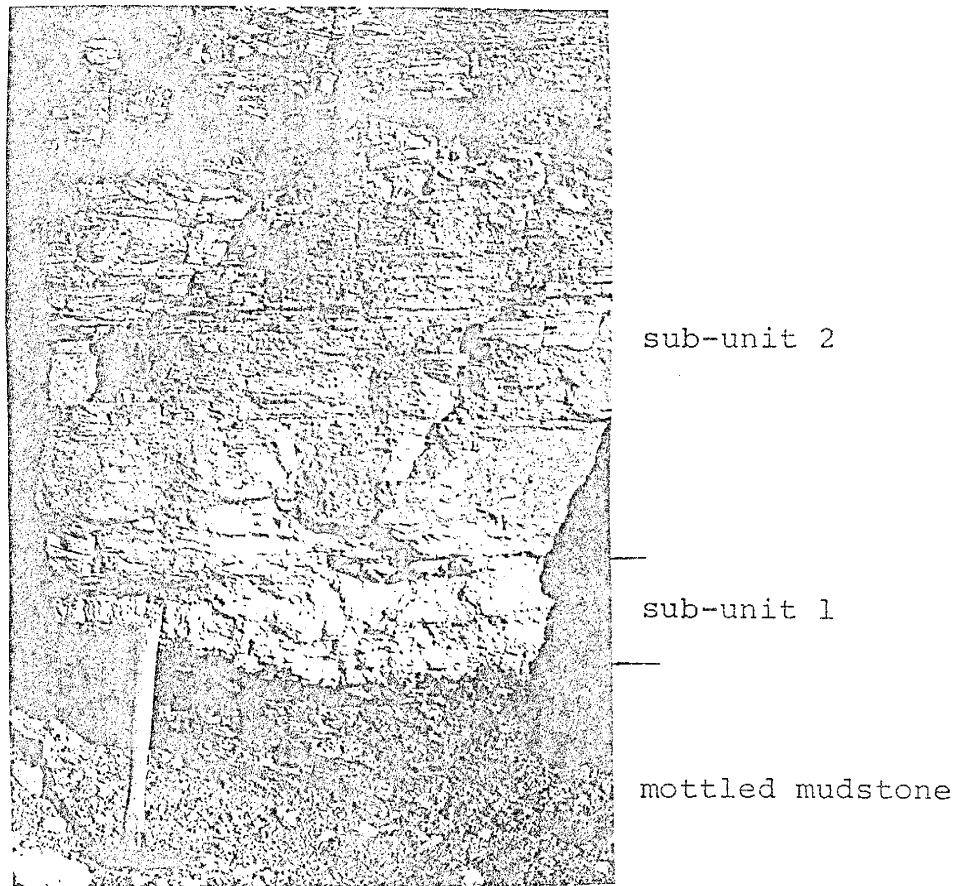


Figure 20. A partial cycle, Unit F, Locality 15. Lower sub-unit is a dark reddish-brown mudstone with mottled texture, overlain by a gray, off-white calcilithite (sub-unit one), overlain by reddish-brown, planar laminated siltstone and minor mudstone (sub-unit two). Hammer is approximately one foot long.

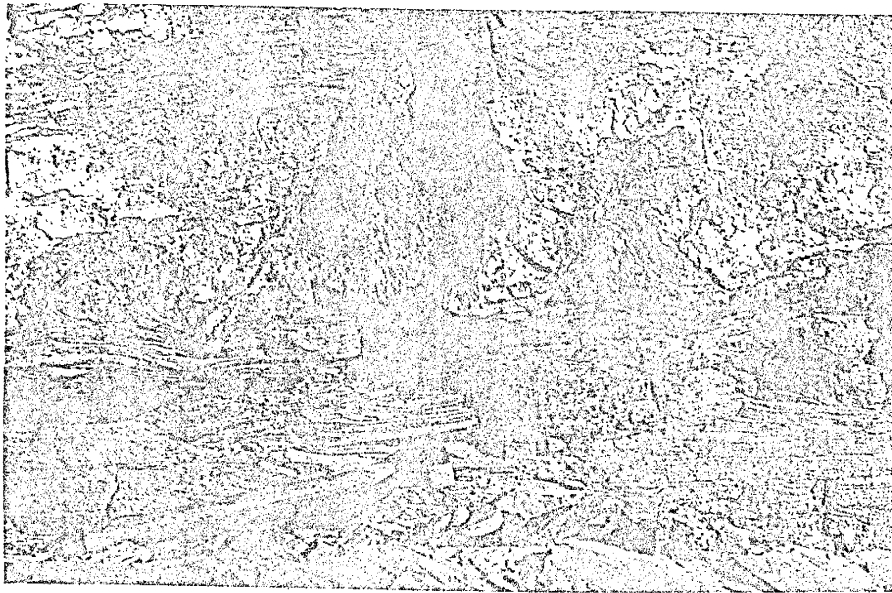


Figure 21. Convolute laminations, Unit F, Locality 15, sub-unit two. Hammer is approximately one foot long.

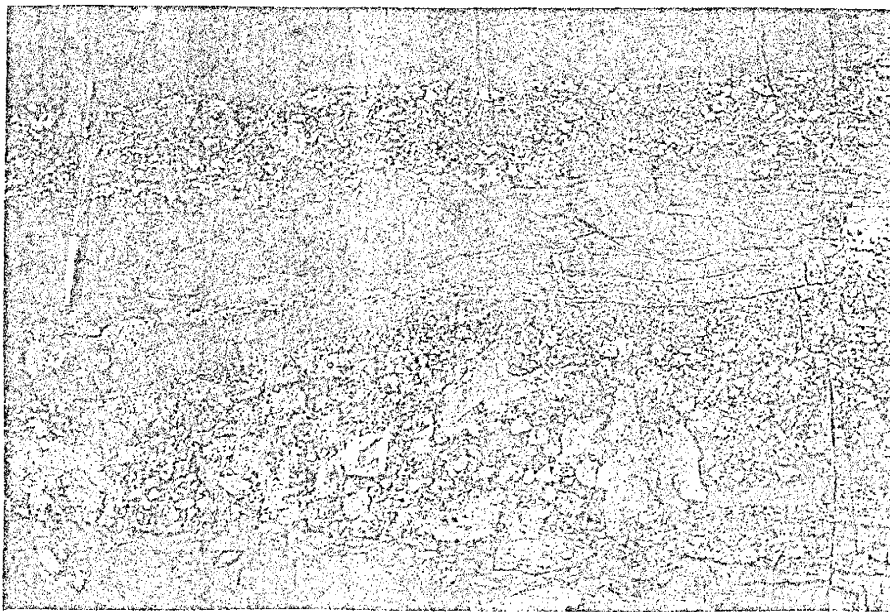


Figure 22. Interbedded calcilithite and siltstone, Unit F, Locality 15, sub-unit three. Note irregular, erosional lower contacts of calcilithite layers. Pencil is six inches long. Note, also, ripple drift cross-lamination in reddish-brown siltstone.

23). The cross lamination occurs in a single tabular set with planar foresets. The lower contact is covered at this locality.

Sub-unit five is predominately a planar-laminated reddish-brown siltstone with minor beds of convolute lamination, small scale cross-lamination and ripple drift cross-lamination.

A detailed stratigraphic section measured in Unit K at Locality 17 (Figure 24) shows a vertical sequence that is in many ways similar to that of Unit F. The basal pebbly calcilithite, sub-unit one, contains a few thin interbeds of small scale cross-laminated reddish-brown siltstone, and has an erosional lower contact. Sub-units two and four are poorly laminated, reddish-brown muddy coarse siltstones. Sub-unit three is the more typical well laminated reddish-brown siltstone.

A detailed stratigraphic section measured in Unit G at Locality 54 (Figure 25) shows some marked differences from the two previously described sections. Sub-unit one has a lenticular trough-shaped form similar to the basal sub-units in the other sections; however, it is composed of poorly to moderately well laminated reddish-brown siltstone. Above sub-unit one is a series of interbedded homogeneous reddish-brown mudstones and reddish-brown siltstone which is either poorly laminated or has small scale cross-lamination and ripple drift. Only sub-unit six contains a few thin lenses of granular calcilithite

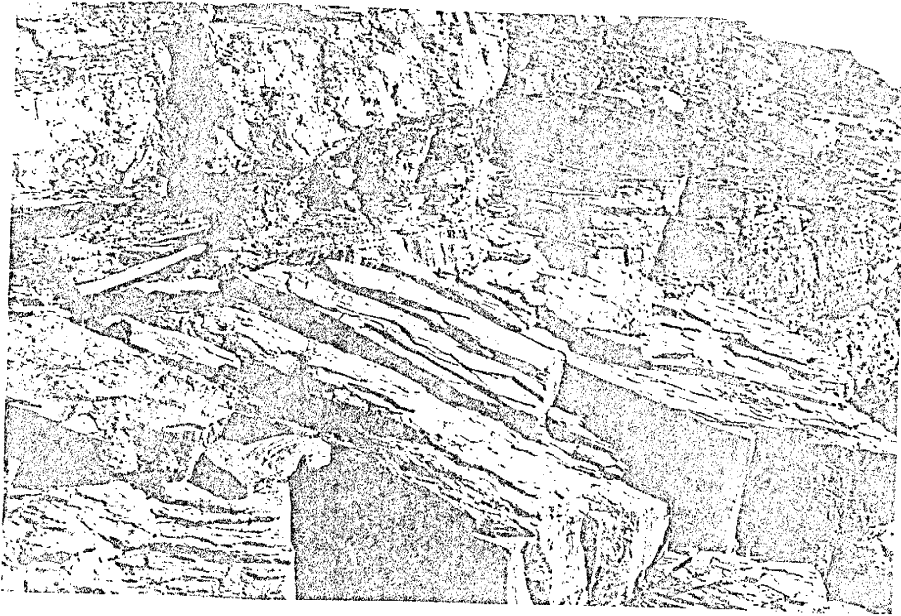


Figure 23. Large scale cross-stratification, Unit F, Locality 15, sub-unit four. Hammer is one foot long.

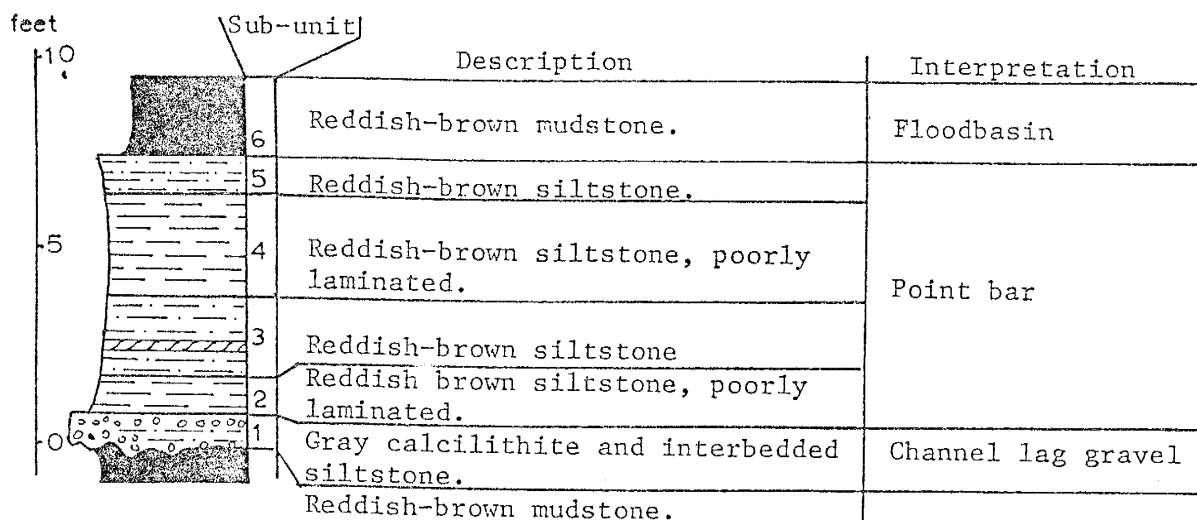


Figure 24. Stratigraphic section of Unit K, Locality 17.

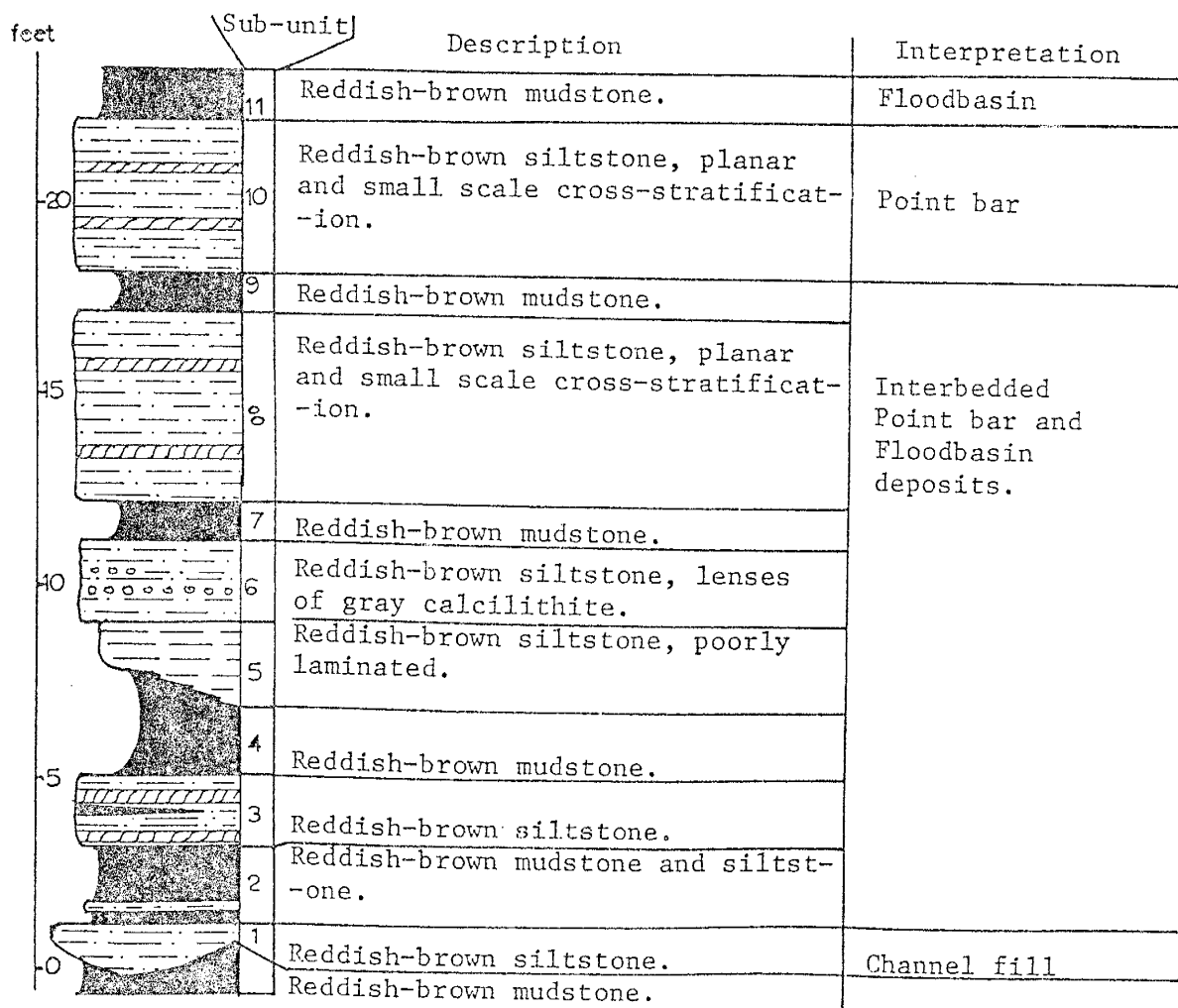


Figure 25. Stratigraphic section of Unit G, Locality 54 (for legend see Figure 19).

(see Table 2, sample no. 54, for clast composition), but is predominately reddish-brown siltstone.

Mudstones: The mudstones of the upper cyclic member of the Abo Formation are generally poorly exposed due to colluvial cover. The mudstones range in thickness from 5 to 70 feet with an average thickness of 28 feet. The mudstones are dark reddish-brown in color and commonly contain numerous "knobby" or thin lenticular beds of calcilithite (see Figure 11), which are approximately four to six inches thick and are laterally continuous from two to twenty feet.

Burrow tubes and plant root networks are common near the mottled tops of the mudstones where they are disconformably overlain by the calcilithites or siltstones of the next cycle.

CHAPTER 5: PALEOCURRENT ANALYSIS

Introduction:

The Abo Formation in the study area and throughout its area of exposure in New Mexico contains abundant and ubiquitous primary sedimentary structures. Many of the primary sedimentary structures in the Abo Formation, such as various types of cross-stratification, ripple marks, tool marks, and channel forms can be used to determine paleocurrent direction.

Procedure

A total of 365 paleocurrent measurements was collected from small to large scale cross-stratification, symmetrical ripple marks, catenary and linguoid ripple marks, plant stems, channel fills, groove marks and tool marks in the Abo Formation within the study area.

The orientation of primary sedimentary structures was measured by a variety of means depending on how much of their forms were exposed. Quite often the three dimensional form of sedimentary structures (such as tabular cross-lamination) was exposed, making direct measurement of the foreset strike and dip a simple and quick procedure. In areas of poorer exposures the apparent dip of the foreset beds was measured from two or more localities (usually intersected joint and fracture faces) to obtain by stereographic procedures the trend and plunge of the foreset beds. In other structures, such as trough cross-lamination and

channel fills, three or more attitudes were measured on a single cross stratum. The measured attitudes were then plotted on a stereonet to obtain the trend and plunge of the trough or channel axis. The exact procedures for the determination of plunge and inclination by stereographic methods are outlined in Phillips (1954). For a description of the type of measurement technique used for the varieties of sedimentary structures within the Abo Formation, see Table 4.

Before measured paleocurrent data from a formation can be utilized, the measured lineations and foliations must be rotated back to their original position at the time of deposition. In areas where there has been no past tectonic deformation and the true bedding remains essentially horizontal, the simple measurement of the lineation or foliation direction and plunge will give the true paleocurrent direction. In areas which have been tectonically deformed four factors must be considered: 1) the structural style of the folding which accompanied the deformation, whether flexural slip folding or shear folding (Ramsey, 1967); 2) the plunge of the fold axes; 3) the possibility of rotation of the beds around an unknown axis; and 4) whether the feature being measured is a foliation or a lineation.

The major deformational style within the study area is normal block faulting. This type of structural displacement can be envisioned as a rotation about a single horizontal axis which is parallel to the strike of the faults, which

Type of sedimentary structure	Abbreviation	How measured	Number of samples
Small scale cross-stratification	SXS	DM, RSN	114
Medium scale cross-stratification	MXS	DM, RSN	66
Large scale cross-stratification	LXS	DM, RSN	9
Ripple marks	RM	DM	62
Plant stems	PS	DM	45
Groove marks	GM	DM	22
Channel cut and fills	CF	RSN	8
Tool marks	TM	DM	39
TOTAL			365

Table 4. Types of primary sedimentary structures used for paleocurrent measurement in this thesis. DM = Direct measurement, RSN = Reduction on a stereonet. For classification schemes see Appendix A.

is generally east to northeast in the study area. There is no evidence of tectonically induced plastic deformation and flowage within the study area; therefore the dominant structural movements can be equated to simple flexural slip folding with horizontal fold axes.

Two minor folds, which involve no more than one siltstone bed and 20 feet of strike length, have essentially horizontal northwest trending fold axes. One other fold in the southeast corner of the area (Plate 1) has a plunging fold axis but it involves only about 40 square feet of area and is spatially associated with a normal fault. No sedimentary structures were measured in the area near the fault.

Beds involved in this type of folding, flexural slip with horizontal fold axes, can be restored to their original position by the standard methods of rotation on a stereonet (Potter and Pettijohn, 1963). For a more complete description and analysis of the effects of flexural slip folding with plunging fold axes, and the more complicated case of shear (or similar) folding on the orientation of sedimentary structures see J. G. Ramsay (1961).

Linear sedimentary structures, such as tool marks and the strike of ripple marks, are not as affected by changes in orientation caused by tilting or folding as are planar structures (foliations) such as the foresets of cross lamination (Potter and Pettijohn, 1963). In areas of low structural dip, such as the study area, the rotation of lineations back to original horizontality can be ignored. It

has been found that angular errors of only 3° are encountered when structural dip is neglected in areas with a structural dip of 25° (Potter and Pettijohn, 1963, Fig. 10-7). These types of computational errors are probably less than the measurement error.

Statistical Treatment

After the measured paleocurrent data were rotated back to their original position, they were statistically analyzed by the methods outlined by High and Picard (1963) and Potter and Pettijohn (1963). Paleocurrent data cannot be treated by standard statistical procedures which utilize data from a normal distribution, because the choice of origin for paleocurrent data or any other vectorial data is a critical decision and has an important affect on the results of the analysis. Another distribution, the circular normal, must be used because it allows analysis of vectorial data without regard to the choice of origin (Jones, 1968).

In order to simplify calculations and the graphical presentation of the paleocurrent data, azimuthal groups of 20° were used to classify the paleocurrent data. The vector resultant (a measure of the central tendency of the paleocurrent data - similar to the mean of a normal distribution) is calculated by the following equation:

$$\text{Tan } \theta = \frac{\sum n_o \sin \theta_i}{\sum n_o \cos \theta_i} \quad (5-1)$$

where,

θ = azimuth of the vector resultant

n_o = number of observations within a specific 20° interval

θ_i = azimuth of the mid point of the i th interval where i ranges from 1 to 18, based on a division of a 360° circle by 20° azimuthal groups. i.e. when $i=1$, $\theta_i=10$; $i=2$, $\theta_i=30$; $i=18$, $\theta_i=350^\circ$.

The magnitude of the resultant vector, R , is given by the following equation:

$$R = \sqrt{(\sum n_o \sin \theta_i)^2 + (\sum n_o \cos \theta_i)^2} \quad (5-2)$$

The magnitude of the resultant vector expressed in percentage terms, L , is given by the following equation:

$$L = \frac{R}{\sum n_o} (100\%) \quad (5-3)$$

When $L = 100\%$ there is no dispersal of data away from the resultant vector - all the data are in one 20° azimuthal group. Decreasing values of L indicate increasing dispersal (more variance) of the data about the resultant vector.

The data are plotted on rose diagrams with a 20° azimuthal grouping according to stratigraphic position and type of sedimentary structure (Plates 3A and 3B). Appendix B presents the paleocurrent data measured at each sample locality within the study area. Some of the paleocurrent data gathered in this study, such as the strike of the crests of symmetrical ripple marks and the strike of plant stems, cannot be treated as a vector with a unique direction and magnitude. These structures can be used to define a resultant strike line which is perpendicular to the current direction. At the onset of this investigation it was not

known that the strike of the plant stems would define a paleocurrent direction. Because the resultant strikes of plant stems and ripple marks within a given unit in the Abo Formation are close to being parallel, it is assumed then that the long axis (strike) of the plant stems are deposited by currents in a direction that is perpendicular to the current flow like the crests of symmetrical ripple marks. This observation is valid for the Abo Formation. It may or may not be valid for other formations. Resultant strikes are calculated using θ_i 's measured in only the northern hemisphere of the compass by equation (5-1). The "magnitude" or variance of the resultant strike line is calculated by equations (5-2) and (5-3). The strike line is then extended into the southern hemisphere of the compass by adding or subtracting 180° to the resultant strike line measured in the northern hemisphere. Strike line data are also plotted on rose diagrams (Plates 3A and 3B). Resultant strikes and their corresponding L value (eqn. 5-3) appear on the summed row and column of Plates 3A and 3B.

Test of Significance

There are numerous statistical methods available for the evaluation of the level of significance of data derived from a circular normal distribution, such as paleocurrent data (Potter and Pettijohn, 1963). The sums of all the types of sedimentary structures (top row on Plate 3B) with $\Sigma n_o \geq 10$ have been evaluated for their level

of significance by a graphical presentation of the Rayleigh test (Curry, 1956) in Figure 26. The diagonal lines on the log-log graph of Figure 26 represent the level of significance evaluated by the following equation:

$$p = e^{(-L^2n)} (10^{-4}) \quad (5-4)$$

where p = probability of obtaining a greater vector magnitude by pure chance combination of random measurements

L = the magnitude of the resultant vector expressed as a percent (eqn. 5-3)

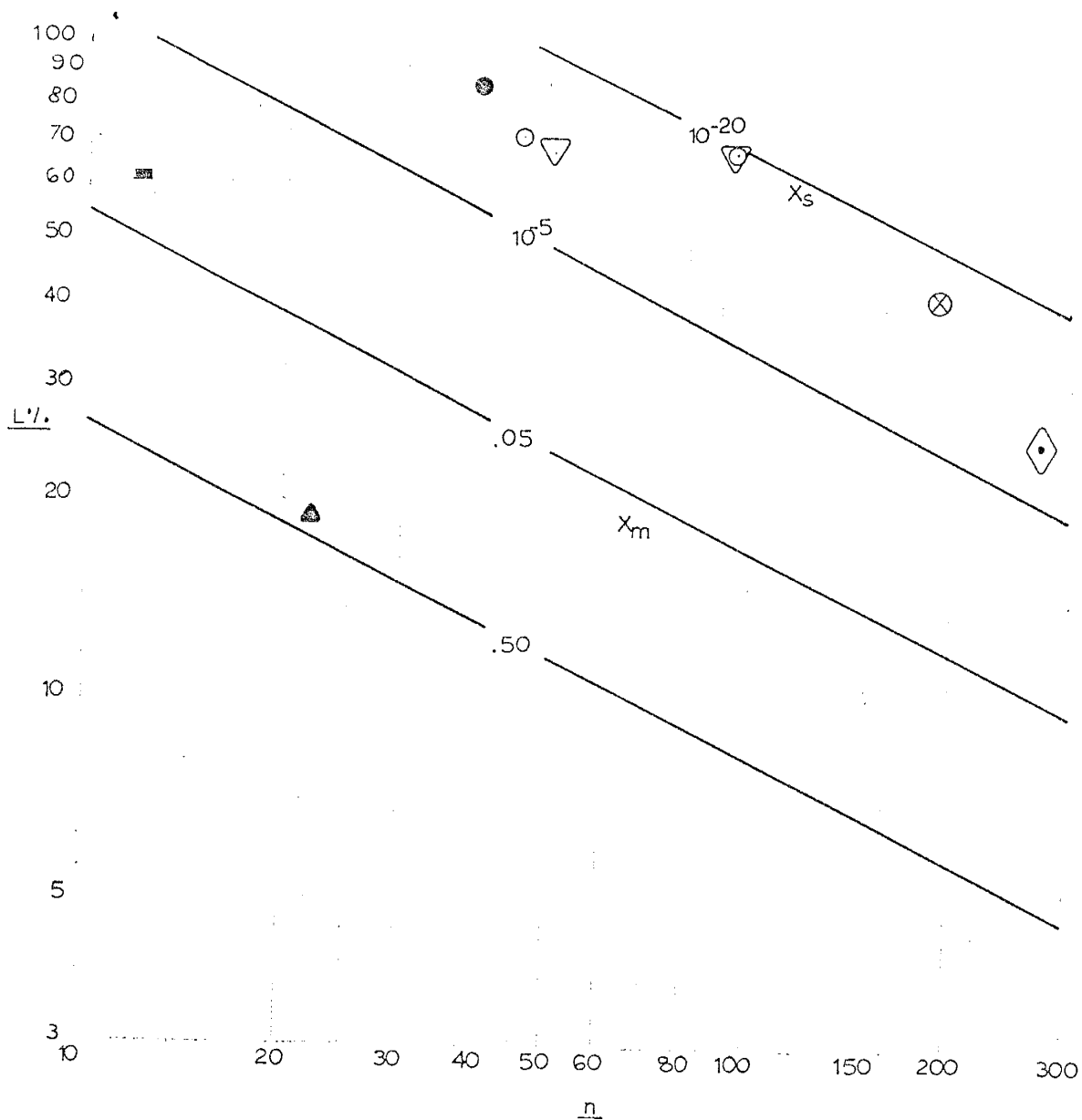
n = $\sum n_o$ (eqn. 5-1)

Thus, all the values falling above the diagonal line labelled $<.05$ in Figure 26 have a probability of less than .05 of being derived from a uniform distribution (equal frequencies assigned to each azimuthal class); those values falling below the $<.05$ diagonal line have a probability of greater than .05 of being derived from a uniform distribution. Only two data points fall below the $<.05$ level of significance: medium scale cross-stratification and groove marks.

Paleocurrent Data:

Small scale cross-lamination: Paleocurrents measured from the small scale cross-lamination have a strong easterly to southeasterly component in Unit A, the lowest siltstone unit in the Abo Formation (Plate 3A).

Paleocurrents measured from Unit C show an increasing dominance of the southerly component as time progressed



LEGEND

X = cross stratification; s = small scale, m = medium scale.
 ⊗ = sum of all cross stratification. ■ = catenary ripple marks.
 ▲ = groove marks. ● = tool marks. ▽ = strike of ripple marks.
 ○ = strike of plant stems. ▽ = sum of all strike structures.
 ◆ = sum of all vectorial structures.

Figure 26. Rayleigh Test of significance on summed sedimentary structures with $n \geq 10$. Sloping lines are the levels of significance. (After Curaray, 1956, Fig. 4).

from the deposition of Unit A to Unit C.

A paleocurrent measurement for a single small scale cross-lamination in Unit D indicates a northerly flowing current. This is in agreement with paleocurrent measurements derived from other sedimentary structures in Unit D.

All the beds above Unit D, with the exception of Units G and M, have southeasterly to southerly flowing paleocurrent directions (Plate 3B). Unit G has a bimodal paleocurrent distribution with a strong easterly component and a lesser southeasterly component. Unit M has a south to southwesterly trending paleocurrent direction.

Medium scale cross-stratification: The paleocurrent directions derived from medium scale cross-stratification are variable. Figure 26 indicates that the sum of all medium scale cross-stratification falls below the .05 level of significance, indicating a statistically high probability of the data being derived from a uniform distribution.

Only in Unit M do the small scale cross-lamination and medium scale cross-stratification have corresponding rose diagrams (Plate 3B). In Unit O through Unit K there is a strong orientation of the medium scale cross-stratification at right angles to the paleocurrent direction defined by the small scale cross-lamination. The summed medium scale cross stratification of all units (top row of Plate 3B), though they have a low L of 19%, show resultant vector that is directed toward the southwest - 90° away from the southeast paleocurrent direction defined by the resultant

vector of the small scale cross-lamination. The origin of the two component flow system described above will be discussed more completely in Chapter 7.

An interesting relationship occurs between the small scale cross-lamination and the medium scale cross-stratification in Unit F. The paleocurrent directions defined by each of these structures are 180° apart. There are four possible explanations for this phenomenon: One) that some tectonic perturbation occurred within the depositional basin or in a nearby source area, two) that two current directions existed at the same locality such as occurs today on tidal flats and some beaches; three) that the reverse paleocurrent direction was formed under the condition of high flow regime (Simons, et al., 1965) when antidunes could form; or four) that the two opposing paleocurrent directions are from different locations in a meandering stream channel.

Large scale cross-stratification: Summed paleocurrent data of the large scale cross-stratification show a strong southerly direction with a high L of 84%. Paleocurrents from Unit C have a strong northerly component.

Catenary and linguoid ripple marks: Catenary and linguoid ripple marks are measured separately from symmetrical ripple marks. Catenary and linguoid ripple marks, because they are assymmetrical, can be used to define a current vector by simply measuring the dip vector of the lee face. Paleocurrent directions measured from Unit H show a southward

flowing current. Paleocurrent directions from Unit G indicate an easterly flowing current as noted previously for the small and medium scale cross-stratification.

Channel cut and fills: Paleocurrent data are often difficult to obtain for the channel fills. Directions and amount of plunge can be obtained by plotting measured attitudes of the channel form on a stereonet. Adjacent sedimentary structures, such as pebble imbrications and large scale cross-stratification, can be used to confirm the suggested paleocurrent direction. The paleocurrent directions from channel fills are quite variable as indicated by the summed rose diagram on Plate 3B. Figure 26 does not show values for any structure with $\Sigma n_0 < 10$, so a simple Rayleigh test can be used to evaluate the data at an .05 level of significance (Potter and Pettijohn, 1963). The test is to compare $2R^{2/n}$ to $\chi^2_{.05}$, d.f.=2. If $2R^{2/n} > \chi^2_{.05}$ then reject the null hypothesis which states that the data are uniformly distributed. The calculations are as follows:

$$2R^{2/n} > \chi^2_{.05}, \text{ where } R = 3.76, n = 8$$

$$1.655 > 5.99$$

This is false so we must accept the null hypothesis that the data have a uniform distribution at an .05 level of significance. That is, the summed paleocurrent data of the channel fills are not statistically significant, and that channel fills should be used only on a unit by unit basis to interpret paleocurrent directions.

Channel fills in Units A and B indicate southerly flowing paleocurrents, but currents from Bed C are variable over 180°. Beds F and G have easterly flowing paleocurrent trends for channel fills.

Groove marks: Figure 26 shows that the summed paleocurrent data for groove marks is not statistically significant at the .05 level and, therefore the paleocurrent patterns for groove marks should be considered only on a unit by unit basis. Paleocurrents from groove marks in Units D and F show northward flowing current patterns which correspond to the pattern produced by other sedimentary structures in these beds. Paleocurrent data from Unit A show the more typical southward flowing current.

Tool marks: The paleocurrent pattern for tool marks has a very high L indicating little dispersal away from resultant vector. The paleocurrent pattern indicates a westward flowing current direction which corresponds to other sedimentary structures in Unit F.

Plant stems: In the Abo Formation the plant stems are oriented with their long stems perpendicular to the prevailing current. The measurement of the strike direction of the plant stems gives two possible unique current directions which are perpendicular to the strike. When these are combined with vectorial paleocurrent data they give a greater degree of confidence to the determined paleocurrent direction.

The measured strike of plant stems from Units A and F is approximately perpendicular to the resultant vectors of other structures in those units. The summed strike of the plant stems is also approximately perpendicular to the sum of all vectorial paleocurrent data, and has a very low probability of being derived from a uniform distribution (see Figure 26).

Assymetrical ripple marks: Like the strike of plant stems, the measured strike of symmetrical ripple marks can be used to give a greater degree of confidence to the measured vectorial paleocurrent direction. The strike of the ripple marks measured from Units A, C, D, F, and G is approximately perpendicular to the calculated resultant vectors for these units. The summed resultant strike for ripple marks is also perpendicular to the summed resultant vectors (top row of Plate 3B). Unit B is somewhat anomalous in that the resultant strike of the ripple marks is approximately parallel to the resultant vector. This may be due to local variations in the current direction and the small number of measurements.

Summary

The sum of all the vectorial paleocurrent data and the corresponding sum of all the strike-type data give a very strong indication of southward flowing currents (top row of Plate 3B). The sum of all the cross-stratification also indicates a strong southward directed current. The above described sums have a very low probability of

being derived from a random distribution.

Some of the beds such as Units D, F and G have rose diagrams and resultant vectors that deviate from the general southward current direction. These are important deviations and may represent variations in sedimentary processes within the depositional basin, variations due to tectonism within the depositional basin or the source area, fluctuations in sea level, or major climatic changes.

CHAPTER 6: DEPOSITIONAL ENVIRONMENT

Introduction

Many workers (see Introduction-Chapter 1) have commented on the continental fluvial and alluvial origin of the Abo Formation. The combination of all the primary sedimentary structures, fossil evidence and the detailed and regional stratigraphic relationships constitute an almost irrefutable interpretation of continental-fluvial deposition for the Abo Formation.

Many recent advances in the study of modern fluvial deposits allow more sophisticated and detailed interpretations of past fluvial processes from observations made in ancient sedimentary rocks (Leopold, et al., 1964; Allen, 1965, 1970).

Fluvial deposits may be classified into two end-member groups: meandering stream systems (high sinuosity) and braided stream systems (low sinuosity). A third possible member mentioned by Moody-Stuart (1966) includes low sinuosity, low braiding index streams such as the Niger-Benue system, the Yellow River in China, and possibly the Kosi River in India.

The following fluvial models are taken largely from the review of the origin and characteristics of alluvial sediments by J. R. L. Allen (1965).

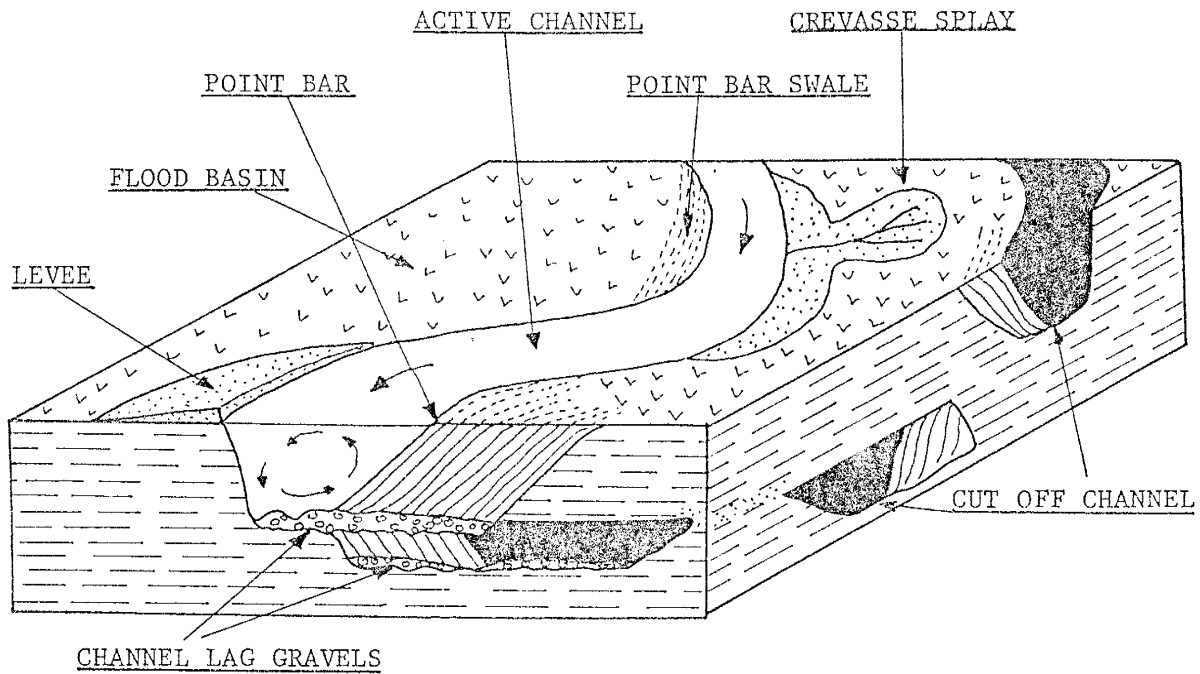
Fluvial Models

Meandering streams: Meandering stream systems can be

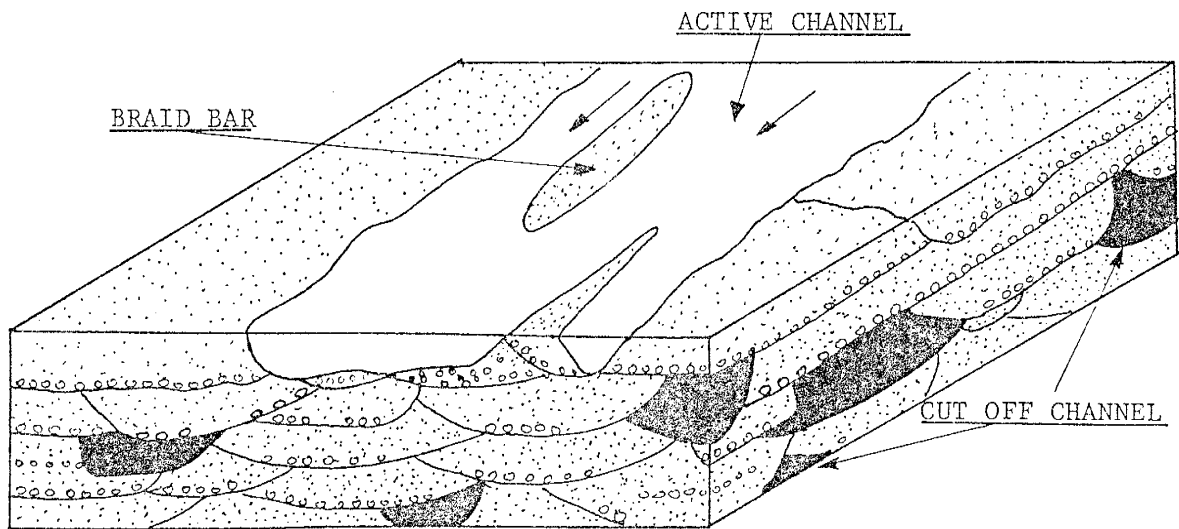
characterized by lateral erosion and aggradation in the streams own alluvial sediment and associated flood basin deposits, as opposed to braided streams, which are dominantly characterized by downstream migration with minor lateral erosion and shifting of banks.

Gravel deposits commonly occur in the deepest part of meandering stream channels where they have been deposited on irregular scour surfaces cut into the underlying flood basin or point bar deposits. The gravels are residual deposits left by the normal processes of stream erosion to form lenticular channel lag deposits. In the Mississippi River, channel lag deposits commonly occur within the overlying finer grained bar sediments. Here the lag deposits occur primarily as thin sheets of pebbles concentrated by the winnowing of sand from an initially mixed deposit (Fisk in Allen, 1965).

One of the most important processes operating in a meandering stream is lateral erosion of the concave, outer banks of meanders and simultaneous deposition on the point bars of the convex, inner banks (Figure 27-A) of meanders. The point bars overlies the channel lag deposits and are approximately as thick as the channel is deep. Point bar deposits come to overlies the channel lag gravels by lateral migration of the point bar. The grain size of sediment deposited in point bars is variable but sand-sized material is the most common, and silts and gravels are less common. Most point bar deposits show a fining-upward



A) MEANDERING STREAM MODEL



B) BRAIDED STREAM MODEL

Figure 27. Fluvial Models (after Allen, 1970; Moody-Stuart, 1966).

sequence. The most important and diagnostic sedimentary structure in point bar deposits is large scale cross-stratification. An abundance of trough-shaped large scale cross-strata was reported from the Beene point bar on the Red River in Louisiana (Harms et al., 1963). Point bars on the Colorado River in Texas and the Amite River in Louisiana have both tabular and trough sets of large scale cross-strata (McGowen and Garner, 1970). Planar, large scale, solitary sets of cross-strata, termed Epsilon cross-strata by Allen (1963), are thought to be typical of point bar deposits. The upper portions of point bar sequences are typically finer grained than the lower portions and have sedimentary structures typical of lesser stream power, such as small scale cross-stratification, ripple marks, and planar lamination.

Channel fills of abandoned or avulsed channels cut off at the neck of a meander loop commonly are composed of silty sands, silts and clay. Coarse bed load sediments occur near the ends of the plugged channel. The dominant fine material in abandoned channel fills is brought in by overbank flow from the main channel and associated flood basins. Abandoned channel fills on the Brazos River flood plain in Texas consist principally of laminated and bedded silt and clay (Bernard and Major, 1963). Abandoned channels can be as large as the active channels and meander belts. Fisk (in Allen, 1965) reports abandoned channel fills in the form of closed meander loops up

to 25 miles in length and having an average thickness of 60 to 90 feet in the flood plain of the Mississippi River.

Channel fills resulting from chute cut-off are generally shorter and less arcuate than neck cut-off channel fills. Coarse bed load sediments are the common filling material. Because of the small angular discordance, the stream continues to flow through the channel for some time depositing bed load material before closure at the cut-off ends is complete.

Levee deposits in meandering stream systems are sinuous, ribbon-like bodies having a triangular cross section (Figure 27-A). They are characterized by interbedding of coarse and fine material. The scale of the interbedding is variable and depends upon many factors, such as stream size, suspended and bed load, and discharge rate. The interbedding of levee deposits is caused by the repeated submergence and construction of levees during flood stage.

Crevasse splay deposits are narrow to broad, localized tongues of coarse sediment, lobate shaped in plan view which are deposited over the lower slopes of levees and flood basins from crevasse channels that tap active streams in flood.

Flood basin deposits are the finest grained material in the meander system. Usually they are composed of silt and clay. Bedding or lamination is generally poorly

developed. Mud cracks are common as are calcretes and ferrocretes in areas of high aridity. Flood basin deposits usually contain abundant mottled soil zones with rootlets and burrows. The geometry of flood basin deposits is of elongated prismatic bodies of rectangular cross-section. The flood basin deposits of the Mississippi River, for example, are up to 50 miles in length, 2 to 15 miles wide and 25 to 140 feet thick (Fisk in Allen, 1965).

Figure 27-A shows the spatial relationships of the deposits of a meandering stream system.

Braided streams: The deposits of braided streams are much less varied than those of meandering streams. They are commonly composed of sand and gravel sized material with fine sand, silt and clay being notably rare. The generally coarser grain sizes are partially due to the fact that braided streams of a given discharge occur on much steeper slopes than meandering streams having the same discharge (Leopold, et al., 1964). Silts and clays, when present, usually occupy channel fills.

Longitudinal channel bars (braid bars) and anastomosing channels are the most common large scale sedimentary structures found in the braided stream system (Williams and Rust, 1969) (see Figure 27-B). According to Allen (1970) small scale sedimentary structures such as cross-bedding and ripple marks are rarely found in the deposits of braided streams; however, Williams and

Rust (1969) report abundant ripple marks and small scale cross-stratification from the modern braided channels of the Donjek River in the Yukon Territory of Canada. The small scale structures have a low preservation potential except in cut-off channels and, therefore, are usually not found in older braided stream deposits. Other important structures found in the Donjek River are large scale trough cross-stratification on the migrating face of channel bars and pebble imbrication.

The deposits of braided streams represent a dominance of bed load under conditions of high flow regime. Channel deposits are usually coarse-grained with rare laminations or bedding and lack the variety of textures and sedimentary structures observed in meandering stream channels.

Most fluvial deposits, ancient and modern, can be characterized by the two models just described. This is not meant to imply that there are no intermediate models or gradations between these two end members of fluvial deposition - surely intermediate models must be the rule rather than the exception. Many modern streams are braided in parts of their lengths and meandering in other parts. Changing discharge rates by natural or artificial means can cause a meandering stream to become braided and vice-versa (Leopold et al., 1964).

Depositional Environment - Upper Member of the Abo

The upper member of the Abo Formation in the study area

is composed of fining upwards cycles of pebbly calcilithite, laminated and cross-stratified reddish-brown siltstone and finally reddish-brown mudstone (see Figure 9). The presence of fining upward cycles and the general fine grained nature give a first indication that the Abo red-beds were deposited by low gradient meandering streams. An analysis of the detailed stratigraphic sections presented in Chapter 4 can be used to amplify the meandering stream concept.

Unit E: Locality 10 in Unit E (see Plate 1 and Figure 28) is a well-exposed point bar deposit. Here gray pebble calcilithites (channel lag deposits) are overlying an irregular scoured surface developed on the underlying mudstone. Overlying the channel lag gravels is a single large scale tabular set of cross-stratified reddish-brown siltstone. Internal structures in the large scale cross-strata are predominantly small scale cross-lamination and ripple drift (Figure 13). The large scale cross-strata are produced by the migration of the face of a point bar. The thickness of the point bar deposits, and therefore the bankfull depth of the channel is six feet. Dark reddish-brown mudstones overlie the siltstones of the point bar deposits, and are interpreted as flood basin deposits.

Unit F: The detailed stratigraphic sections of many of the siltstone units, such as Unit F, are more complex than

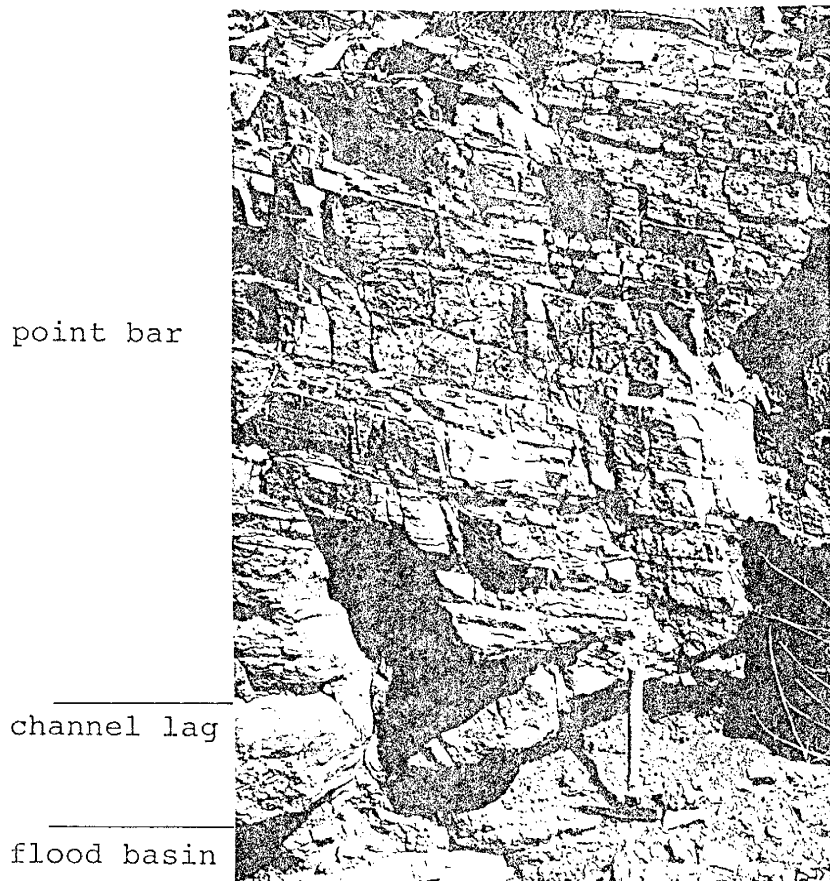


Figure 28. A typical meandering stream deposit in Unit E, Locality 10. Reddish-brown mudstones (flood basin deposits) are overlain disconformably by pebbly calcilithite (channel lag gravels) which are overlain by a single set of large scale cross-strata (point bar). Regional dip is 10° to the north (left side of photograph) but cross strata are dipping south. Note smaller scale cross-stratification within the large scale cross-strata of the point bar. Hammer is one foot long.

the simple section just described for Unit E. The detailed stratigraphic section of Unit F (Figure 19) is a partial cycle and is remarkably similar to other fluvial cycles formed by ancient meandering streams in the old Red Sandstone of Devonian age in the Anglo-Welsh Basin of England (Allen, 1964). Referring to Figure 19, sub-unit one, a gray pebble calcilithite, is interpreted as a channel lag gravel deposited on an irregular scoured surface of mottled mudstone. Above the lag gravels there is an eight foot section of planar laminated, ripple drift cross-laminated, and small scale cross-laminated reddish brown siltstone (sub-unit two), which is best interpreted as a channel fill deposit after avulsion of the active channel.

The mud cracked surfaces in the channel fill of sub-unit two represent periods of areal exposure and dessication. If most of the sediment in the channel fills comes from overbank flow from distant active channels then the mud cracks also represent low discharge (less than bankful) stages for these active channels. The convolute laminations of the channel fill are more difficult to interpret. Some of the convolute laminations which have sharp, peaked antiforms, a dipping axial plane and broad synforms can be attributed to laminar shear flow acting upon slightly plastic penecontemporaneously deposited current ripples. Other convolute laminations have broad domical antiforms and vertical axial planes. The lack of dipping axial planes indicates plastic

deformation under conditions of vertical loading. The cause and modus operandi of the vertical loading is unknown.

Sub-unit three, interbedded pebbly calcilithite and planar laminated to cross-laminated reddish-brown siltstone, appears to represent a levee deposit (Figure 19).

Overlying the levee deposits is a single 2.5 foot thick tabular set of cross-laminated reddish brown siltstone. These cross-strata (sub-unit four, Figure 19) are the migrating convex face of a point bar. The thin calcilithites at the base of the cross-strata are probably poorly developed channel lag gravels.

Sub-unit five is similar to sub-unit two in texture and associated sedimentary structures and probably represents a channel fill deposit. Sub-unit six is reddish-brown, poorly laminated mudstone with a few "knobby" calcilithite beds and calcareous concretions, and is interpreted as a flood basin deposit. The concretions probably indicate soil forming conditions similar to those found today in many arid to semi-arid regions. The calcareous concretions are probably incipient caliche zones which never developed into full scale soil horizons.

The sub-unit underlying Unit F is a reddish-brown mottled mudstone. The mottled texture is indicative of a root network of plants or burrows, which suggests development of soil, and plant growth and maturation of the flood plain before the channel deposits of Unit F were deposited on it.

In summary, the cycle at Unit F indicates deposition of lag gravels upon a well established flood plain; then the channel was partially filled with overbank flows. Levee deposits from a nearby active channel overlie the channel fill. The channel became reactivated and the deposition of large scale tabular cross-strata on the migrating face of a point bar occurred. Again active bed load sedimentation ceased in the channel, and silt sized material was deposited from overbank flows. A flood basin of mud and silt sized material developed over the point bar deposits. The thickness of the point bar deposits is eighteen feet and is an indication of the channel depth at bankfull discharge.

Fining upward sequences are thought to be typical of meandering stream deposits (Allen, 1964; Leopold, et al., 1964), and are reflected not only in grain size, but also in flow regime as determined by sedimentary structures (Harms and Fahnestock, 1965). The grain size of a cycle from Unit F (Figure 19) decreases upward from pebbly calcilithite to siltstone to mudstone. Sedimentary structures decrease upward in flow regime from the channel lag gravels which are deposited only under conditions of upper flow regime (Harms and Fahnestock, 1965) to the transitional flow regime planar laminated siltstone beds of sub-unit two (Figure 19). Overlying the levee deposits of Unit F are the large scale cross-stratification (dunes of Harms and Fahnestock, 1965) which are formed in the

upper part of the low flow regime. The upper sub-units of Unit F contain ripple cross-lamination, planar lamination, and small scale cross-lamination which are formed in the lower part of the low flow regime. The mudstone which overlies the siltstone is formed by the settling of fine silt and clay size material from suspension.

The Type A and Type B ripple drift in the siltstone beds indicate suspended load sedimentation in the lower flow regime (Jopling and Walker, 1968).

Unit K: A partial cycle of Unit K is presented in Figure 24. Sub-unit one of this stratigraphic section is a channel lag gravel deposited on an irregular scoured surface of the underlying reddish-brown mudstones. Interbedded, cross-laminated, reddish-brown siltstones indicate a less complete winnowing of fine-grained material during low discharge states in this channel. Above sub-unit one there is a sequence of four sub-units which appear to represent avulsion of the active channel, and filling with alternating cross-laminated and planar laminated silt and poorly laminated silty mud. Sub-unit six (Figure 24) is composed of poorly laminated reddish-brown mudstone which is typical of flood basin deposits.

Unit G: The partial cycle of Unit G (Figure 25) shows a markedly different fluvial history than the two preceding sections. Sub-unit one in Unit G has the morphology of a channel lag deposit, but is composed of laminated reddish-brown

mudstone. The remainder of the section of Unit G is composed of alternating reddish-brown mudstone and planar-laminated and cross-laminated reddish-brown siltstone. All the above described units represent a channel fill deposit primary from overbank flow of a nearby active channel. All of the sedimentary structures indicate low flow regime deposition of bed load silt-sized material for the siltstones, and suspended load deposition for the mudstones. Some erosion of the mudstone before deposition of the overlying siltstone is indicated by the rapid thinning of sub-unit four. The thin lenses of calcilithites in sub-unit six are either crevasse splay or levee deposits.

Much of the medium and large scale cross-stratification in the Abo Formation is probably formed by the migration of point bars in meander loops, though rarely are the relationships with the other depositional features of a meandering stream system as well exposed as in the above described localities. The general stratigraphic column of the Abo Formation (Figure 9) indicates that many of the siltstone units are underlain by a pebbly calcilithite.

The mudstones of the Abo Formation are interpreted as suspended load, overbank flood basin deposits, mainly because of their very fine-grained character (silt and clay) and the presence of poorly developed lamination. The mudstones have abundant evidence of areal exposure: mud cracks and mottled zones which indicate burrow tubes or plant root networks. They also have calcareous

concretions which were probably formed by a process similar to that observed in the formation of caliche soils in arid to semi-arid climates. Within the mudstones there are thin sheet-like calcilithites and a few lenticular, channel-like beds (Figure 11). The thin sheet-like beds lack the characteristic channel form and may be blanket lag deposits similar to those described by Fisk (in Allen, 1965) in the bar sediments of the Mississippi River, or they may be the distal portions of crevasse splay or levee deposits.

Siltstone from portions of Unit G (Locality 53) contain very coarse sand to granule-sized clasts of hematized siltstone. The location of the samples examined petrographically is one foot above an obvious channel form which was filled with laminated siltstone. If the channel fill was transported primarily by overbank flows, then the siltstone clasts may represent flood basin or channel deposits that were "ripped-up" by a local increase in the stream power. It is interesting to note that the siltstone clasts had already been hematized before they were eroded and redeposited. It is impossible to estimate the amount of time between the deposition and diagenetic hematization of the siltstone and its erosion and redeposition in Unit G, but Walker (1967) estimates that the "generation of well crystallized hematite, during diagenesis under natural conditions in arid climates, may take hundreds of thousands to several million years."

Depositional Environment - Lower Member of the Abo

Due to the poor exposures of the lower arkosic unit of the Abo Formation, it is difficult to determine the large scale and medium scale sedimentary structures that are necessary for a detailed environmental interpretation. The general lack of fine-grained deposits, the thick bedding, pebble imbrication, the rare graded bedding, the size and angularity of the clasts and the internal homogeneity of the lower arkoses suggest deposition by upper flow regime streams transporting coarse debris from a nearby source area - possibly a braided stream.

The thin, nodular, argillaceous, micritic limestones may represent local basins of either fresh water or marine to brackish waters.

The lower member is a transitional deposit between the dominantly near shore marine rocks of the underlying Bursum Formation and the fluvial meandering stream deposits of the upper member of the Abo Formation.

Fluvial Paleochannels

From the work of Schumm (1972) it is possible to estimate the ancient hydrologic and flood plain characteristics from the measurement of the width and depth of paleochannels. Schumm (1972) empirically derived equations from cross sections of many different types of rivers which relate the measured width-depth ratio of modern fluvial channels to several hydrologic and flood plain characteristics (see Table 5-A).

Fluvial Parameters	Symbol	Equation	Dimensions
Width	W		feet
Depth	d		feet
Width-Depth ratio	F	$F = W/d$	dimensionless
Meander wavelength	L	$L = 18 (F^{.53} W^{.69})$	feet
Meander amplitude	A	$A = 2.7 W^{1.1}$	feet
Gradient	S	$S = 30 (F^{.95} / W^{.98})$	feet/mile
Sinuosity	P	$P = 3.5 F^{.27}$	dimensionless
Mean annual flood	Qma	$Qma = 16 (W^{1.56} / F^{.66})$	cubic feet/second
Mean annual discharge	Qm	$Qm = W^{2.43} / 18 F^{1.13}$	cubic feet/second

Table 5-A. Fluvial parameters and equations. All equations are from Schumm (1972) except meander amplitude, A, which is from Leopold and Wolman (1960)

Location	$F = W/d$	L	A	S	P	Qma	Qm
E-10	$6.66 = 40/6$	626	156	5	2.1	1447	51
F-15	$1.66 = 30/18$	244	114	2	3.1	2325	122

Table 5-B. Fluvial parameters from two localities in the Abo Formation.

The depth of the ancient channels at bankfull discharge is obtained by measuring the thickness of the point bar deposits (Leopold et al., 1964). The width of the ancient channels was measured in near normal cross-sections of channel cut-and-fills. Only two localities within the study area are sufficiently well exposed to allow a confident interpretation of the point bar deposit and measurement of the corresponding width and depth (see Table 5-B).

All the parameters in Table 5-A are straightforward and require no explanation with the exception of P, the sinuosity index, which is described by Leopold et al. (1964) as the ratio between channel length and downvalley distance. Rivers having a sinuosity of greater than 1.5 are termed meandering and those with a sinuosity of less than 1.5 are termed sinuous or straight. The value of 1.5 is an arbitrarily defined limit. For purposes of illustration, a meandering channel consisting of semi-circles in a map view would have a sinuosity of approximately 1.5.

It must be realized that the quantitative estimation of these various hydrologic and flood plain characteristics from paleochannels is fraught with many difficulties and the numerical values listed in Table 5-B are probably subject to a great deal of variation. Such quantitative estimations can, at best, be used to visualize a general picture of hydrologic conditions on the flood plain.

The sinuosity index, slope and discharge data for the two fluvial paleochannels of the Abo Formation indicate

a meandering stream depositional environment (Leopold et al., 1964, Fig. 7-39) with many small channels all capable of only relatively low discharge rates. Modern streams with comparable l , Q_{ma} , and Q_m have relatively small drainage areas - approximately 100 to 200 square miles (Leopold, et al., 1964).

CHAPTER 7: PROVENANCE AND DISPERSAL
PATTERNS OF THE ABO FORMATION

Provenance

Based on petrographic and X-ray diffraction evidence, models of "source rocks" of the detrital material in the Abo Formation were presented in Chapter 3.

The distribution of the late Paleozoic land masses is shown in Figure 2. These areas are composed predominantly of Precambrian igneous and metamorphic rocks. The land masses are thought to have been positive areas during most of Pennsylvanian and Permian time in New Mexico (Thompson, 1942; McKee, 1967). The trends of the late Paleozoic land masses are similar to the observed trends in the modern southern Rocky Mountains. For this reason they have been termed the "ancestral Rockies."

Lower coarse arkosic member: The lower coarse arkosic member requires a nearby source of metamorphic rock of granitic composition. Less than five miles south of the study area there are six well exposed outcrops of Precambrian granitic gneiss (Wilpolt and Waneck, 1951) which may represent part of a late Paleozoic land mass. Three of these outcrops have been visited by the author and they are all composed of granitic gneiss with minor quartzite. Locally, large pink poikiloblastic microclines similar to the microcline clasts in the lower coarse arkose member occur.

The Precambrian rocks of the Joyita Hills, which lie ten miles north of the study area, have been described by L. Herber (1963). The Joyita Hills are composed dominantly (75%) of quartz-potassium feldspar-biotite gneiss. The potassium feldspar makes up 45% to 60% of the gneiss, and is either microcline or perthitic microcline. The microclines, which have an average crystal size of 6 mm, commonly enclose crystals of plagioclase, biotite and quartz. Myrmekitic textures are common. Quartz, which comprises about 25% to 35% of the gneiss, occurs in clear elongate crystals, which have sutured boundaries and undulatory extinction. Brown biotite is also common, making up 5% to 15% of the total composition of the gneiss. Small crystals of sodic plagioclase (albite and oligoclase ranging up to An_{26}) make up 5% to 20% of the gneiss. Other rock types noted by Herber (1963) in the Precambrian of the Joyita Hills are amphibolite, quartz-potassium feldspar schist, epidosite, pegmatite and aplite.

The descriptive petrography of the gneiss of the Joyita Hills matches very well with the petrography of the detritus in the lower coarse arkose member described in Chapter 3, except for the relative percentages of potassium feldspar, plagioclase and quartz. In any weathering and transportational sequence, feldspars will be selectively weathered and destroyed with respect to quartz. The markedly similar petrography of the lower arkose and the granitic gneiss of the Joyita Hills make the Joyita Hills a highly likely

candidate for the provenance of the lower coarse arkose member of the Abo Formation.

The Abo Formation in the Joyita Hills contains a basal lenticular pebble to cobble conglomerate composed of angular shard-like quartz which is in depositional contact with the Precambrian granitic gneiss. Kottowski and Stewart (1970) suggest that the higher parts of the Joyita uplift were exposed until deposition of the middle Abo covered them completely.

The outcrops of Precambrian granite gneiss south of the study area are not as likely candidates for the provenance of the lower coarse arkose member because of two reasons: 1) All the Precambrian rocks are depositio-ly overlain by the clastic rocks of the Sandia Formation of Pennsylvanian age and have for the most part been exposed only recently by Tertiary normal faulting. (Wilpolt and Waneck, 1951), so they were not exposed during the Permian, and 2) paleocurrent directions measured from the upper cyclic member indicate southerly flowing currents for most of the Abo Formation, therefore, a source area to the north of the study area seems more likely.

Upper cyclic member: The provenance of the calcilithites in the Abo Formation requires a mixed sequence of micrite, biomicrite, sparite, microsparite and quartzose siltstone. Sedimentary rocks of Pennsylvanian age are found in abundance throughout New Mexico (Dane and Bachman, 1965).

According to regional and other studies (Wilpolt and Waneck, 1951; Kottowski, 1963; T. Siemers, personal communication, 1975) the Pennsylvanian rocks of central New Mexico can be broadly grouped into two formations. The lower formation (Sandia Formation) consists largely of quartz arenites, feldspathic sandstones and shales with minor carbonate rock. The upper formation (Madera Formation) is dominantly micrite and biomicrite with lesser amounts of sparite and interbedded shales. Locally, the Madera Formation has an upper clastic member of arkosic limestone and micrite (Wilpolt and Waneck, 1951). Because of their: 1) petrographic similarity with the calcilithites of the Abo Formation, 2) widespread occurrence throughout New Mexico, and 3) stratigraphic position directly below the Permian System; the Pennsylvanian rocks are likely source rocks for the calcilithites.

In the calcilithites approximately 10% of the clasts are siltstones which are petrographically similar to the Abo siltstones. This similarity suggests that some or all of the siltstone clasts in the calcilithites may have an intraformational origin. Within the study area and probably throughout central New Mexico the Abo Formation contains a low percentage of thin, minor, lenticular limestone beds. Therefore, an intraformational source for the carbonate clasts, which compose approximately 90% of the calcilithite clasts, seems highly unlikely.

Rocks of the Mississippian System principally occur

in southern New Mexico. Mississippian rocks in central New Mexico are composed of algal and crinoidal limestones, shales and limy sandstones (Kottowski, 1963). Because of their: 1) limited occurrence throughout New Mexico, and 2) poor lithologic correspondence with the clasts in the Abo calcilithites, the Mississippian rocks are not regarded as important source rocks for the calcilithites.

Sedimentary rocks of Lower Paleozoic age generally do not occur in northern or central New Mexico, but are well exposed in southern New Mexico in the western escarpment of the Sacramento Mountains (Pray, 1961). Lower Paleozoic rocks consist primarily of dolomite and glauconitic sandstone. There is a possibility that these rocks were exposed in northern and central New Mexico and were being eroded in Permian time. As there are very rare clasts of dolomite and no clasts of glauconite sandstone in the Abo Formation the probability of the Lower Paleozoic rocks as source rocks for the calcilithites is very low, at least in the study area, if not elsewhere. If these rocks were deposited in northern and central New Mexico, it is more probable that they were stripped by erosion before late Paleozoic time.

There are two possible sources for the clastic quartz, plagioclase and biotite found in the siltstones and in the mudstones of the Abo Formation: 1) the "granitic" rocks of the late Paleozoic land masses - in particular those which are north of the study area such as

the Pedernal land mass, Uncompaghre Uplift, and the Zuni Uplift (Figure 2); or 2) Pennsylvanian and/or Mississippian clastic rocks which originally derived their clasts from the erosion of late Paleozoic land masses.

The petrography of the Precambrian rocks of the Pedernal Hills, a remnant of the late Paleozoic Pedernal land mass, has been studied by R. Gonzalez (1965), and he described four major rock types: 1) granite gneiss containing idioblastic microcline and microperthite up to one cm in size and containing inclusions of quartz and plagioclase, 2) quartzite, quartz-mica and quartz-specular hematite schist, 3) intrusive granite, and 4) cataclasite.

The Precambrian rocks of the Zuñi Mountains are similar to that of the Pedernal Hills: mostly granite gneiss and metarhyolite with lesser amounts of aplitic rocks, quartzites and gneisses of various composition (Goddard, 1966).

Both of these Precambrian rock masses fit the petrography of the Abo siltstones and mudstone and, on this basis, are likely candidates for the provenance of siltstones and mudstone either directly or through a second cycle process after being deposited in Mississippian and/or Pennsylvanian sedimentary rocks.

The Abo Formation on the northeastern side of the Zuñi Mountains is the oldest Paleozoic Formation in that area and disconformably overlies the Precambrian metamorphic

rocks. The lower Abo in the Zuñi Mountains contains beds of calcilithite which are very similar to those found in the Abo red-beds of the study area (Read et al., 1967). This implies that if the Zuñi Uplift was a positive area in Permian time (McKee, 1967), then Pennsylvanian carbonate and clastic rocks were deposited along the flanks and possibly over the Zuñi crystalline complex before it was uplifted and exposed to erosion presumably toward the end of Pennsylvanian time.

Clasts of Pennsylvanian rocks found in the calcilithites of the study area also probably had a local source. Some of the clasts in the calcilithites have irregular shapes which could not have survived the 75 miles to 100 miles of transport from the Zuñi Uplift. It is probable that there were local positive areas on the developing flood plain during Lower Permian time. These positive areas may have been composed of Pennsylvanian carbonate and clastic rocks. These local uplifts of Pennsylvanian rocks may have been, in part, caused by tectonic events represented in the local unconformity separating Pennsylvanian and Permian rocks in parts of south-central New Mexico (Kottlowski, 1963).

Lenses of conglomerate in outcrops of the Abo Formation, which lie near the Pedernal land mass and which were presumably derived from it, contain no clasts of carbonate rocks. In the Sacramento Mountains, conglomerates of arkosic composition occur in the upper fine-grained member of the Abo Formation (Pray, 1961). Further north

along the Pedernal land mass trend at the Gallinas Mountains, small outcrops of the Abo Formation are composed of a lower conglomeratic arkose member and an upper silty member which contains lenticular conglomerates with clasts of metamorphic rock fragments (Perhac, 1970).

The above evidence suggests that the Pedernal land mass did not supply any coarse material to the Abo fluvial deposits within the study area, but silt-sized quartz and minor plagioclase could have been derived from the Pedernal land mass, the Zuñi uplift, or the southern part of the Uncompaghre uplift (see Figure 2). Other sources of silt-sized quartz may have been the previously described local uplifts of Pennsylvanian clastic and carbonate sequences exposed on the Abo flood plain.

Dispersal Patterns

Dispersal patterns, as defined by Potter and Pettijohn (1963), are "map pattern(s)...of one or more variable whose distribution was controlled by a current system... ." As the study area of this thesis is very small (one square mile) it is not practical to study dispersal patterns in the strictest sense of the definition. However, it is possible to observe changes in current-formed variables, such as small and medium scale cross-stratification, in a vertical stratigraphic sense rather than on a map view.

Variations of sedimentation patterns and depositional mechanisms in a fluvial-alluvial system are complex.

Cyclic sequences, such as the upper member of the Abo Formation, and the origin of the variations within such sequences, have been discussed by J. R. Beerbower (1964). Autocyclic sequences, as defined by Beerbower (1964), are caused by variations generated within the sedimentary prism, and are, basically, responses to changes in the energy distribution on an alluvial flood plain. Some of the mechanisms which cause autocyclic variations are channel migration and crevasse splaying. Autocyclic variations generally produce cycles of the asymmetric type (a-b-c/a-b-c) or some variation on that theme. Allocyclic variations are changes in slope, load, discharge, biological activity and chemical deposition that are induced by some mechanism outside the sedimentary prism. The mechanisms of allocyclic variations are eustatic variations of sea level, climatic shifts, and diastrophic movements (Beerbower, 1964).

The regular asymmetric cyclic sequence, a-b-c/a-b-c, (where a = calcilithite, b = siltstone, and c = mudstone) of the upper member of the Abo Formation suggests that, in a gross manner, the entire upper member was formed by autocyclic variations induced by a meandering stream system. Many of the changes in paleocurrent directions observed between siltstone beds may be caused by autocyclic or allocyclic variations.

Small changes in paleocurrent direction, such as the change from easterly flowing currents to southerly

flowing currents as observed in the small scale cross-stratification from Unit A to Unit C, may indicate the operation of allocyclic mechanisms, such as a shifting source area, or autocyclic mechanisms, such as channel migration.

Paleocurrents measured from the small and medium scale cross-stratification in Unit D indicate northward flowing currents. Because the paleocurrent measurements were taken over 3000 feet of strike, which is greater than the calculated meander wavelength (see Chapter 6), it is probable that this is not an autocyclic variation but an allocyclic variation. It is proposed that either differentials of compaction, subsidence on the developing flood plain, or local diastrophic movements may have created a small positive area just south of the study area. The brief interlude of northward flowing currents would have been superceded by the more typical southward flowing currents as sedimentation covered the small positive area. If there was a change in source area, then it was thought that the mineralogical and textural characteristics of the siltstones from Bed D might in some ways be different than the surrounding siltstones, provided that the source rocks differ. However, there is no petrographic difference between siltstones from Unit D and any other siltstone in the upper member. The above evidence suggests that much of the detritus in Unit D could be intraformational - derived from the erosion

of previously deposited fluvial sediments to the south of the study area. Considering the meandering stream model it is probable that the detritus was deposited and re-eroded many times before final deposition and burial (see Figure 27). Therefore, intraformational detritus would be common in meandering stream deposits.

Paleocurrent directions defined by small scale cross-lamination and medium scale cross-stratification from Unit E differ by almost 90°. Different primary sedimentary structures which are formed in different parts of a meandering stream system can have paleocurrent patterns which differ appreciably in direction (Allen, 1966). In Unit F the westerly trending paleocurrents directions from the medium scale cross-stratification are interpreted as being formed by the lateral migration of point bar deposits. The southerly trending paleocurrent directions from the small scale cross-laminations were probably formed by deposition on the upper part of the point bar or associated flood basin.

Paleocurrent patterns from Unit G are more difficult to interpret because there is no striking angular discordance between paleocurrent directions defined by small scale cross-lamination and medium scale cross-stratification. The easterly trending paleocurrents and the low value of L (high variance) (see Plate 3B) for Unit G suggest that this unit was deposited by a predominantly eastwardly flowing reach of a meandering stream system.

The angular discordance between paleocurrent directions defined by medium scale cross-stratification, and the dominantly southerly direction defined by the small scale cross-lamination in Unit H through Unit O, can be attributed to the autocyclic variations of dispersal variables in a meandering stream system as described above for Unit F. The small amount of angular variation of paleocurrent directions from bed to bed suggests that normal meandering stream processes were the major cause of the variation.

CHAPTER 8: SUMMARY AND CONCLUSIONS

Summary

Lower arkosic member: The coarse to pebbly arkoses of the lower member of the Abo Formation were deposited by streams transporting coarse, angular debris under upper flow regime conditions. The presence of graded bedding, poorly developed pebble imbrication, medium scale, trough-shaped cross-stratification, and lack of fine-grained detritus suggest that the depositional environment was that of a braided stream.

The detrital material in the arkoses of the lower member, as suggested by the coarseness and angularity of the clasts of microcline and composite grains of quartz, was derived from a nearby source. The petrographic characteristics of the composite grains of quartz, the microcline, and the sodic plagioclase in the arkose suggest a moderately foliated metamorphic rock with a granitic composition as the most likely source.

The Precambrian granite gneiss of the Joyita Hills is petrographically almost identical to the detritus in the arkose and is only ten miles to the north of the study area, and therefore is the most likely source area for the arkoses of the Abo Formation.

Upper cyclic member: The upper member of the Abo Formation consists of fourteen cycles of gray, coarse to pebbly

calcilithite overlain by pale to dark reddish-brown siltstone which is, in turn, overlain by dark reddish-brown mudstone. These cycles are fining-upwards in grain size and in the scale of sedimentary structures. Each of the fourteen cycles represents deposition by meandering streams. The calcilithites which disconformably overlie the mudstones of the underlying cycle were deposited as channel lag gravels (see Figure 27). The siltstones which overlie the calcilithites contain a wide variety of primary sedimentary structures, such as ripple marks, ripple drift cross-lamination, small to large scale cross-stratification, planar laminations (all of which indicate deposition under low flow regime conditions), mud cracks, convolute laminations, deformed bedding, vertebrate tracks, raindrop impressions, tool marks, plant fossils, and channel cut and fills. The siltstones are interpreted as point bar deposits (Figure 27). Other genetic units can also be identified within the siltstone beds, such as levee deposits, crevasse splay deposits and channel cut-offs. The overlying mudstones were deposited in flood basins.

Analysis of the hydrological and geological parameters of the flood plain indicate that there were many small meandering streams (no wider than 40 feet, no deeper than 18 feet) with gradients of two to five feet per mile, having relatively low discharge rates, and draining relatively small drainage basins (100 to 200 square miles).

Paleocurrent measurements in the upper member of the Abo Formation indicate dominantly southerly flowing streams. The resultant vectors defined by the sum of the small scale cross-stratification and the medium scale cross-stratification have an angular separation of approximately 70° (see Plate 3B). The medium scale cross-stratification is interpreted as having formed by a process of lateral accretion on the migrating convex face of a point bar. The small scale cross-stratification was formed by down-current migration of ripples on the upper point bar, point bar swale, or possibly the flood basin itself.

Not all the paleocurrents measured from the upper member indicate southward flowing streams. Measurements from Unit D indicate northward flowing currents. These differences in paleocurrent direction are allocyclic variations (Beerbower, 1964) which were probably caused by local diastrophic events in the Abo flood plain.

The clasts in the calcilithites are petrographically similar to Pennsylvanian carbonate and clastic sequences within Socorro County, New Mexico. It is most probable that the calcilithites were derived from the erosion of these sedimentary sequences, either from small local uplifts on the flood plain or from sedimentary deposits on or surrounding the late Paleozoic land masses (Figure 2) north of the study area.

The fine grained clastic material in the siltstone and mudstones was probably derived either from the

weathering and erosion of crystalline rocks of one or more of the late Paleozoic land masses and/or from the erosion of Pennsylvanian clastic rocks.

Conclusions

During the earliest period of deposition of the Abo Formation there were small local highlands of Precambrian metamorphic and igneous rock exposed on the flood plain. Braided streams carrying coarse debris formed around the Joyita uplift north of the study area. After the Joyita uplift was covered, the Abo flood plain consisted of many small meandering stream systems which carried mostly silt and clay and small amounts of bed load gravel. These streams flowed sluggishly toward the south to the Early Permian sea. The gradient of the flood plain was approximately two to five feet per mile. Local small uplifts of Abo silts and muds and Pennsylvanian carbonate and clastic rocks produced some relief within the Abo flood plain and acted as local source areas.

Recommendations for Further Work

A more complete understanding of Lower Permian sedimentation in New Mexico would be gained by studying the depositional environments, the paleocurrent patterns and the provenance of the Abo Formation on a regional scale.

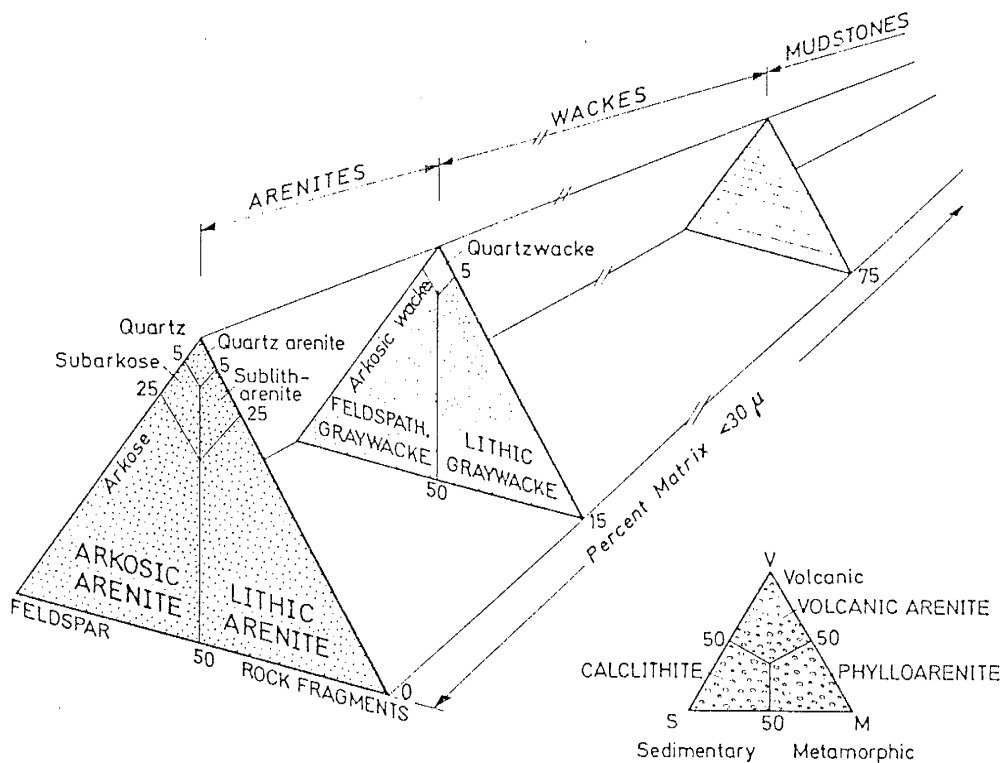
The measurement of 100 to 200 paleocurrent directions from small, medium and large scale cross-stratification

would be enough to define a paleocurrent direction at one locality.

The determination of the depositional environment of the Abo Formation at a specific locality, the changes in depositional environment through time, and the location of the source areas, would add greatly to our knowledge of the Lower Permian paleogeography in New Mexico.

Appendix A
Classification Systems

A.1 - Petrographic Classification



A.1a - Classification of terrigenous sandstones and siltstones (modified from Dott, 1964 in Pettijohn et al., 1973).

	OVER 2/3 LIME MUD MATRIX				SUBEQUAL SPAR AND LIME MUD	OVER 2/3 SPAR CEMENT		
Percent Allochems	0-1%	1-10%	10-50%	OVER 50%		SORTING POOR	SORTING GOOD	ROUNDED AND ABRADED
Representative Rock Terms	Micrite and Dismicrite	Fossiliferous Micrite	Sparse Biomicrite	Packed Biomicrite	Poorly Washed Biosparite	Unsorted Biosparite	Sorted Biosparite	Rounded Biosparite
1959 Terminology	Micrite and Dismicrite	Fossiliferous Micrite	Biomicrite		Biosparite			
Terrigenous Analogues	Claystone		Sandy Claystone	Clayey or Immature Sandstone	Submature Sandstone	Mature Sandstone	Supermature Sandstone	

Lime mud matrix
 Sparry calcite cement

CARBONATE TEXTURAL SPECTRUM

A.1b - Folks classification of carbonate rocks (after Blatt, et al., 1972).

Note: Microsparite is composed of carbonate crystals with a size range of 5μ to 20μ . Carbonate crystals in micrite are usually less than 5μ (Blatt *et al.*, 1972).

A.2 - Textural Classification

Wentworth's Size Classification

<u>Grade limits</u>	<u>(diameter in mm)</u>
>256	boulder
64 - 256	cobble
4 - 64	pebble
2 - 4	granule
1 - 2	very coarse sand
.5 - 1	coarse sand
.25 - .5	medium sand
.12 - .25	fine sand
.062 - .12	very fine sand
.031 - .062	coarse silt
.0039 - .031	medium to very fine silt
<.0039	clay

A.3 - Sedimentary Structures

A.3a - Cross-stratification

Thickness of set

small scale:

<5 cm

medium scale:

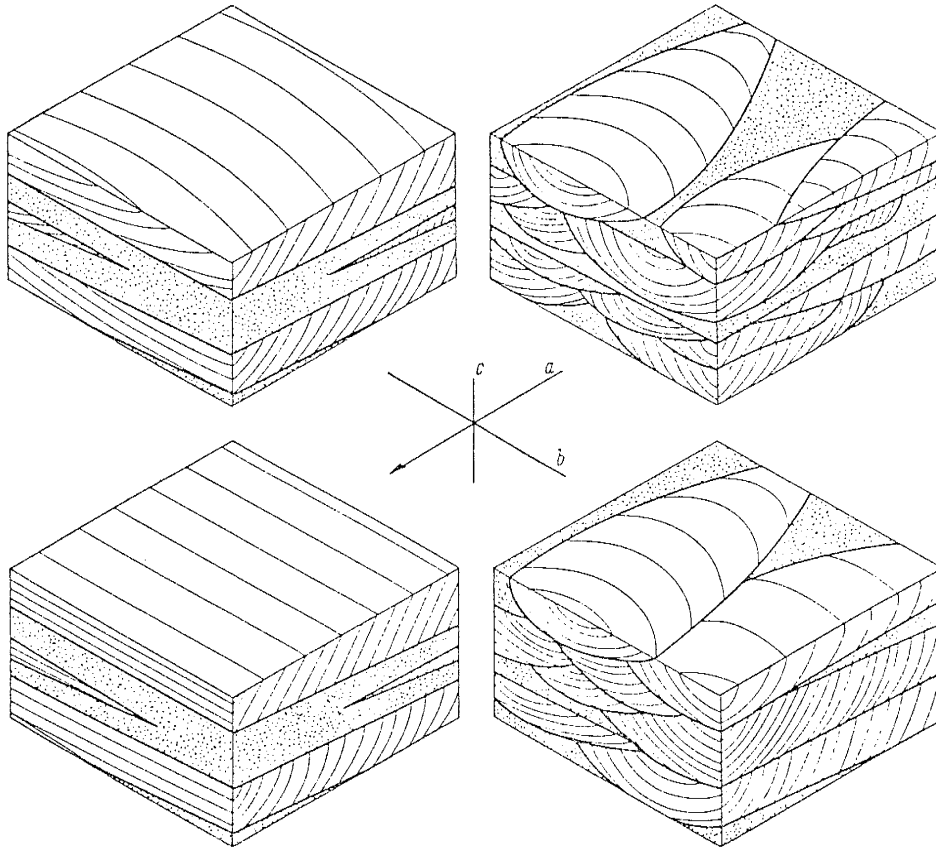
5cm-60cm

large scale:

>60 cm

A.3b - Cross-stratification

shape



Block diagrams of the two end members of cross-bedding, tabular (left) and trough (right) and standard reference system (after Potter and Pettijohn, 1963).

Appendix B

Catalogue of Directional Sedimentary Structures from the
Abo Formation

notes: See Table 4 for meaning of abbreviations in the type column.

1) The corrected trend and plunge of the sedimentary structures was obtained by the rotation of true bedding back to its original assumed horizontal position on a stereonet.

2) IPB = In the plane of bedding. These sedimentary structures marked with IPB are linear features (e.g., tool marks) as opposed to planar features (e.g., the foreset beds of a set of planar cross strata). The rotation of linear sedimentary structures can be treated differently than planar structures as is described in Chapter 4.

3) Some localities were noted during early reconnaissance and were eliminated later because they lacked sufficient information to be useful.

Appendix B: Catalogue of Directional Sedimentary Structures from the Abo Formation

Sample Locality	Unit	Type	True Bedding	Measured Strike	Measured Trend, Plunge ^o	Corrected ¹ Strike	Corrected ¹ Trend, Plunge ^o
1	A	SXS	N50E - 06N		S15E, 08		S27E, 13
	"	SXS	" "		S00, 12		S11E, 17
	"	MXS	N72E - 17N		S77W, 10		S15W, 19
	"	MXS	N61E - 12N		N22E, 15		N72E, 12
	"	MXS	" "		N43W, 6		S14E, 07
2	C	LXS	N83W - 05N		N28E, 03		S23E, 02
	"	LXS	N80W - 04N		N08W, 47		N10W, 43
	"	MXS	N52E - 18N		N24W, 27		N30W, 24
	C	CF	N80E - 07N		N64W, 12		S80W, 09
3	"	LXS	" "		S10W, 17		S04W, 24
	A	GM	N07E - 25W		N22E, IPB		N22E, 0
	"	GM	" "		N12E, IPB		N12E, 0
	"	GM	" "		N05E, IPB		N05E, 0
	"	GM	" "		N04E, IPB		N05E, 0
	"	SXS	N10W - 16W		N49W, 02		S70 E, 15
	"	SXS	N15W - 18W		S03E, 02		N85E, 17
5 6	Eliminated						
	C	SXS	N75E - 22N		N10W, 17		S35E, 05
7	"	CF	" "		N89W, 06		N01E, 21
	"	MXS	N55E - 16N		N85W, 27		S61W, 20
	A	PS	N82E - 25N		N40E, IPB		N40E, 0
8	Eliminated						
	Eliminated						
9	E	LXS	N84E - 15N		S02W, 11		S02E, 26
	"	LXS	" "		S20E, 16		S14E, 31
	"	LXS	" "		S10E, 11		S08E, 26
	"	LXS	" "		S40E, 20		S26E, 34
	"	MXS	N84E - 10N		S05W, 10		S00, 20

Sample Locality	Unit	Type	True Bedding	Measured Strike	Measured Trend, Plunge°	Corrected ¹ Strike	Corrected ¹ Trend, Plunge°
11	G	RM	N70W - 05N	N42E		N42E	
	"	RM	" "	N37E		N37E	
	"	RM	" "	N35E		N35E	
12	G	MXS	N67W - 15N		S62E, 06		S08E, 12
	"	MXS	" "		S86W, 19		S65W, 25
	"	MXS	" "		N75W, 14		S73W, 18
	"	SXS	" "		S70W, 17		S53W, 25
	"	SXS	" "		N33E, 21		N42E, 11
	"	SXS	" "		N49E, 23		N57E, 15
	"	SXS	" "		N40E, 27		N49E, 17
	"	SXS	" "		N48E, 24		N62E, 16
13	Eliminated						
14	Eliminated						
15	F	SXS	N52E - 10N		S25E, 13		S30E, 23
	"	SXS	" "		S30E, 05		S37E, 15
	"	SXS	" "		N48E, 07		S00, 12
	"	SXS	" "		S88E, 03		S48E, 12
	"	SXS	" "		S42E, 05		S39E, 15
	"	SXS	" "		S47E, 11		S43E, 21
	"	SXS	" "		S52E, 13		S46E, 23
	"	SXS	" "		S55E, 14		S49E, 24
16	Eliminated	RM		N40E		N40E	
17	K	MXS	N82E - 09N		N59W, 21		N31W, 17
	"	SXS	" "		S07W, 18		S03W, 28
	"	SXS	" "		S30E, 12		S22E, 21
	"	SXS	" "		S25E, 11		S17E, 19
	"	SXS	" "		S10E, 03		S07E, 12
	"	SXS	" "		S47W, 14		S37W, 20
18	G	MXS	N75E - 16N		N65E, 22		S77E, 25
	"	MXS	" "		N50E, 19		S80E, 19
	"	MXS	" "		N80E, 13		S53E, 21

Sample Locality	Unit	Type	True Bedding	Measured Strike	Measured Trend, Plunge°	Corrected ¹ Strike	Corrected ¹ Trend, Plunge°	
18	G	MXS	N75E - 16N		N72E, 21		S72E, 25	
	"	MXS	" "		S20E, 04		S17E, 20	
	"	SXS	" "		S55W, 02		S08E, 17	
	"	SXS	" "		S55E, 03		S22E, 18	
	"	RM	N80E - 20N	N05W				
19	F	RM	" "	N03W		N05W		
	"	MXS	" "			N03W		
	F	MXS	N72E - 07N		S10E, 11		S10E, 31	
	"	MXS	" "		N45E, 30		N55E, 27	
	"	MXS	" "		N25E, 24		N38E, 20	
20	"	MXS	" "		N45E, 14		N75E, 12	
	"	MXS	" "		N20E, 15		N45E, 10	
	"	RM	" "	N40W				
	"	SXS	" "					
	"	SXS	" "		S75E, 08		S50E, 13	
	"	SXS	" "		S05W, 15		S02E, 22	
	"	SXS	" "		S25W, 07		S03W, 13	
	"	SXS	" "		S05E, 07		S11E, 14	
	"	SXS	" "		S10E, 07		S13E, 17	
	"	CRM	N90W - 10N		N25E, 31		N35E, 23	
21	G	CRM	" "		N45E, 22		N70E, 16	
	"	CRM	" "		N42E, 17		N70E, 14	
	"	CRM	" "		N51E, 23		N76E, 19	
	"	CRM	" "		N38E, 30		N51E, 23	
	"	CRM	" "		N47E, 30		N63E, 24	
	"	CRM	" "		N60E, 26		N81E, 23	
	"	CRM	" "		N68E, 18		S80E, 17	
	"	CRM	" "		N58E, 27		N78E, 23	
	"	SXS	N78E - 11N		S40E, 09		S25E, 18	
	"	SXS	" "		S04E, 12		S08E, 23	
	"	SXS	" "		S60E, 13		S39E, 22	
	"	SXS	" "		S05W, 04		S07E, 15	
	"	SXS	" "		S80W, 15		S45W, 18	
	22	"	CRM	" "				
		"	CRM	" "				
"		CRM	" "					
"		CRM	" "					
"		CRM	" "					
"		CRM	" "					
"		CRM	" "					
"		CRM	" "					
"		CRM	" "					
"		CRM	" "					
"		CRM	" "					
"		CRM	" "					
"		CRM	" "					
"		SXS	" "					
"		SXS	" "					

Sample Locality	Unit	Type	True Bedding	Measured Strike	Measured Trend, Plunge ^o	Corrected ¹ Strike	Corrected ¹ Trend, Plunge ^o
23	F	CF	N75E - 04N		S81W, 09		S55W, 09
	"	CF	" "		N32W, 09		N41W, 05
24	F	TM	N45E - 13N		S84W, IPB		S84W, 0
	"	TM	" "		N88W, IPB		N88W, 0
	"	TM	" "		S82W, IPB		S82W, 0
	"	TM	" "		N61W, IPB		N61W, 0
	"	TM	" "		N90W, IPB		N90W, 0
	"	TM	" "		S88W, IPB		S88W, 0
	"	TM	" "		N90W, IPB		N90W, 0
	"	TM	" "		N88W, IPB		N88W, 0
	"	TM	" "		N86W, IPB		N86W, 0
	"	TM	" "		N80W, IPB		N80W, 0
	"	TM	" "		N86W, IPB		N86W, 0
	"	TM	" "		N75W, IPB		N75W, 0
	"	TM	" "		N90W, IPB		N90W, 0
	"	TM	" "		S80W, IPB		S80W, 0
	"	TM	" "		N86W, IPB		N86W, 0
	25	"	TM	" "		S90W, IPB	
"		TM	" "		S87W, IPB		S87W, 0
"		TM	" "		N78W, IPB		N78W, 0
"		TM	" "		N89W, IPB		N89W, 0
"		TM	" "		S88W, IPB		S88W, 0
"		TM	" "		N05E, IPB		N05E, 0
A		PS	N13E - 07W		N40E, IPB		N40E, 0
"		PS	" "		N70E, IPB		N70E, 0
"		PS	" "		N50E, IPB		N50E, 0
"		PS	" "		N18E, IPB		N18E, 0
"		PS	" "		N17W, IPB		N17W, 0
"		PS	" "		N90W, IPB		N90W, 0
"		PS	" "		N30W, IPB		N30W, 0
"		MXS	N07W - 14W		N28E, 16		N52E, 26

Sample Locality	Unit	Type	True Bedding	Measured Strike	Measured Trend, Plunge ^o	Corrected ¹ Strike	Corrected ¹ Trend, Plunge ^o
26	A	CF	N35E - 17N		N90W, 10		S20E, 10
	"	MXS	"		N20W, 12		N80E, 10
	"	PS	"		N75E, IPB		N75E, 0
	"	PS	"		N70E, IPB		N70E, 0
	"	PS	"		N73E, IPB		N73E, 0
	"	PS	"		N77E, IPB		N77E, 0
	"	PS	"		N25E, IPB		N25E, 0
	"	PS	"		N21E, IPB		N21E, 0
	"	SXS	N56E - 15N		N65E, 16		S75E, 24
	"	SXS	"		S60E, 8		S44E, 23
27	"	SXS	"		N78E, 20		N60E, 33
	"	SXS	N60E - 15N		S66E, 13		S47E, 26
	"	GM	N65E - 05N		S33E, IPB		S33E, 0
	"	GM	"		S33E, IPB		S33E, 0
	"	GM	"		S48E, IPB		S48E, 0
	"	GM	"		S43E, IPB		S43E, 0
	"	GM	"		S35E, IPB		S35E, 0
	"	MXS	N88E - 14N		S47E, 11		S23E, 23
	"	RM	"			N73E	
	"	SXS	N55E - 11N				
28	A	SXS	"		N80E, 28		S83E, 34
	"	SXS	"		S88E, 10		S62E, 18
	"	SXS	"		N63E, 18		S89E, 22
	"	PS	"		N40E, IPB		N40E, 0
	"	PS	"		N05W, IPB		N05W, 0
	"	PS	"		N25E, IPB		N25E, 0
	"	PS	"		N47E, IPB		N47E, 0
	"	PS	"		N72W, IPB		N72W, 0
	"	PS	"		N25W, IPB		N25W, 0
	"	PS	"		N58E, IPB		N58E, 0
29	A	PS	N24E - 19W		S76W, IPB		S76W, 0
	"	PS	"		S88W, IPB		S88W, 0
	"	PS	"		S84E, IPB		S84E, 0
	"	PS	"				

Sample Locality	Unit	Type	True Bedding	Measured Strike	Measured Trend, Plunge ^o	Corrected ¹ Strike	Corrected ¹ Trend, Plunge ^o
29	A	PS	N24E - 19W		S87W, IPB		S87W, 0
	"	PS	" "		S87W, IPB		S87W, 0
	"	PS	" "		S40E, IPB		S40E, 0
	"	PS	" "		S66W, IPB		S66W, 0
	"	PS	" "		S76E, IPB		S76E, 0
	"	SXS	N62W - 25N		S75E, 25		S27E, 30
30	"	SXS	" "		S72E, 13		S03E, 26
	B	CF	N85W - 15N		N64E, 06		S17E, 13
31	B	MXS	N83W - 23N		S57E, 04		S03E, 25
32	B	SXS	N88E - 19N		S13E, 27		S09E, 46
	"	SXS	N60E - 16N		S03E, 11		S18E, 26
33	B	RM	N68E - 19N	N43W		N43W	
	"	RM	" "	N26W		N26W	
	"	RM	" "	N27W		N27W	
	"	RM	" "	N31W		N31W	
	"	RM	" "	" "	N50W		N50W
	"	RM	N75W - 08N	N80E		N80E	
34	C	RM	" "	N75W		N75W	
	"	RM	" "		N48E, 33		N72E, 27
35	C	SXS	N85E - 14N		N16W, 20		N35W, 07
	"	SXS	" "				
36	C	RM	N65E - 15N	N20E		N20E	
	"	RM	" "	N31E		N31E	
	"	RM	" "	N08E		N08E	
	"	RM	" "	N01E		N01E	
	"	SXS	N76W - 10N		S30W, 27		S26W, 36
	"	SXS	" "		S85E, 15		S49E, 16
37	"	SXS	" "		S35E, 20		S19E, 27
	"	SXS	" "		S25W, 07		S17W, 17
	"	SXS	" "		S14W, 16		S14W, 26
	"	SXS	N88W - 17N		N55E, 02		S05E, 16
	"	SXS	" "		N68E, 21		S66E, 20
	"	SXS	" "		N67E, 13		S45E, 16
38	C	SXS	" "				
	"	SXS	" "				

Sample Locality	Unit	Type	True Bedding	Measured Strike	Measured Trend, Plunge°	Corrected ¹ Strike	Corrected ¹ Trend, Plunge°
39	C	CFE	N42E - 24N	N90W	N68W, 22	N90W	S14W, 08
40	D	RM	N70E - 13N	N65W		N65W	
	"	RM	"	N80E		N80E	
	"	RM	"	N70W		N70W	
	"	RM	"	N60W		N60W	
	"	RM	"	N45E		N45E	
	"	RM	"	N35E		N35E	
	"	RM	"	N72E		N72E	
41	D	RM	N65E - 08N	N70E		N70E	
	"	RM	"		N15W, 27		N10W, 18
	"	MXS	"				
42	D	RM	N90W - 07N	N30W		N30W	
	"	MXS	"		N18E, 26		N23E, 19
43	D	MXS	N85W - 20N		N15E, 34		N29E, 15
	"	MXS	"		N48E, 15		S43E, 13
	"	RM	"	N42W		N42W	
	"	RM	"	N75E		N75E	
	"	RM	"	N77E		N77E	
	"	RM	"	N85W		N85W	
	"	RM	"	N90W		N90W	
	"	RM	"	N87W		N87W	
44	Eliminated						
45	D	GM	N65E - 10N		N20E, IPB		N20E, 0
	"	GM	"		N20E, IPB		N20E, 0
	"	GM	"		N20E, IPB		N20E, 0
	"	GM	"		N20E, IPB		N20E, 0
	"	GM	"		N20E, IPB		N20E, 0
	"	GM	"		N20E, IPB		N20E, 0
46	E	LXS	N84E - 10N		S00W, 17		S02E, 27
	"	LXS	"		S50W, 14		S27W, 21
47	F	TM	N75W - 15N		N58W, IPB		N58W, 0

Sample Locality	Unit	Type	True Bedding	Measured Strike	Measured Trend, Plunge ^o	Corrected ¹ Strike	Corrected ¹ Trend, Plunge ^o	
47	F	TM	N75W - 15N		N62W, IPB		N62W, 0	
	"	TM	"		N62W, IPB		N62W, 0	
	"	TM	"		N73W, IPB		N73W, 0	
	"	TM	"		N80W, IPB		N80W, 0	
	"	TM	"		N80E, IPB		N80E, 0	
	"	TM	"		N80E, IPB		N80E, 0	
	"	TM	"		N52W, IPB		N52W, 0	
	"	TM	"		N02W, IPB		N02W, 0	
	"	TM	"		N35W, IPB		N35W, 0	
	"	TM	"		N60W, IPB		N60W, 0	
	"	TM	"		N45W, IPB		N45W, 0	
	"	TM	"		N88W, IPB		N88W, 0	
	48	F	PM	N73E - 20N	N43W		N43W	
		"	PM	"	N53W		N53W	
49	"	MXS	"		S35W, 09		SOLE, 26	
	"	MXS	"		S50W, 16		S14W, 30	
	"	MXS	"		S25W, 13		S00W, 31	
	"	MXS	"		S80W, 26		S42W, 31	
	"	MXS	"		S75W, 25		S38W, 31	
	"	MXS	"		S80W, 23		S38W, 28	
	"	MXS	"		N70W, 24		S59W, 20	
	"	MXS	"		N75W, 24		S54W, 21	
	"	MXS	N86E - 12N		N67W, 33		N87W, 29	
	"	MXS	"		N52W, 24		N80W, 18	
	"	MXS	"		N63W, 30		N86W, 25	
	"	MXS	"		N40W, 35		N56W, 26	
	"	MXS	"		N52W, 25		N81W, 19	
	"	MXS	"		N52W, 25		N81W, 19	
	"	MXS	"		N55W, 39		N69W, 32	
	"	MXS	"		N55W, 29		N75W, 23	
	"	MXS	"		N57W, 33		N75W, 28	
"	MXS	"		N55W, 35		N72W, 29		

Sample Locality	Unit	Type	True Bedding	Measured Strike	Measured Trend, Plunge °	Corrected ¹ Strike	Corrected ¹ Trend, Plunge °
50	F	RM	N57E - 10N	N35E		N35E	
	"	RM	" "	N30E		N30E	
51	F	PS	N63E - 11N		N67W, IPB		N67W, 0
	"	PS	" "		N88W, IPB		N88W, 0
	"	PS	" "		N68W, IPB		N68W, 0
	"	PS	" "		N60W, IPB		N60W, 0
	"	PS	" "		N22E, IPB		N22E, 0
	"	PS	" "		N35W, IPB		N35W, 0
	"	PS	" "		N46E, IPB		N46E, 0
	"	PS	" "		N35E, IPB		N35E, 0
	"	PS	" "		N68E, IPB		N68E, 0
	"	PS	" "		N20W, IPB		N20W, 0
	"	PS	" "		N23W, IPB		N23W, 0
	"	PS	" "		N58W, IPB		N58W, 0
	"	PS	" "		N25W, IPB		N25W, 0
	"	PS	" "		N08W, IPB		N08W, 0
	"	PS	" "		N80E, IPB		N80E, 0
52	F	MXS	N38E - 13N		N65E, 20		N65E, 28
53	G	CF	N85W - 08N		N70W, 10		S88W, 19
	"	RM	" "	N80W		N80W	
	"	RM	" "	N78W		N78W	
	"	RM	" "	N81W		N81W	
	"	RM	" "	N77E		N77E	
	"	RM	" "	N30W		N30W	
54	G	RM	N87W - 04N		N26W		
	"	RM	" "	N26W		N26W	
	"	RM	" "	N23W		N23W	
	"	RM	" "	N27W		N27W	
	"	RM	" "	N20W		N20W	
	"	RM	" "	N36W		N36W	
	"	RM	" "	N38W		N38W	
	"	MXS	N87W - 04N		N10E, 34		N11E, 29
	"	MXS	N67E - 10N		N06E, 13		N44E, 04

Sample Locality	Unit	Type	True Bedding	Measured Strike	Measured Trend, Plunge ^o	Corrected ¹ Strike	Corrected ¹ Trend, Plunge ^o
54	G	MXS	N67E - 10N		N15W, 20		N10W, 10
	"	MXS	" "		N02E, 27		N08E, 17
	"	MXS	" "		N08E, 16		N46E, 09
	"	MXS	" "		N17E, 10		N87E, 06
	"	MXS	" "		N15E, 26		N33E, 18
	"	MXS	" "		N22E, 15		S88E, 17
	G	SXS	N55E - 18N		S77E, 10		S28E, 13
	G	SXS	N70W - 10N		S32E, 20		S17E, 28
	"	SXS	" "		S10E, 23		S03E, 32
	"	SXS	" "		S65E, 17		S35E, 21
55	"	SXS	" "		N20E, 23		N39W, 06
	"	SXS	N55W - 20N		N33E, 13		S42W, 07
	"	SXS	" "		N51E, 24		S79E, 07
	"	SXS	" "		N63E, 27		S73E, 12
	"	SXS	" "		N53E, 22		S60E, 06
	"	SXS	" "		N23E, 26		N07W, 08
	"	SXS	" "		N26E, 38		N17E, 19
	"	SXS	" "		N20E, 35		N02E, 17
	"	SXS	" "		N26E, 26		N00W, 06
	"	SXS	" "		N03E, 32		N29W, 18
58	"	SXS	" "		N52E, 29		N73E, 26
	G	SXS	N78E - 11N		N53E, 24		N79E, 22
	"	SXS	" "		N48E, 20		N79E, 17
	"	SXS	" "		N41E, 29		N60E, 24
	"	SXS	" "		N50E, 23		N79E, 20
	"	SXS	" "		S60W, 05		S03W, 22
	"	SXS	N80E - 19N		S70W, 09		S25W, 22
	"	SXS	" "		S53W, 16		S20W, 30
	"	SXS	" "		S57W, 15		S20W, 28
	"	SXS	" "		S12W, 37		S09W, 45
59	"	CRM	N82E - 09N		S20W, ?		S15W, ?
	"	CRM	" "		S03W, 39		S01W, 48
	"	CRM	" "				
	"	CRM	" "				

Sample Locality	Unit	Type	True Bedding	Measured Strike	Measured Trend, Plunge ^o	Corrected ¹ Strike	Corrected ¹ Trend, Plunge ^o
61	K	SXS	N82E - 27N		N23E, 32		N78E, 15
	"	SXS	"		N80E, 32		S56W, 33
	"	SXS	"		S73W, 26		S34W, 39
	K	SXS	N50E - 07N		S30E, 19		S33E, 25
62	"	SXS	"		S47W, 22		S31W, 23
	"	SXS	"		S07W, 10		S11E, 16
	"	SXS	"		S00W, 11		S15E, 17
	"	SXS	"		S20E, 12		S26E, 18
	"	SXS	"		S05E, 22		S05E, 27
	"	SXS	"		S15E, 15		S23E, 22
	"	SXS	"		S39W, 13		S27W, 22
	M	SXS	N80W - 10N		S48W, 15		S34W, 23
	"	SXS	"		S07W, 06		S09W, 16
	"	SXS	"		S32W, 02		S15W, 12
	"	SXS	"		S65W, 20		S47W, 27
	63	"	SXS	"		S72W, 19	
"		SXS	"		S14W, 04		S10W, 14
"		SXS	"		S63W, 24		S49W, 31
"		SXS	"		S50W, 20		S38W, 29
"		SXS	"		S24W, 14		S18W, 24
"		SXS	"		N55W, 24		N88W, 15
"		SXS	"		N83W, 26		S65W, 23
"		SXS	"		S66W, 11		S17W, 19
"		SXS	"		N58W, 33		S53W, 20
"		SXS	"		N60E, 22		N90E, 15
"		SXS	"		N90W, 30		S60W, 28
64		"	SXS	"		N82W, 29	
	"	SXS	"		N70W, 26		S73W, 20
	"	SXS	"		N71W, 21		S62W, 16
	"	SXS	"		N76E, 15		N65E, 18
	"	SXS	"		N70E, 09		S50E, 13
	"	SXS	"		N57E, 07		S39E, 09
	"	SXS	"		N68E, 07		S42E, 12
	"	SXS	"		N72E - 15N		
	"	SXS	"		"		
	"	SXS	"		"		
	"	SXS	"		"		
	"	SXS	"		"		
65	M	SXS	N72E - 15N				
	"	SXS	"				
	"	SXS	"				
66	M	SXS	N70E - 32N				
	N	SXS	N70W - 13N				
67	N	SXS	N70E - 16N				
	"	SXS	"				
68	"	SXS	"				
	"	SXS	"				
	"	SXS	"				
	"	SXS	"				
	O	SXS	N82E - 12N				
	"	SXS	"				

Sample Locality	Unit	Type	True Bedding	Measured Strike	Measured Trend, Plunge ^o	Corrected ¹ Strike	Corrected ¹ Trend, Plunge ^o
68	0	SXS	N82E - 12N		N65E, 20		S80E, 20
69	0	SXS	N58E - 09N		S42E, 08		S36E, 17
	"	SXS	" "		S55E, 11		S45E, 20
	"	SXS	" "		S75E, 07		S50E, 15
	"	SXS	" "		S70E, 05		S43E, 13
	"	SXS	" "		S87E, 13		S67E, 19
	"	SXS	" "		S78E, 14		S59E, 22
	"	SXS	" "		N65E, 06		N90E, 21
	"	SXS	" "		N72E, 09		S70E, 14
70	0	MXS	N80W - 07N		S73W, 23		S65W, 36
	"	MXS	" "		S81W, 24		S70W, 27
	"	MXS	" "		N80W, 30		S88W, 31
	"	MXS	" "		S70W, 24		S59W, 28

REFERENCES

- Allen, J. R. L., 1963, The classification of cross-stratified units. With notes on their origin: *Sedimentology*, v. 2, p. 93-114.
- _____, 1964, Studies in fluvial sedimentation: six cyclothems from the Lower Old Red Sandstones, Anglo-Welsh Basin: *Sedimentology*, v. 3, p. 163-198.
- _____, 1965, A review of the origin and characteristics of Recent alluvial sediments: *Sedimentology*, v. 5, p. 89-191.
- _____, 1966, On bed forms and paleocurrents: *Sedimentology*, v. 6, p. 153-190.
- _____, 1970, Physical processes of sedimentation: New York, American Elsevier Publishing Co., 248 p.
- _____, 1973, A classification of climbing-ripple cross lamination: *Jour. Geol. Soc. London*, v. 129, p. 537-541.
- Baars, D. L., 1961, Permian strata of central New Mexico: *New Mexico Geol. Soc. Guidebook*, 12th field conference, p. 113-120.
- _____, 1962, Permian System of the Colorado Plateau: *Am. Assoc. Petroleum Geologists Bull.*, v. 46, p. 149-218.
- Bachman, G. O., 1964, Southwestern edge of the Paleozoic land mass in southwestern New Mexico: *New Mexico Geol. Soc. Guidebook*, 15th field conference, p. 70-72.
- Basu, A., Calvin, J. W., Mack, G. H., Suttner, L. J., and Young, S. W., 1974, Re-evaluation of the use of strained

- monocrystalline quartz in provenance interpretation:
Geol. Soc. America, Abs. with Programs (Ann. Mtg.),
v. 6, no. 7, p. 1021.
- Beerbower, J. R., 1964, Cyclothems and cyclic depositional
mechanisms in alluvial plain sedimentation: Kansas
Geol. Surv. Bull. 169, p. 31-42.
- Bernard, H. A., and Major, C. F., 1963, Recent meander belt
deposits of the Brazos River: An alluvial "sand"
model: Am. Assoc. Petroleum Geologists Bull.,
v. 47, p. 350.
- Blatt, H., and Christie, J. M., 1963, Undulatory extinction
in quartz of igneous and metamorphic rocks and its
significance in provenance studies of sedimentary
rocks: Jour. Sedimentary Petrology, v. 33, p. 550-579.
- Blatt, H., Middleton, G., and Murray, R., 1972, Origin of
sedimentary rocks: Englewood Cliffs, New Jersey,
Prentice-Hall Inc., 634 p.
- Curray, J. R., 1956, The analysis of two-dimensional
orientation data: Jour. Geology, v. 64, p. 117-131.
- Dane, C. H., and Bachman, G. O., 1965, Geologic map of
New Mexico: U. S. Geol. Survey, 2 sheets.
- Darton, N. H., 1928, "Red Beds" and associated formations
in New Mexico: U. S. Geol. Survey Bull. 794,
356 p.
- Dunbar, C. O., (chairman) et al., 1960, Correlation of
the Permian formations of North America: Geol.
Soc. America Bull., v. 71, p. 1763-1806.

- Folk, R. L., 1965, Some aspects of recrystallization in ancient limestones: (in) L. C. Pray and R. C. Murray (editors), Dolomitization and limestone diagenesis: a symposium: Soc. Econ. Paleontologists and Mineralogists, Spec. Pub. 13, p. 14-48.
- _____, 1974, Petrology of sedimentary rocks: Austin Texas, Hemphill Publishing Co., 182 p.
- Goddard, E. N., 1966, Geologic map and sections of the Zuni Mountains fluorspar district, Valencia county, New Mexico: U. S. Geol. Survey Misc. Geol. Investigations Map, I-454.
- Gonzalez, R. A., 1965, Petrography and structure of the Pedernal Hills, Torrance County, New Mexico: Univ. of New Mexico, unpublished M.S. thesis, 78 p.
- Harms, J. C., MacKenzie, D. B., McCubbin, D. G., 1963, Stratification in the modern sands of the Red River, Louisiana: Jour. Geology, v. 71, p. 566-580.
- Harms, J. C., and Fahnestock, R. K., 1965, Stratification, bed forms and flow phenomena (with an example from the Rio Grande): (in) G. V. Middleton (editor), Primary sedimentary structures and their hydrodynamic interpretation: Soc. Econ. Paleontologists and Mineralogists, Spec. Pub. 12, p. 84-110.
- Herber, L., 1963, Structural petrology and economic features of the Precambrian rocks of the La Joyita Hills: New Mexico Instit. Mining and Tech., unpublished M.S. thesis, 36 p.

- High, L. R., and Picard, M. D., 1971, Mathematical treatment of orientation data: (in) R. E. Carver (editor), Procedures in sedimentary petrology: New York, John Wiley and Sons Inc., p. 21-44.
- Hills, J. M., 1961, Correlation of Permian formations of North America: Am. Assoc. Petroleum Geologists Bull., v. 45, p. 1412-1414.
- Jaworski, M. J., 1973, Copper mineralization of the Upper Moya Sandstone, Chupadero Mines area, Socorro County, New Mexico: New Mexico Instit. Mining and Tech., unpublished M.S. thesis, 102 p.
- Jerome, S. E., Campbell, D. D., Wright, J. S., and Vitz, H. E., 1965, Geology and ore deposits of the Sacramento (High Rolls) Mining district, Otero County, New Mexico: New Mexico Instit. Mining and Tech., State Bureau Mines and Min. Res., Bull. 86, 29 p.
- Johns, W. D., Grim, R. E., and Bradley, W. F., 1954, Quantitative estimations of clay minerals by diffraction methods: Jour. Sedimentary Petrology, v. 24, p. 242-251.
- Jones, T. A., 1968, Statistical analysis of orientation data: Jour. Sedimentary Petrology, v. 38, p. 61-67.
- Jopling, A. V., and Walker, R. G., 1968, Morphology and origin of ripple drift cross-lamination, with examples from the Pleistocene of Massachusetts: Jour. Sedimentary Petrology, v. 38, p. 971-984.
- Kelley, V. C., and Silver, C., 1952, Geology of the Caballo Mountains: Univ. New Mexico Pubs. in

- Geology, number 4, 285 p.
- Kelley, V. C., 1963, Geological map of the Sandia Mountains and vicinity: New Mexico Instit. Mining and Tech., State Bureau Mines and Min. Res., Map 18.
- King, P. B., 1942, Permian of west Texas and southwestern New Mexico: Am. Assoc. Petroleum Geologists Bull., v. 26, p. 535-763.
- King, R. E., 1945, Stratigraphy and oil producing zones of the pre-San Andres formations of southeastern New Mexico: New Mexico School of Mines, State Bureau Mines and Min. Res., Bull. 23, 34 p.
- Kottowski, F. E., Flower, R. H., Thompson, M. L., and Foster, R. W., 1956, Stratigraphic studies of the San Andres Mountains, New Mexico: New Mexico Instit. Mining and Tech., State Bureau Mines and Min. Res., Memoir 1, 132 p.
- Kottowski, F. E., 1963, Paleozoic and Mesozoic strata of southwestern and south-central New Mexico: New Mexico Instit. Mining and Tech., State Bureau Mines and Min. Res., Bull. 79, 100 p.
- _____, 1965, Sedimentary basins of south-central and southwestern New Mexico: Am. Assoc. Petroleum Geologists Bull., v. 49, p. 2120-2139.
- Kottowski, F. E., and Stewart, W. J., 1970, The Wolfcampian Joyita uplift in central New Mexico: New Mexico Instit. of Mining and Tech., State Bureau Mines and Min. Res., Memoir 23, Part 1, p. 1-31.

- LaPoint, D., 1974, Possible source areas for sandstone copper deposits in northern New Mexico: New Mexico Geol. Soc. Guidebook, 25th Field conference, p. 305-307.
- Lee, W. T., and Girty, G. H., 1909, The Manzano Group of the Rio Grande Valley of New Mexico: U. S. Geol. Survey Bull. 389, 141 p.
- Leopold, L. B., and Wolman, M. G., 1960, River meanders: Geol. Soc. America Bull., v. 71, p. 769-794.
- Leopold, L. B., Wolman, M. G., and Miller, J. P., 1964, Fluvial processes in geomorphology: San Francisco, W. H. Freeman and Co., 522 p.
- Meyer, R. F., 1966, Geology of the Pennsylvanian and Wolfcampian rocks in southeastern New Mexico: New Mexico Instit. Mining and Technology, State Bureau Mines and Min. Res., Memoir 17, 123 p.
- Miller, J. P., Montgomery, A., and Sutherland, P. K., 1963, Geology of the southern part of the Sangre de Cristo Mountains, New Mexico: New Mexico Instit. Mining and Tech., State Bureau Mines and Min. Res., Memoir 11, 106 p.
- Moody-Stuart, M., 1966, High- and Low-sinuosity stream deposits with examples from the Devonian of Spitsbergen: Jour. Sedimentary Petrology, v. 36, p. 1102-1117.
- McGowen, J. H., and Garner, L. E., 1970, Physiographic features and stratification types of coarse-grained

- point bars: modern and ancient examples: *Sedimentology*, v. 14, p. 77-111.
- McKee, E. D., 1965, Experiments on ripple lamination: (in) G. V. Middleton (editor), *Primary sedimentary structures and their hydrodynamic interpretation: Soc. Econ. Paleontologists and Mineralogists, Spec. Pub. 12*, p. 66-83.
- _____, 1967, Paleotectonic investigations of the Permian System in the United States - Arizona and western New Mexico: *U. S. Geol. Survey Prof. Paper 515*, p. 203-223.
- Needham, C. E., and Bates, R. L., 1943, Permian type sections in central New Mexico: *Geol. Soc. America Bull.*, v. 54, p. 1653-1667.
- New Mexico Geological Society, 1963, The Abo Formation in the area around Socorro, New Mexico: *New Mexico Geol. Soc. Guidebook, 14th Field conference*, p. 98-99.
- Otte, C. Jr., 1959, Late Pennsylvanian and Early Permian stratigraphy of the northern Sacramento Mountains, Otero County, New Mexico: *New Mexico Instit. Mining and Tech., State Bureau Mines and Min. Res., Bull. 50*, 111 p.
- Perhac, R. M., 1970, Geology and mineral deposits of the Gallinas Mountains, Lincoln and Torrance Counties, New Mexico: *New Mexico Instit. Mining and Tech., State Bureau Mines and Min. Res., Bull. 95*, 51 p.
- Pettijohn, F. J., Potter, P. E., and Siever, R., 1973,

- Sand and sandstone: New York, Springer-Verlag,
618 p.
- Phillips, F. C., 1954, The use of the stereographic
projection in structural geology: London, Edwin
Arnold (Publishers) Ltd., 86 p.
- Potter, P. E., and Pettijohn, F. J., 1963, Paleocurrents
and basin analysis: Berlin, Springer Verlag Inc.,
296 p.
- Pray, L. C., 1961, Geology of the Sacramento Mountains
escarpment, Otero County, New Mexico: New Mexico
Instit. Mining and Tech., State Bureau Mines and
Min. Res., Bull. 35, 144 p.
- Price, N. J., 1966, Fault and joint development in brittle
and semi-brittle rock: New York, Pergammon Press
Inc., 176 p.
- Ramsay, J. G., 1961, The effects of folding on the
orientation of sedimentary structures: Jour.
Geology. v. 69, p. 84-100.
- _____, 1967, Folding and fracturing of rocks: New
York, McGraw-Hill Book Co., 568 p.
- Read, C. B., and Mamay, S. B., 1964, Upper Paleozoic
floral zones and floral provinces: U. S. Geol.
Survey Prof. Paper 454-K, 35 p.
- Read, C. B., Trauger, F. D., and Werts, L. L., 1967,
Road log from Gallup through the Zuni Mountains to
Thoreau and return to Gallup via Smith Lake, Mariano
Lake and Pinedale: New Mexico Geol. Soc. Guidebook,

- 18th field conference, p. 99-119.
- Rejas, A., 1965, Geology of the Cerros de Amado area, Socorro County, New Mexico: New Mexico Instit. of Mining and Tech., unpublished M.S. thesis, 128 p.
- Schumm, S. A., 1972, Fluvial paleochannels: (in) J. K. Rigby and W. K. Hamblin (editors), Recognition of ancient sedimentary environments: Soc. Econ. Paleontologists and Mineralogists: Spec. Pub. 16, p. 98-107.
- Simons, D. B., Richardson, E. V., and Nordin, C. F. Jr., 1965, Sedimentary structures generated by flow in alluvial channels: (in) G. V. Middleton (editor), Primary sedimentary structures and their hydrodynamic interpretation: Soc. Econ. Paleontologists and Mineralogists, Spec. Pub. 12, p. 34-52.
- Smith, C. T., 1957, Geology of the Zuni Mountains, Valencia and McKinley Counties, New Mexico: (in) Geology of the southwestern San Juan Basin, Four Corners Geological Society, 2nd field conference Guidebook, p. 53-61.
- Thompson, M. L., 1942, Pennsylvanian System in New Mexico: New Mexico School of Mines, State Bureau of Mines and Min. Res., Bull. 17, 92 p.
- Tonking, W. H., 1957, Geology of the Puertocito quadrangle, Socorro County, New Mexico: New Mexico Instit. Mining and Tech., State Bureau Mines and Min. Res., Bull. 41, 67 p.

- U. S. Geological Survey, 1965, Mineral and water resources of New Mexico: New Mexico Instit. Mining and Tech., State Bureau Mines and Min. Res., Bull. 87, 437 p.
- Walker, T. R., 1967, Formation of red beds in modern and ancient deserts: Geol. Soc. America Bull., v. 78, p. 353-368.
- _____, 1974, Formation of red beds in moist tropical climates: A hypothesis: Geol. Soc. America Bull., v. 85, p. 633-638.
- Williams, P. F., and Rust, B. R., 1969, The sedimentology of a braided river: Jour. Sedimentary Petrology, v. 39, p. 649-679.
- Wilpolt, R. H., et al., 1946, Geological map and stratigraphic sections of Paleozoic rocks of Joyita Hills, Los Piños Mountains, and northern Chupadero Mesa, Valencia, Torrance, and Socorro Counties, New Mexico: U. S. Geol. Survey, Oil and Gas Invest. Prelim. Map, OM 61.
- Wilpolt, R. H., and Waneck, A. A., 1951, Geology of the region from Socorro and San Antonio east to Chupadera Mesa, Socorro County, New Mexico: U. S. Geol. Survey, Oil and Gas Invest. Map, OM 121.
- Winters, S. L., 1963, The Supai Formation (Permian) of eastern Arizona: Geol. Soc. America, Memoir 89, 99 p.
- Wright, F., 1962, Abo Reef: prime west Texas target, part 1: Oil and Gas Jour., v. 60, n. 31, p. 226-235.

This thesis is accepted on behalf of the faculty of the
Institute by the following committee:

John R. Miller

W. T. Pudding

Frank E. [unclear]

Date June 27, 1975